SUPPLEMENTARY DATA

Synthesis, Characterisation and Influence of Lipophilicity on Cellular Accumulation and Cytotoxicity of Unconventional Platinum(IV) Prodrugs as Potent Anticancer Agents

Krishant M. Deo,[a] Jennette Sakoff,[b] Jayne Gilbert,[b] Yingjie Zhang[c] and Janice R. Aldrich Wright[a]

[a] *Nanoscale Organisation and Dynamics Group, Western Sydney University, Campbelltown, NSW 2560, Australia*

[b] *Calvary Mater Newcastle, Waratah, NSW 2298, Australia*

[c] *Australian Nuclear Science and Technology Organisation, Locked Bag 2001, Kirrawee DC, NSW 2232, Australia*

Contents

A. Characterisation Data

[Pt(PHEN)(SSDACH)(OH)(Decanoate)](NO_3)$_2$ (1)

Yield (445.3 mg, 80 %). Electronic spectrum λ_{max} nm (ε/mol^{-1}.dm^3.cm^{-1}, MeOH): 279 (27 500 ± 530). CD spectrum λ_{max} nm (mdeg.mol/L, MeOH:H_2O (1:4)): 279 (-3.3). ^{1}H NMR (400 MHz, MeOD): δ 9.46 (dd, J_1 = 11.82 Hz, J_2 = 5.30 Hz, 2 H), 9.23 (d, J = 8.28 Hz, 2 H), 8.47 (s, 2 H), 8.40 (dd, J_1 = 8.30 Hz, J_2 = 5.54 Hz, 2 H), 3.21 (m, 2H), 2.48 (m, 2 H), 2.07 (t, J = 7.32 Hz, 2 H), 1.81 (m, 4 H), 1.44 (m, 2 H), 1.31 – 1.10 (m, 8 H), 1.03 – 0.88 (m, 7 H), 0.76 (pnt, J = 7.70 Hz, 2 H). ^{1}H-^{195}Pt HMQC (400/86 MHz, MeOD): δ 9.45, 8.39/480. ^{195}Pt NMR (86 MHz, MeOD): δ 481 ppm. HPLC t_R: 7.8 min. HRMS-ESI: Calc. [M-H]$^+$ = 676.2826, Found = 676.2816.

[Pt(PHEN)(SSDACH)(Decanoate)$_2$](NO_3)$_2$ (2)

Yield (122.6 mg, 55 %). Electronic spectrum λ_{max} nm (ε/mol^{-1}.dm^3.cm^{-1}, MeOH): 279 (29 000 ± 120). CD spectrum λ_{max} nm (mdeg.mol/L, MeOH:H_2O (1:4)): 279 (-5.3). ^{1}H NMR (400 MHz, MeOD): δ 9.59 (d, J = 5.52 Hz, 2 H), 9.24 (d, J = 8.24 Hz, 2 H), 8.47 (s, 2H), 8.40 (d, J_1 = 8.26 Hz, J_2 = 5.58 Hz, 2 H), 3.22 (m, 2H), 2.51 (m, 2H), 2.12 (t, J = 7.28 Hz, 4 H), 1.83 (m, 4 H), 1.45 (m, 2 H), 1.31 – 1.06 (m, 16 H), 1.03 – 0.88 (m, 14 H), 0.72 (pnt, J = 7.43 Hz, 4 H). ^{1}H-^{195}Pt HMQC (400/86 MHz, MeOD): δ 9.59, 8.40/688. ^{195}Pt NMR (86 MHz, MeOD): δ 692 ppm. HPLC t_R: 10.3 min. HRMS-ESI: Calc. [M-H]$^+$ = 830.4184, Found = 830.4158.

[Pt(PHEN)(SSDACH)(OH)(DoDecanoate)](NO_3)$_2$ (3)

Yield (105.4 mg, 55 %). Electronic spectrum λ_{max} nm (ε/mol^{-1}.dm^3.cm^{-1}, MeOH): 279 (27 000 ± 190). CD spectrum λ_{max} nm (mdeg.mol/L, MeOH:H_2O (1:4)): 279 (-2.8). ^{1}H NMR (400 MHz, MeOD): δ 9.46 (dd, J_1 = 12.74 Hz, J_2 = 5.58 Hz, 2 H), 9.24 (d, J = 8.32 Hz, 2 H), 8.47 (s, 2 H), 8.40 (dd, J_1 = 8.30 Hz, J_2 = 5.54 Hz, 2 H), 3.21 (m, 2H), 2.48 (m, 2 H), 2.07 (t, J = 7.34 Hz, 2 H), 1.81 (m, 4 H), 1.43 (m, 2 H), 1.35 – 1.09 (m, 12 H), 1.04 – 0.89 (m, 7 H), 0.77 (pnt, J = 7.70 Hz, 2 H). ^{1}H-^{195}Pt HMQC (400/86 MHz, MeOD): δ 9.45, 8.40/479. ^{195}Pt NMR (86 MHz, MeOD): δ 480 ppm. HPLC t_R: 9.1 min. HRMS-ESI: Calc. [M-H]$^+$ = 704.3139, Found = 704.3135.

[Pt(PHEN)(SSDACH)(DoDecanoate)$_2$](NO_3)$_2$ (4)

Yield (118.8 mg, 51 %). Electronic spectrum λ_{max} nm (ε/mol^{-1}.dm^3.cm^{-1}, MeOH): 279 (29 000 ± 350). CD spectrum λ_{max} nm (mdeg.mol/L, MeOH:H_2O (1:4)): 279 (-5.7). ^{1}H NMR (400 MHz, MeOD): δ 9.59 (d, J = 5.52 Hz, 2 H), 9.24 (d, J = 8.24 Hz, 2 H), 8.47 (s, 2H), 8.40 (dd, J_1 = 8.28 Hz, J_2 = 5.60 Hz, 2 H), 3.22 (m, 2H), 2.52 (m, 2H), 2.12 (t, J = 7.28 Hz, 4 H), 1.83 (m, 4 H), 1.45 (m, 2 H), 1.35 – 1.07 (m, 24 H), 1.03 – 0.89 (m, 14 H), 0.73 (pnt, J = 7.48 Hz, 4 H). ^{1}H-^{195}Pt HMQC (400/86 MHz, MeOD): δ 9.59, 8.40/686. ^{195}Pt NMR (86 MHz, MeOD): δ 690 ppm. HPLC t_R: 12.1 min. HRMS-ESI: Calc. [M-H]$^+$ = 886.4810, Found = 886.4784.

[Pt(PHEN)(SSDACH)(OH)(TetraDecanoate)](NO_3)$_2$ (5)

Yield (98.4 mg, 50 %). Electronic spectrum λ_{max} nm (ε/mol^{-1}.dm^3.cm^{-1}, MeOH): 279 (27 500 ± 100). CD spectrum λ_{max} nm (mdeg.mol/L, MeOH:H_2O (1:4)): 279 (-3.3). ^{1}H NMR (400 MHz, MeOD): δ 9.45 (dd, J_1 = 12.76 Hz, J_2 = 5.58 Hz, 2 H), 9.24 (d, J = 8.28 Hz, 2 H), 8.47 (s, 2 H), 8.40 (dd, J_1 = 8.30 Hz, J_2 = 5.54 Hz, 2 H), 3.21 (m, 2H), 2.48 (m, 2 H), 2.07 (t, J = 7.32 Hz, 2 H), 1.81 (m, 4 H), 1.44 (m, 2 H), 1.35 – 1.11 (m, 16 H), 1.04 – 0.90 (m, 7 H), 0.77 (pnt, J = 7.34 Hz, 2 H). ^{1}H-^{195}Pt HMQC (400/86 MHz, MeOD): δ 9.45, 8.39/480. ^{195}Pt NMR (86 MHz, MeOD): δ 481 ppm. HPLC t_R: 10.3 min. HRMS-ESI: Calc. [M-H]$^+$ = 732.3452, Found = 732.3438.

[Pt(PHEN)(SSDACH)(TetraDecanoate)$_2$](NO_3)$_2$ (6)

Yield (116.5 mg, 47 %). Electronic spectrum λ_{max} nm (ε/mol^{-1}.dm^3.cm^{-1}, MeOH): 279 (29 000 ± 500). CD spectrum λ_{max} nm (mdeg.mol/L, MeOH:H_2O (1:4)): 279 (-5.7). ^{1}H NMR (400 MHz, MeOD): δ 9.59 (d, J = 5.52 Hz, 2 H), 9.24 (d, J = 8.28 Hz, 2 H), 8.47 (s, 2H), 8.40 (d, J_1 = 8.28 Hz, J_2 = 5.60 Hz, 2 H), 3.22 (m, 2H), 2.51 (m, 2H), 2.12 (t, J = 7.30 Hz, 4 H), 1.83 (m, 4 H), 1.45 (m, 2 H), 1.36 – 1.07 (m, 32 H), 1.04 – 0.90 (m, 14 H), 0.72 (pnt, J = 7.48 Hz, 4 H). ^{1}H-^{195}Pt HMQC (400/86 MHz, MeOD): δ 9.58, 8.40/688. ^{195}Pt NMR (86 MHz, MeOD): δ 692 ppm. HPLC t_R: 14.1 min. HRMS-ESI: Calc. [M-H]$^+$ = 942.5436, Found = 942.5400.

[Pt(PHEN)(SSDACH)(OH)(HexaDecanoate)](NO_3)$_2$ (7)

Yield (102.3 mg, 50 %). Electronic spectrum λ_{max} nm (ε/mol^{-1}.dm^3.cm^{-1}, MeOH): 279 (27 000 ± 420). CD spectrum λ_{max} nm (mdeg.mol/L, MeOH:H_2O (1:4)): 279 (-2.6). ^{1}H NMR (400 MHz, MeOD): δ 9.46 (dd, J_1 = 11.88 Hz, J_2 = 5.56 Hz, 2 H), 9.23 (d, J = 8.36 Hz, 2 H), 8.47 (s, 2 H), 8.40 (dd, J_1 = 8.30 Hz, J_2 = 5.54 Hz, 2 H), 3.21 (m, 2H), 2.48 (m, 2 H), 2.07 (t, J = 7.34 Hz, 2 H), 1.81 (m, 4 H), 1.44 (m, 2 H), 1.36 – 1.11 (m, 20 H), 1.04 – 0.90 (m, 7 H), 0.77 (pnt, J = 7.29 Hz, 2 H). ^{1}H-^{195}Pt HMQC (400/86 MHz, MeOD): δ 9.45, 8.40/480. ^{195}Pt NMR (86 MHz, MeOD): δ 481 ppm. HPLC t_R: 11.7 min. HRMS-ESI: Calc. [M-H]$^+$ = 760.3765, Found = 760.3747.

[Pt(PHEN)(SSDACH)(OH)(OctaDecanoate)](NO_3)$_2$ (8)

Yield (96.5 mg, 46 %). Electronic spectrum λ_{max} nm (ε/mol^{-1}.dm^3.cm^{-1}, MeOH): 279 (28 000 ± 70). CD spectrum λ_{max} nm (mdeg.mol/L, MeOH:H_2O (1:4)): 279 (-2.5). ^{1}H NMR (400 MHz, MeOD): δ 9.46 (dd, J_1 = 11.82 Hz, J_2 = 5.54 Hz, 2 H), 9.23 (d, J = 8.32 Hz, 2 H), 8.47 (s, 2 H), 8.40 (dd, J_1 = 8.28 Hz, J_2 = 5.52 Hz, 2 H), 3.21 (m, 2H), 2.48 (m, 2 H), 2.07 (t, J = 7.32 Hz, 2 H), 1.81 (m, 4 H), 1.44 (m, 2 H), 1.36 – 1.10 (m, 24 H), 1.04 – 0.90 (m, 7 H), 0.77 (pnt, J = 7.30 Hz, 2 H). ^{1}H-^{195}Pt HMQC (400/86 MHz, MeOD): δ 9.45, 8.40/478. ^{195}Pt NMR (86 MHz, MeOD): δ 479 ppm. HPLC t_R: 13.1 min. HRMS-ESI: Calc. [M-H]$^+$ = 788.4078, Found = 788.4059.

[Pt(56Me$_2$PHEN)(SSDACH)(OH)(Decanoate)](NO$_3$)$_2$ (9)

Yield (377.8 mg, 68 %). Electronic spectrum λ_{max} nm (ε/mol^{-1}.dm^3.cm^{-1}, MeOH): 289 (25 500 ± 80). CD spectrum λ_{max} nm (mdeg.mol/L, MeOH:H$_2$O (1:4)): 289 (-2.7). SRCD spectrum λ_{max} nm (mdeg.mol/L, MeOH:H$_2$O (1:4)): 209 (-3.4), 290 (-0.8). ^{1}H NMR (400 MHz, MeOD): δ 9.38 (m, 4 H), 8.37 (d, J_1 = 8.56 Hz, J_2 = 5.48 Hz, 2 H), 3.20 (m, 2H), 2.98 (s, 6 H), 2.47 (m, 2H), 2.06 (t, J = 7.26 Hz, 2 H), 1.80 (m, 4 H), 1.43 (m, 2 H), 1.30 – 1.09 (m, 8 H), 1.00 – 0.87 (m, 7 H), 0.71 (pnt, J = 7.36 Hz, 2 H). ^{1}H-^{195}Pt HMQC (400/86 MHz, MeOD): δ 9.38, 8.36/468. ^{195}Pt NMR (86 MHz, MeOD): δ 468 ppm. HPLC t_R: 8.2 min. HRMS-ESI: Calc. [M-H]$^+$ = 704.3139, Found = 704.3135.

[Pt(56Me$_2$PHEN)(SSDACH)(Decanoate)$_2$](NO$_3$)$_2$ (10)

Yield (121.3 mg, 56 %). Electronic spectrum λ_{max} nm (ε/mol^{-1}.dm^3.cm^{-1}, MeOH): 289 (27 000 ± 130). CD spectrum λ_{max} nm (mdeg.mol/L, MeOH:H$_2$O (1:4)): 239 (-5.8), 289 (-5.8). SRCD spectrum λ_{max} nm (mdeg.mol/L, MeOH:H$_2$O (1:4)): 205 (-2.5), 241 (-1.0), 290 (-2.7). ^{1}H NMR (400 MHz, MeOD): δ 9.53 (d, J = 5.52 Hz, 2 H), 9.38 (d, J = 8.36 Hz, 2 H), 8.37 (d, J_1 = 8.58 Hz, J_2 = 5.54 Hz, 2 H), 3.20 (m, 2H), 2.97 (s, 6 H), 2.51 (m, 2H), 2.11 (t, J = 7.26 Hz, 4 H), 1.82 (m, 4 H), 1.44 (m, 2 H), 1.30 – 1.06 (m, 16 H), 1.01 – 0.86 (m, 14 H), 0.68 (pnt, J = 7.47 Hz, 4 H). ^{1}H-^{195}Pt HMQC (400/86 MHz, MeOD): δ 9.53, 8.37/674. ^{195}Pt NMR (86 MHz, MeOD): δ 678 ppm. HPLC t_R: 10.7 min. HRMS-ESI: Calc. [M-H]$^+$ = 858.4497, Found = 858.4490.

[Pt(56Me$_2$PHEN)(SSDACH)(OH)(DoDecanoate)](NO$_3$)$_2$ (11)

Yield (110.5 mg, 58 %). Electronic spectrum λ_{max} nm (ε/mol^{-1}.dm^3.cm^{-1}, MeOH): 289 (25 500 ± 250). CD spectrum λ_{max} nm (mdeg.mol/L, MeOH:H$_2$O (1:4)): 289 (-3.7). ^{1}H NMR (400 MHz, MeOD): δ 9.38 (m, 4 H), 8.37 (d, J_1 = 8.56 Hz, J_2 = 5.48 Hz, 2 H), 3.19 (m, 2H), 2.98 (s, 6 H), 2.47 (m, 2H), 2.06 (t, J = 7.26 Hz, 2 H), 1.80 (m, 4 H), 1.44 (m, 2 H), 1.34 – 1.08 (m, 12 H), 1.00 – 0.86 (m, 7 H), 0.71 (pnt, J = 7.42 Hz, 2 H). ^{1}H-^{195}Pt HMQC (400/86 MHz, MeOD): δ 9.37, 8.36/465. ^{195}Pt NMR (86 MHz, MeOD): δ 466 ppm. HPLC t_R: 9.4 min. HRMS-ESI: Calc. [M-H]$^+$ = 732.3452, Found = 732.3428.

[Pt(56Me$_2$PHEN)(SSDACH)(DoDecanoate)$_2$](NO$_3$)$_2$ (12)

Yield (96.1 mg, 42 %). Electronic spectrum λ_{max} nm (ε/mol^{-1}.dm^3.cm^{-1}, MeOH): 289 (27 500 ± 180). CD spectrum λ_{max} nm (mdeg.mol/L, MeOH:H$_2$O (1:4)): 239 (-3.2), 289 (-3.2). ^{1}H NMR (400 MHz, MeOD): δ 9.54 (d, J = 5.48 Hz, 2 H), 9.37 (d, J = 8.52 Hz, 2 H), 8.37 (d, J_1 = 8.58 Hz, J_2 = 5.54 Hz, 2 H), 3.21 (m, 2H), 2.97 (s, 6 H), 2.51 (m, 2H), 2.11 (t, J = 7.26 Hz, 4 H), 1.82 (m, 4 H), 1.44 (m, 2 H), 1.34 – 1.05 (m, 24 H), 1.01 – 0.86 (m, 14 H), 0.69 (pnt, J = 7.46 Hz, 4 H). ^{1}H-^{195}Pt HMQC (400/86 MHz, MeOD): δ 9.52, 8.36/673. ^{195}Pt NMR (86 MHz, MeOD): δ 678 ppm. HPLC t_R: 12.6 min. HRMS-ESI: Calc. [M-H]$^+$ = 914.5123, Found = 914.5088.

[Pt(56Me$_2$PHEN)(SSDACH)(OH)(TetraDecanoate)](NO$_3$)$_2$ (13)

Yield (78.9 mg, 40 %). Electronic spectrum λ_{max} nm (ε/mol^{-1}.dm^3.cm^{-1}, MeOH): 289 (25 500 ± 280). CD spectrum λ_{max} nm (mdeg.mol/L, MeOH:H$_2$O (1:4)): 289 (-3.0). ^{1}H NMR (400 MHz, MeOD): δ 9.38 (m, 4 H), 8.37 (d, J_1 = 8.54 Hz, J_2 = 5.54 Hz, 2 H), 3.19 (m, 2H), 2.98 (s, 6 H), 2.47 (m, 2H), 2.06 (t, J = 7.24 Hz, 2 H), 1.80 (m, 4 H), 1.44 (m, 2 H), 1.36 – 1.08 (m, 16 H), 1.00 – 0.86 (m, 7 H), 0.71 (pnt, J = 7.43 Hz, 2 H). ^{1}H-^{195}Pt HMQC (400/86 MHz, MeOD): δ 9.38, 8.37/467. ^{195}Pt NMR (86 MHz, MeOD): δ 469 ppm. HPLC t_R: 10.7 min. HRMS-ESI: Calc. [M-H]$^+$ = 760.3765, Found = 760.3740.

[Pt(56Me$_2$PHEN)(SSDACH)(TetraDecanoate)$_2$](NO$_3$)$_2$ (14)

Yield (97.4 mg, 40 %). Electronic spectrum λ_{max} nm (ε/mol^{-1}.dm^3.cm^{-1}, MeOH): 289 (27 500 ± 190). CD spectrum λ_{max} nm (mdeg.mol/L, MeOH:H_2O (1:4)): 239 (-5.7), 289 (-5.5). ^{1}H NMR (400 MHz, MeOD): δ 9.53 (d, J = 5.24 Hz, 2 H), 9.37 (d, J = 8.48 Hz, 2 H), 8.37 (d, J_1 = 8.56 Hz, J_2 = 5.56 Hz, 2 H), 3.20 (m, 2H), 2.97 (s, 6 H), 2.51 (m, 2H), 2.11 (t, J = 7.24 Hz, 4 H), 1.83 (m, 4 H), 1.45 (m, 2 H), 1.35 – 1.06 (m, 32 H), 1.01 – 0.86 (m, 14 H), 0.68 (pnt, J = 7.50 Hz, 4 H). ^{1}H-^{195}Pt HMQC (400/86 MHz, MeOD): δ 9.54, 8.40/672. ^{195}Pt NMR (86 MHz, MeOD): δ 677 ppm. HPLC t_R: 14.7 min. HRMS-ESI: Calc. [M-H]$^+$ = 970.5749, Found = 970.5714.

[Pt(56Me$_2$PHEN)(SSDACH)(OH)(HexaDecanoate)](NO$_3$)$_2$ (15)

Yield (96.5 mg, 48 %). Electronic spectrum λ_{max} nm (ε/mol^{-1}.dm^3.cm^{-1}, MeOH): 289 (26 000 ± 120). CD spectrum λ_{max} nm (mdeg.mol/L, MeOH:H_2O (1:4)): 289 (-3.2). ^{1}H NMR (400 MHz, MeOD): δ 9.38 (m, 4 H), 8.36 (d, J_1 = 8.60 Hz, J_2 = 5.52 Hz, 2 H), 3.20 (m, 2H), 2.98 (s, 6 H), 2.47 (m, 2H), 2.06 (t, J = 7.26 Hz, 2 H), 1.80 (m, 4 H), 1.43 (m, 2 H), 1.36 – 1.08 (m, 20 H), 1.00 – 0.86 (m, 7 H), 0.71 (pnt, J = 7.46 Hz, 2 H). ^{1}H-^{195}Pt HMQC (400/86 MHz, MeOD): δ 9.38, 8.36/467. ^{195}Pt NMR (86 MHz, MeOD): δ 467 ppm. HPLC t_R: 12.1 min. HRMS-ESI: Calc. [M-H]$^+$ = 788.4078, Found = 788.4044.

[Pt(56Me$_2$PHEN)(SSDACH)(OH)(OctaDecanoate)](NO$_3$)$_2$ (16)

Yield (91.5 mg, 44 %). Electronic spectrum λ_{max} nm (ε/mol^{-1}.dm^3.cm^{-1}, MeOH): 289 (25 500 ± 200). CD spectrum λ_{max} nm (mdeg.mol/L, MeOH:H_2O (1:4)): 289 (-3.7). ^{1}H NMR (400 MHz, MeOD): δ 9.38 (m, 4 H), 8.37 (d, J_1 = 8.56 Hz, J_2 = 5.52 Hz, 2 H), 3.19 (m, 2H), 2.98 (s, 6 H), 2.47 (m, 2H), 2.06 (t, J = 7.26 Hz, 2 H), 1.80 (m, 4 H), 1.43 (m, 2 H), 1.36 – 1.08 (m, 24 H), 1.00 – 0.86 (m, 7 H), 0.71 (pnt, J = 7.31 Hz, 2 H). ^{1}H-^{195}Pt HMQC (400/86 MHz, MeOD): δ 9.38, 8.37/467. ^{195}Pt NMR (86 MHz, MeOD): δ 467 ppm. HPLC t_R: 13.7 min. HRMS-ESI: Calc. [M-H]$^+$ = 816.4391, Found = 816.4379.

B. NMR Spectra

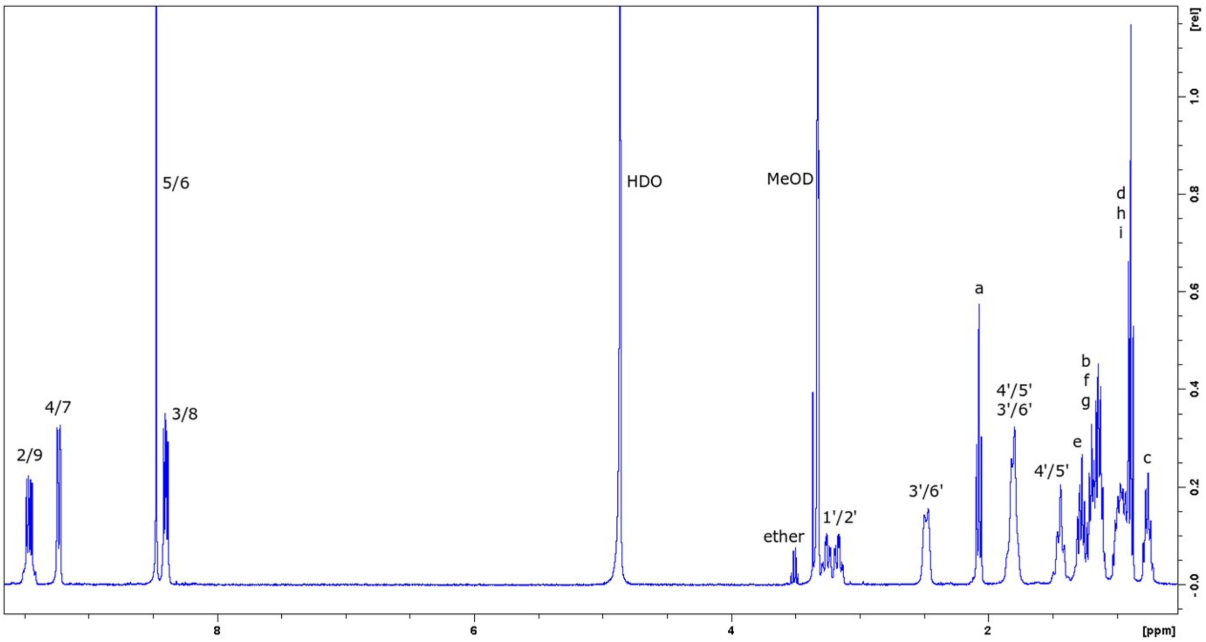

Figure B.1 [1]H NMR of **[Pt(PHEN)(SSDACH)(OH)(Decanoate)]$(NO_3)_2$ (1)** in MeOD at 298 K. Inset below: Structure and proton numbering scheme of **1**.

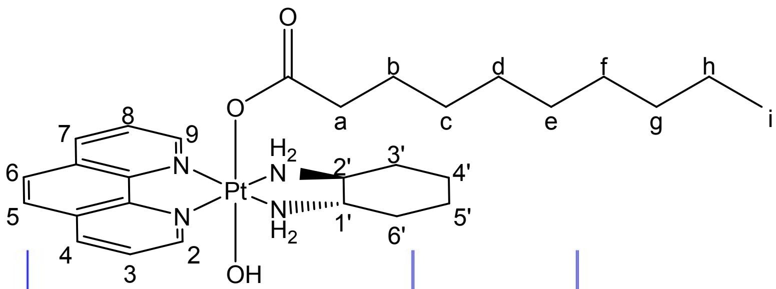

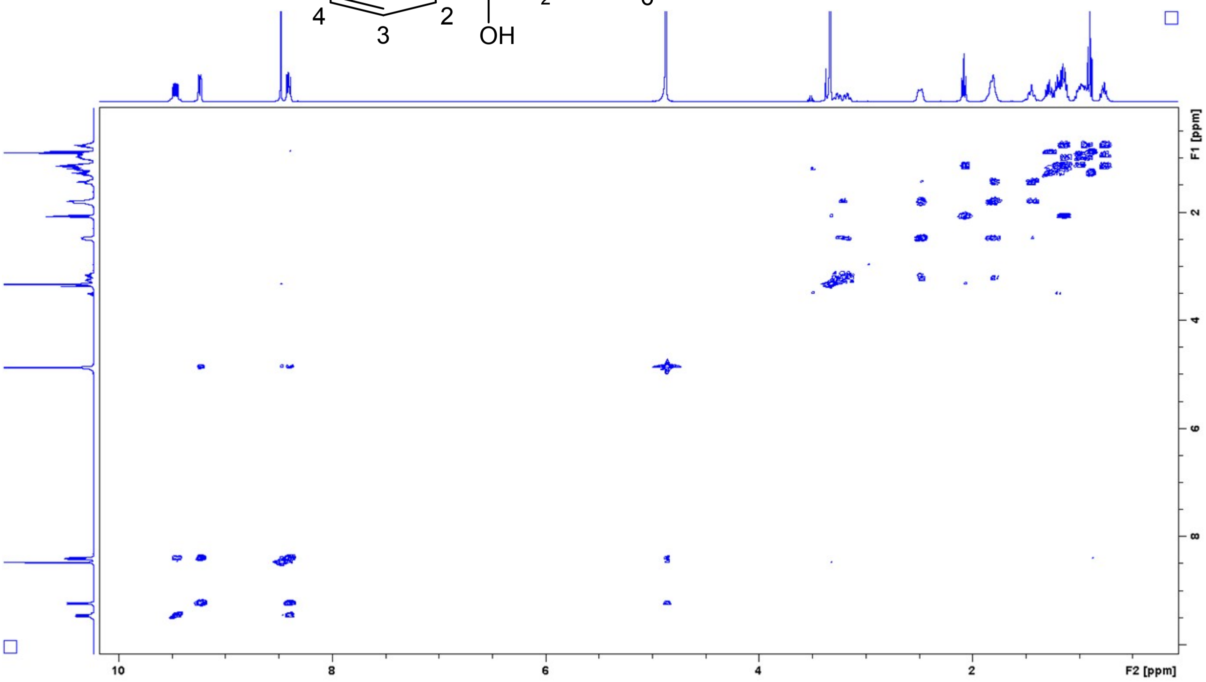

Figure B.2 COSY NMR of **1** in MeOD at 298 K.

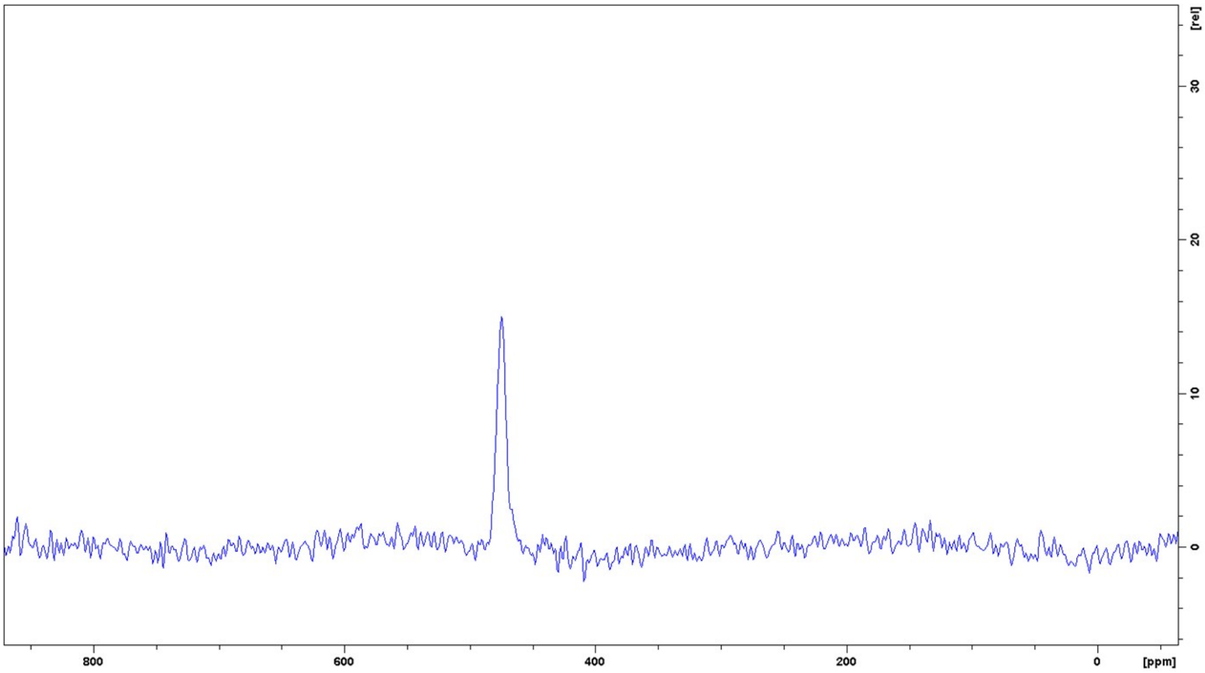

Figure B.3 ^{195}Pt NMR of **1** in MeOD at 298 K, showing a peak at 481 ppm.

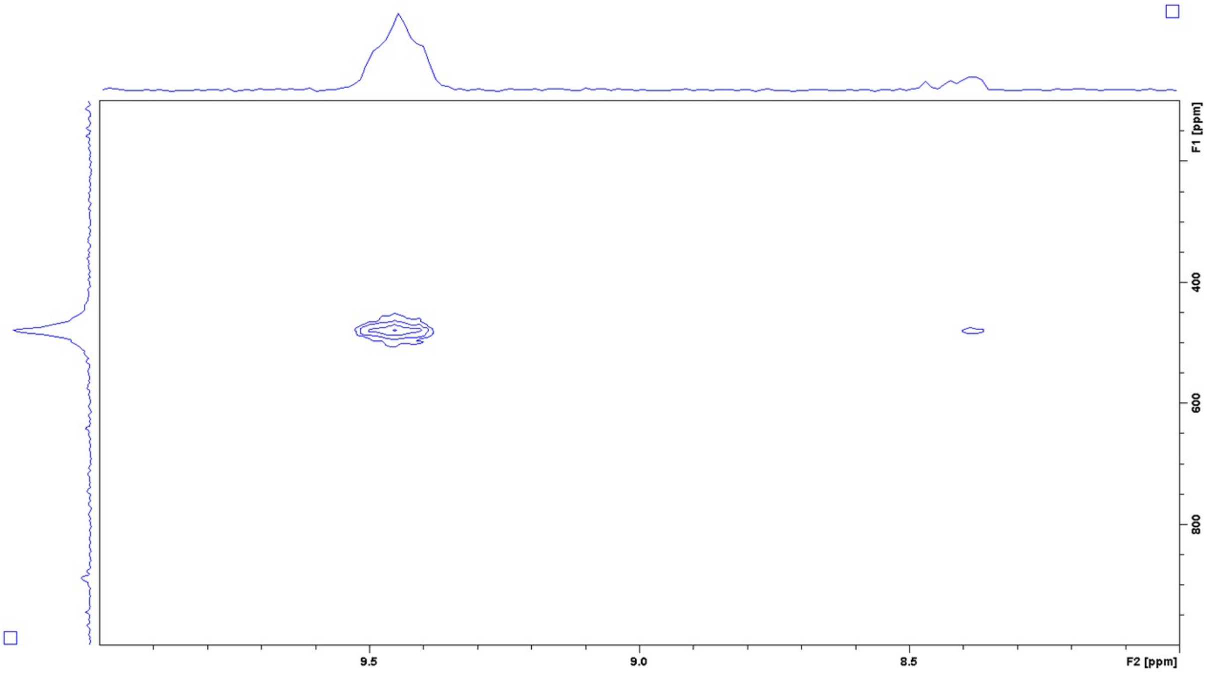

Figure B.4 ^{1}H-^{195}Pt HMQC NMR of **1** showing proton and platinum coupling resonances, in MeOD at 298 K.

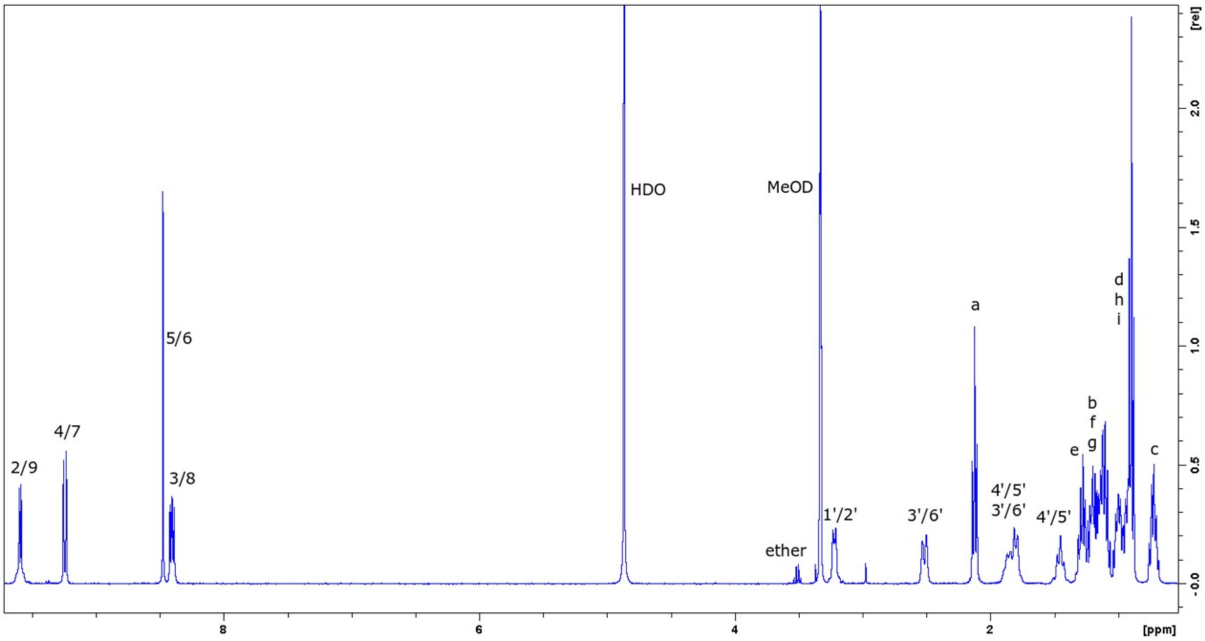

Figure B.5 ^{1}H NMR of **[Pt(PHEN)(SSDACH)(Decanoate)$_2$](NO$_3$)$_2$** (**2**) in MeOD at 298 K. Inset below: Structure and proton numbering scheme of **2**.

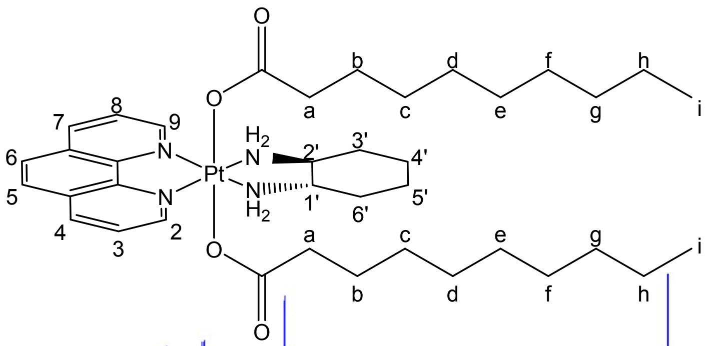

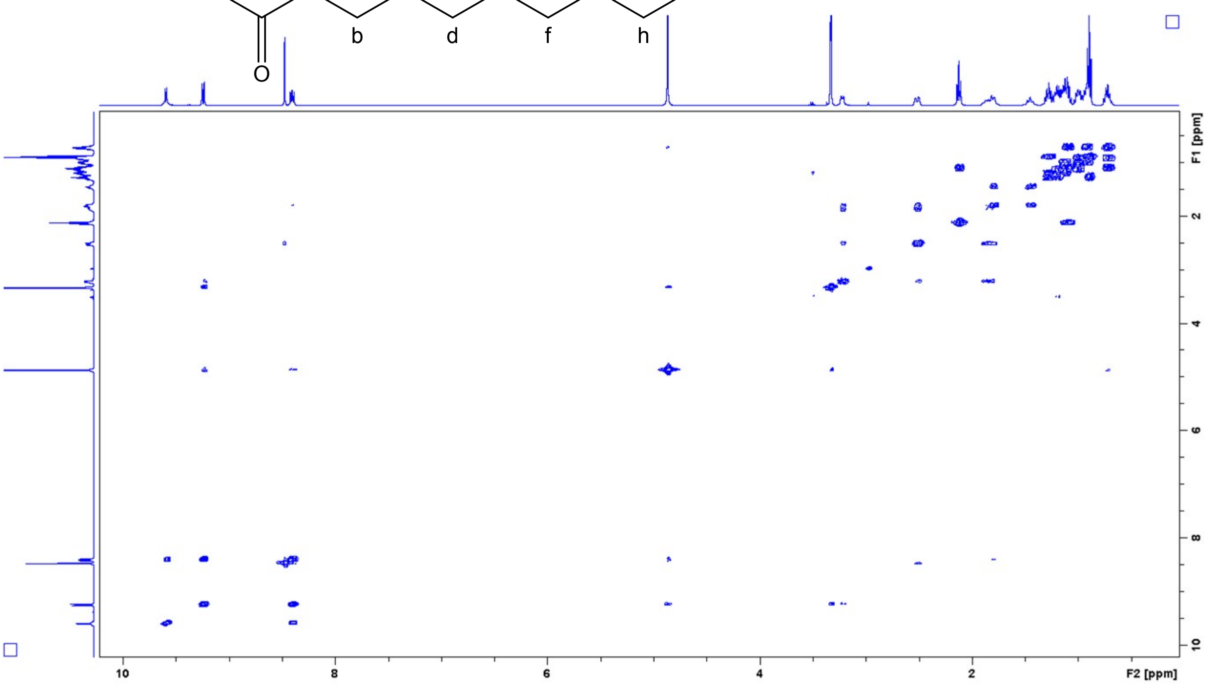

Figure B.6 COSY NMR of **2** in MeOD at 298 K.

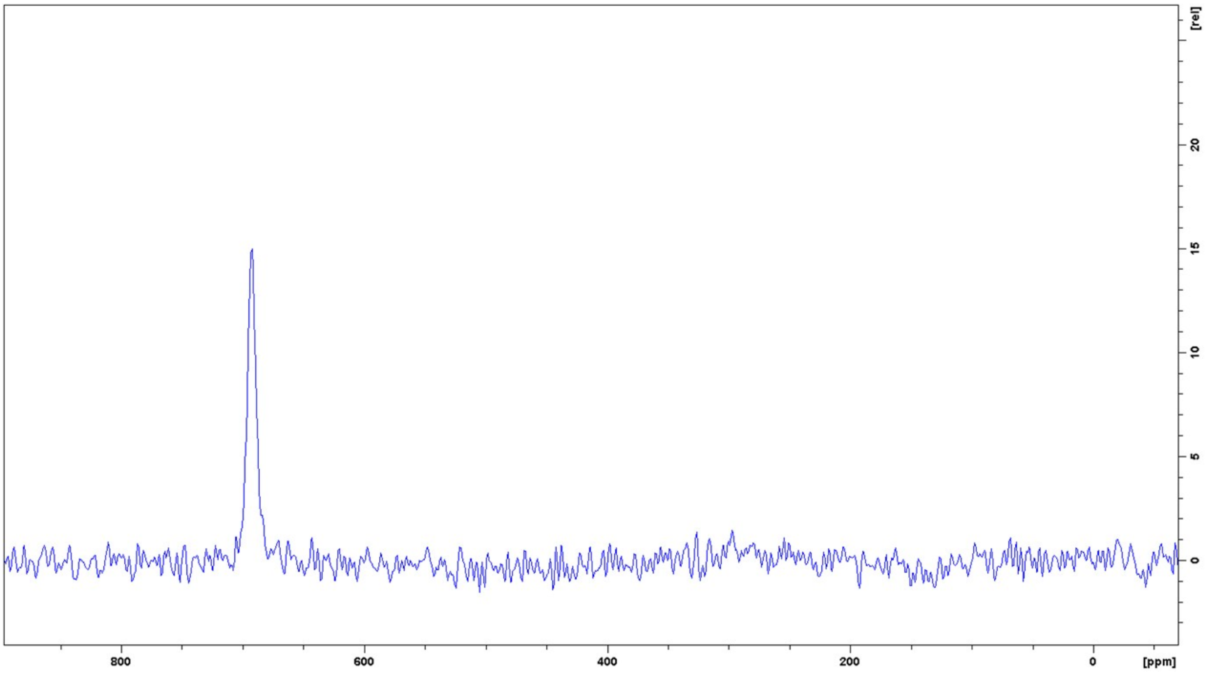

Figure B.7 ^{195}Pt NMR of **PHENSS(Dec)$_2$** in MeOD at 298 K, showing a peak at 692 ppm.

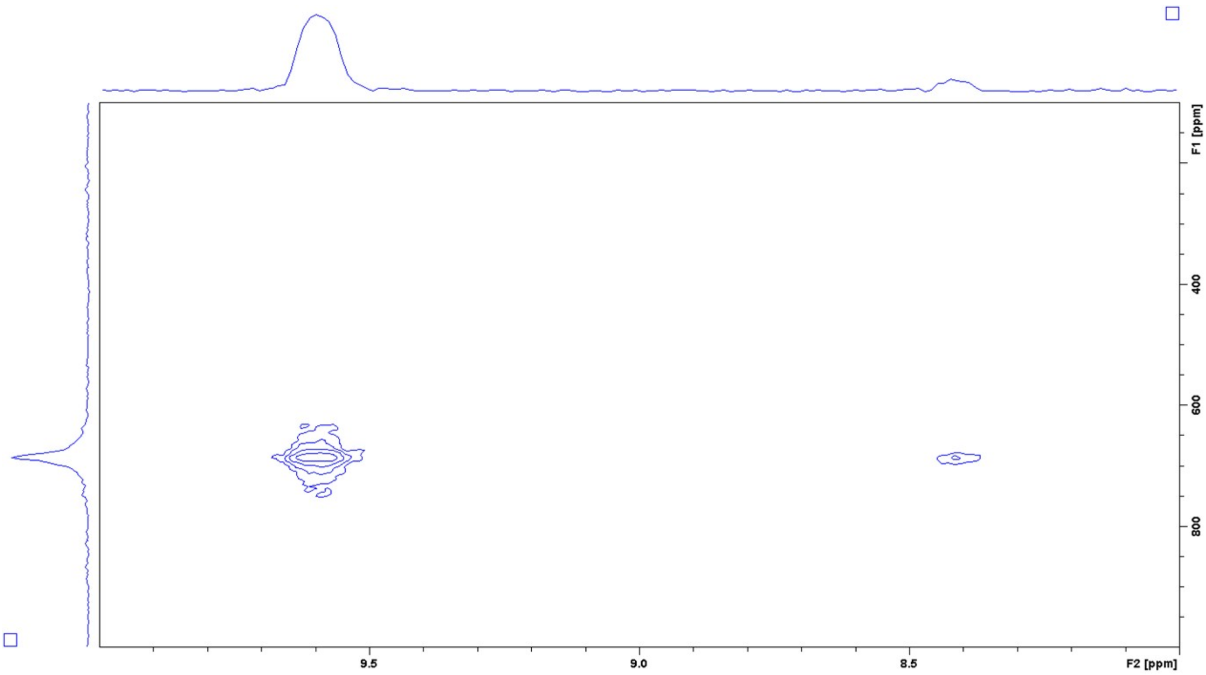

Figure B.8 ^{1}H-^{195}Pt HMQC NMR of **2** showing proton and platinum coupling resonances, in MeOD at 298 K.

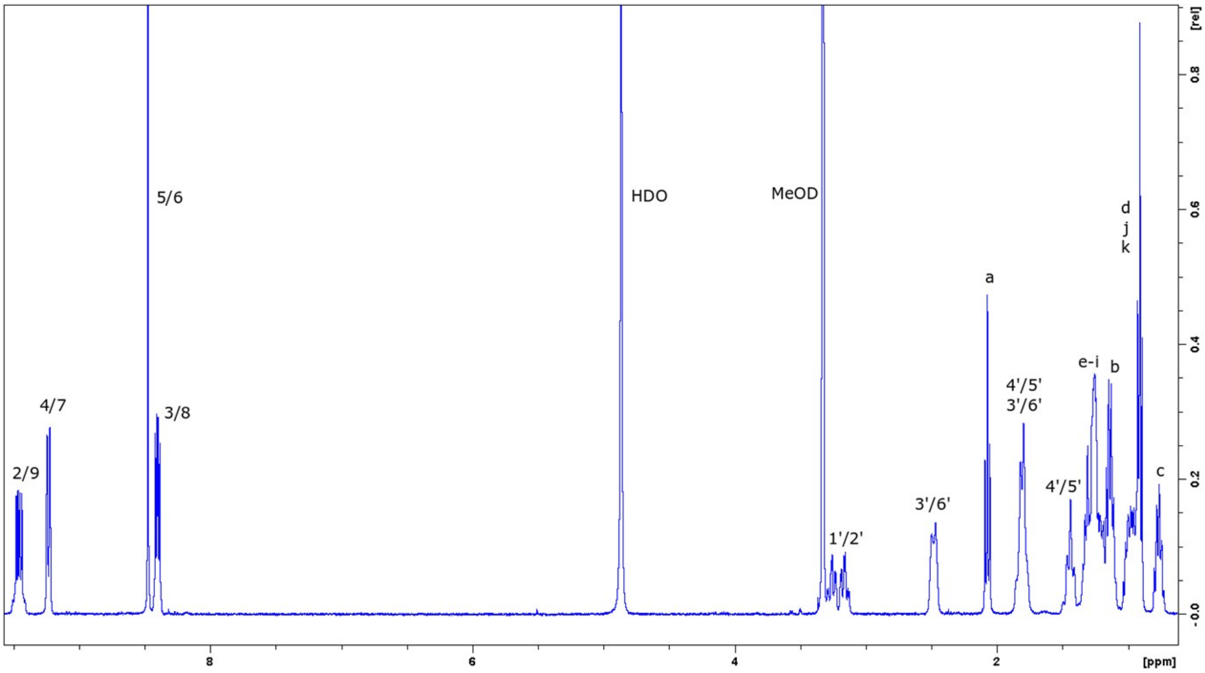

Figure B.9 ^{1}H NMR of **[Pt(PHEN)(SSDACH)(OH)(Dodecanoate)]$(NO_3)_2$** (**3**) in MeOD at 298 K. Inset below: Structure and proton numbering scheme of **3**.

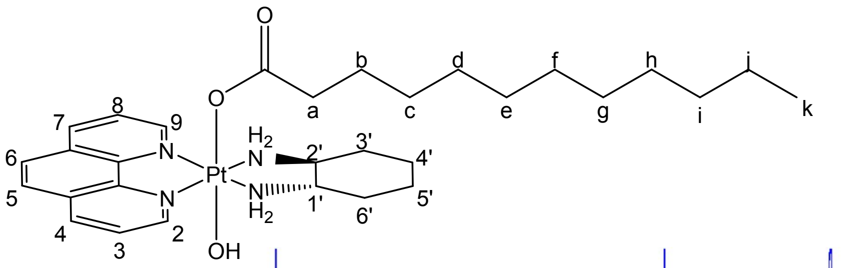

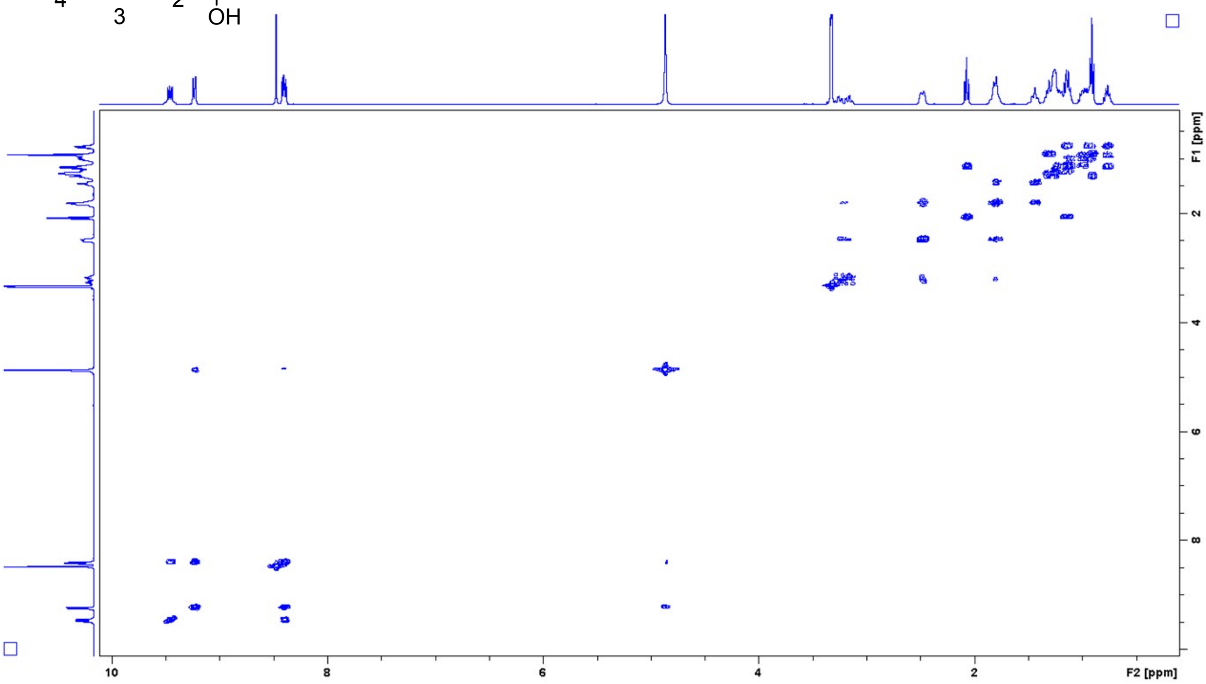

Figure B.10 COSY NMR of **3** in MeOD at 298 K.

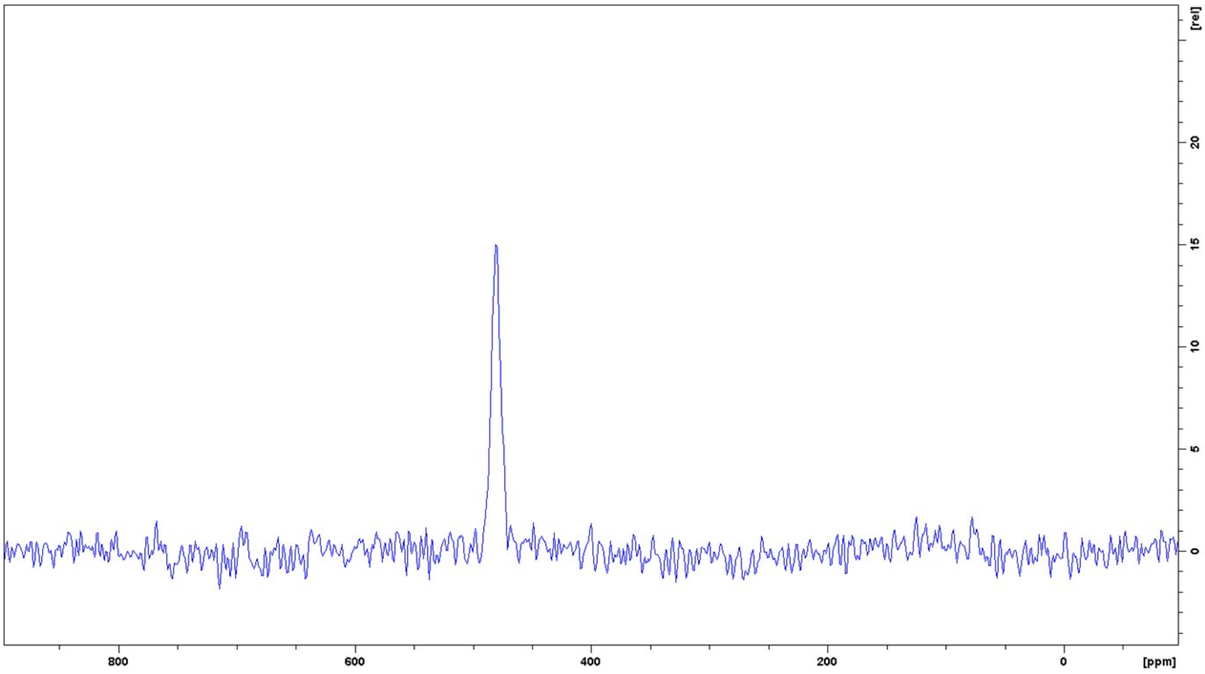

Figure B.11 ^{195}Pt NMR of **3** in MeOD at 298 K, showing a peak at 480 ppm.

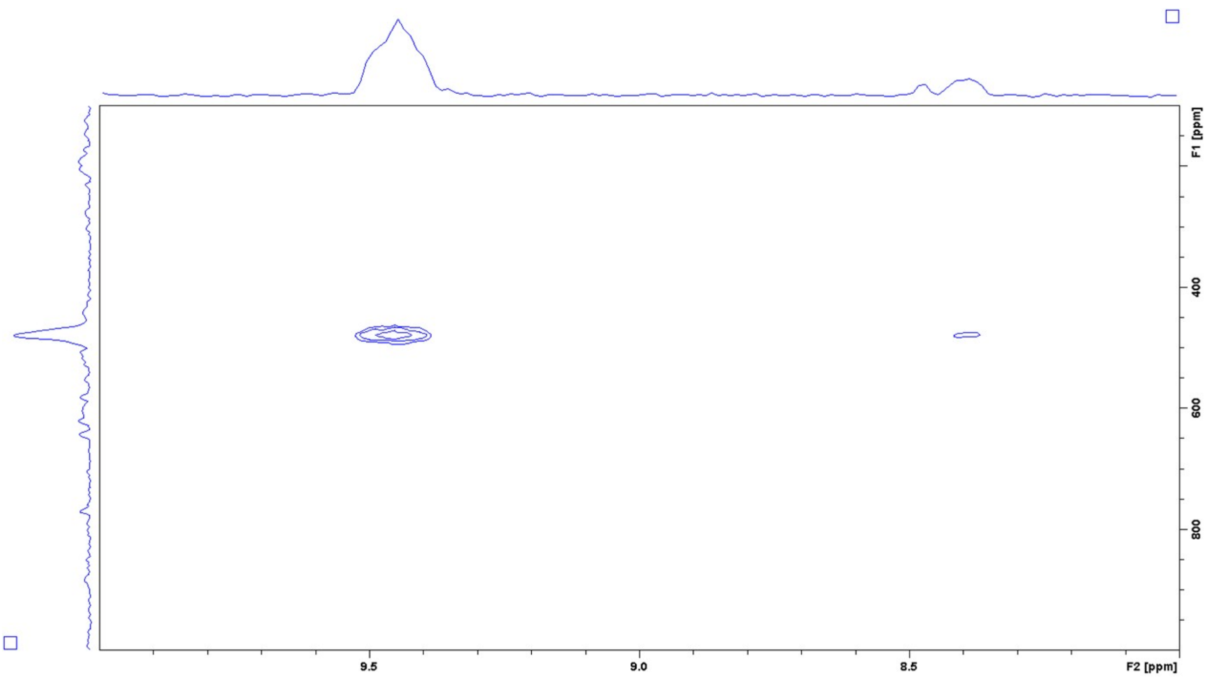

Figure B.12 ^{1}H-^{195}Pt HMQC NMR of **3** showing proton and platinum coupling resonances, in MeOD at 298 K.

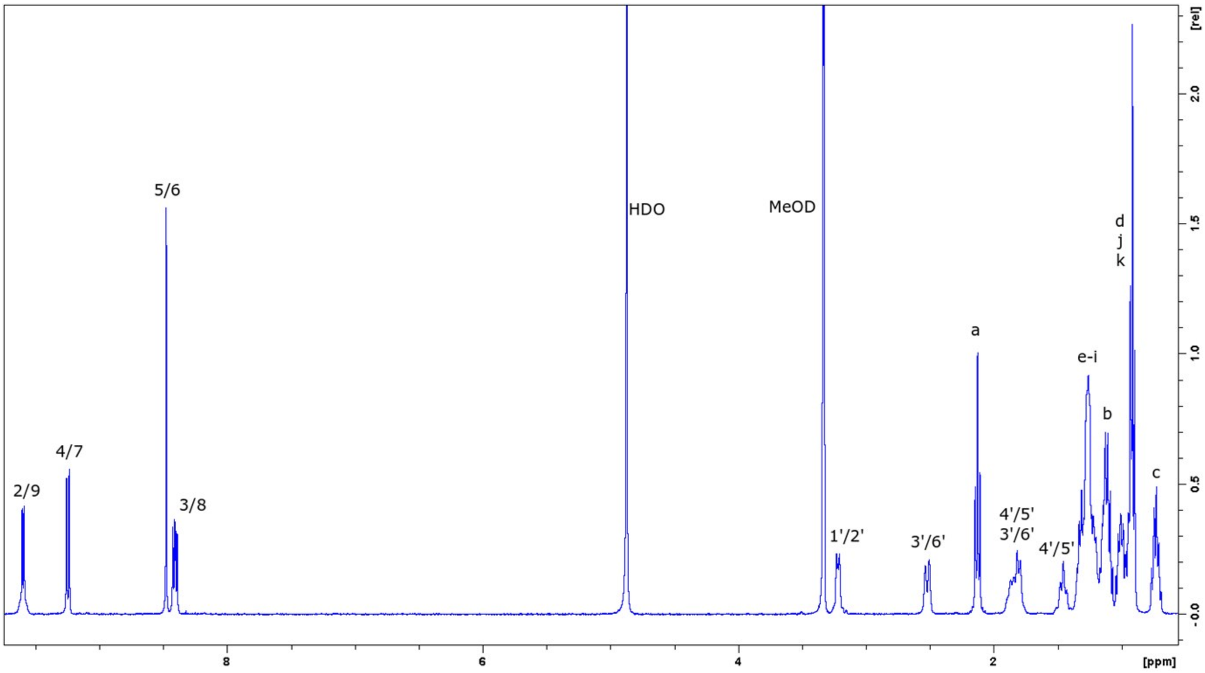

Figure B.13 ^{1}H NMR of **[Pt(PHEN)(SSDACH)(Dodecanoate)$_2$](NO$_3$)$_2$ (4)** in MeOD at 298 K. Inset below: Structure and proton numbering scheme of **4**.

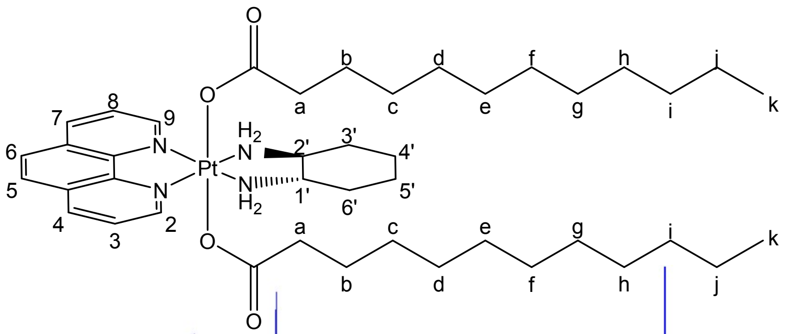

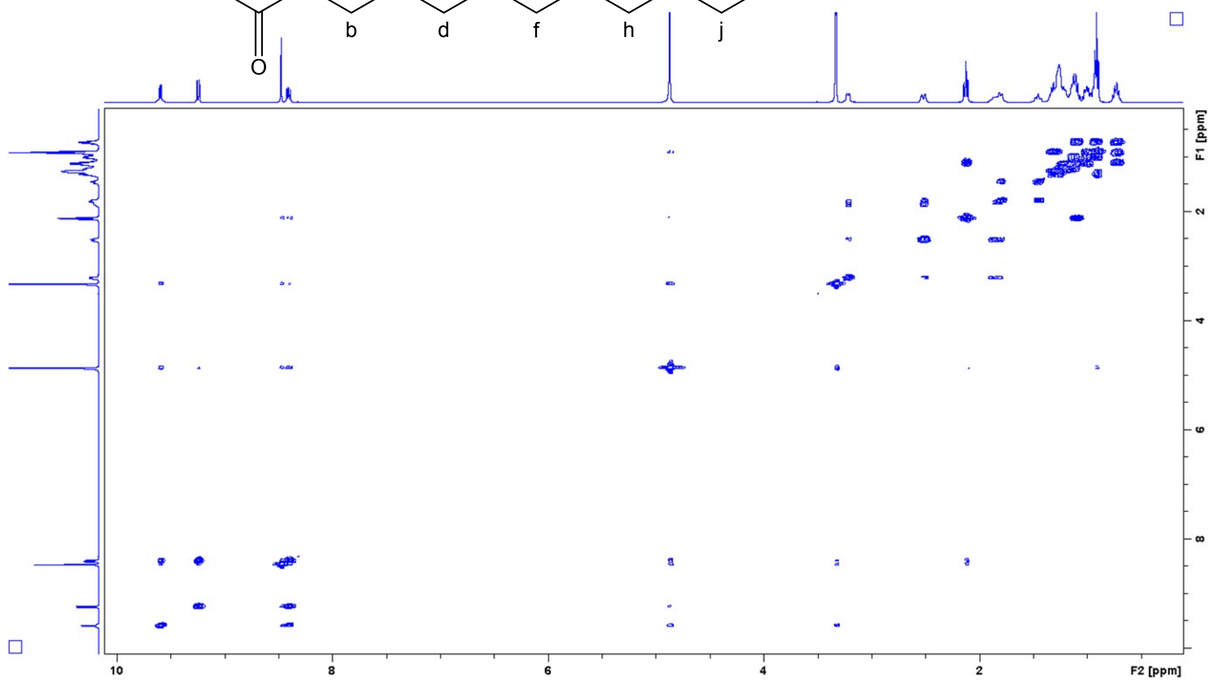

Figure B.14 COSY NMR of **4** in MeOD at 298 K.

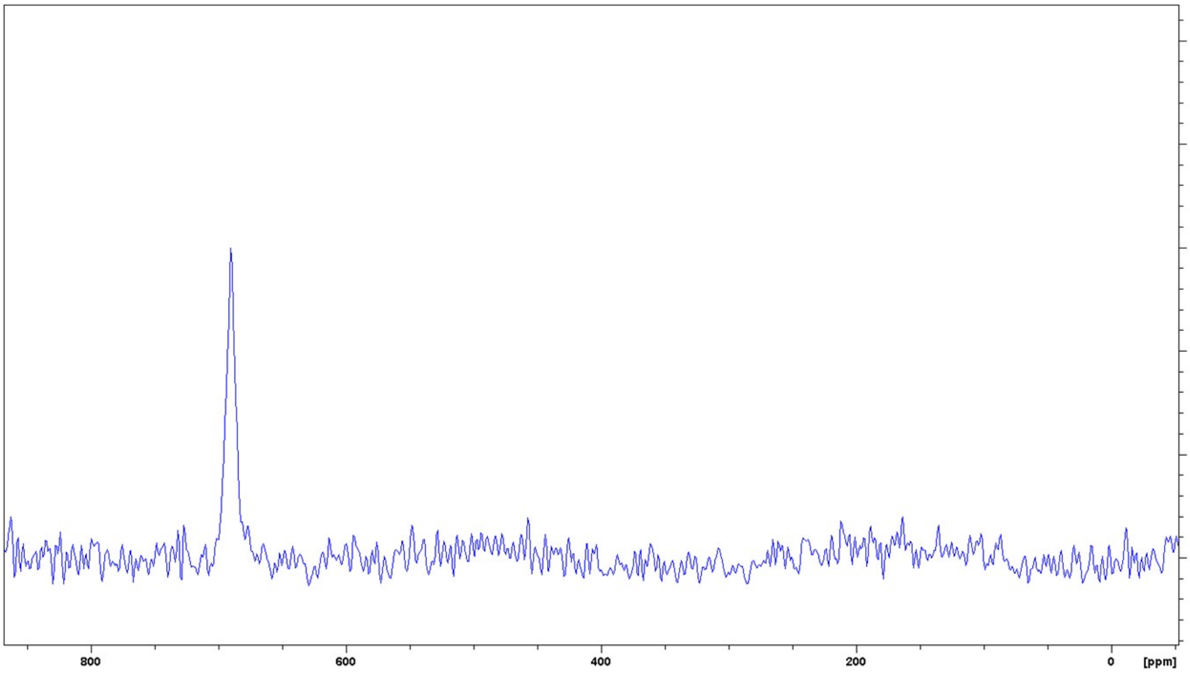

Figure B.15 ^{195}Pt NMR of **4** in MeOD at 298 K, showing a peak at 690 ppm.

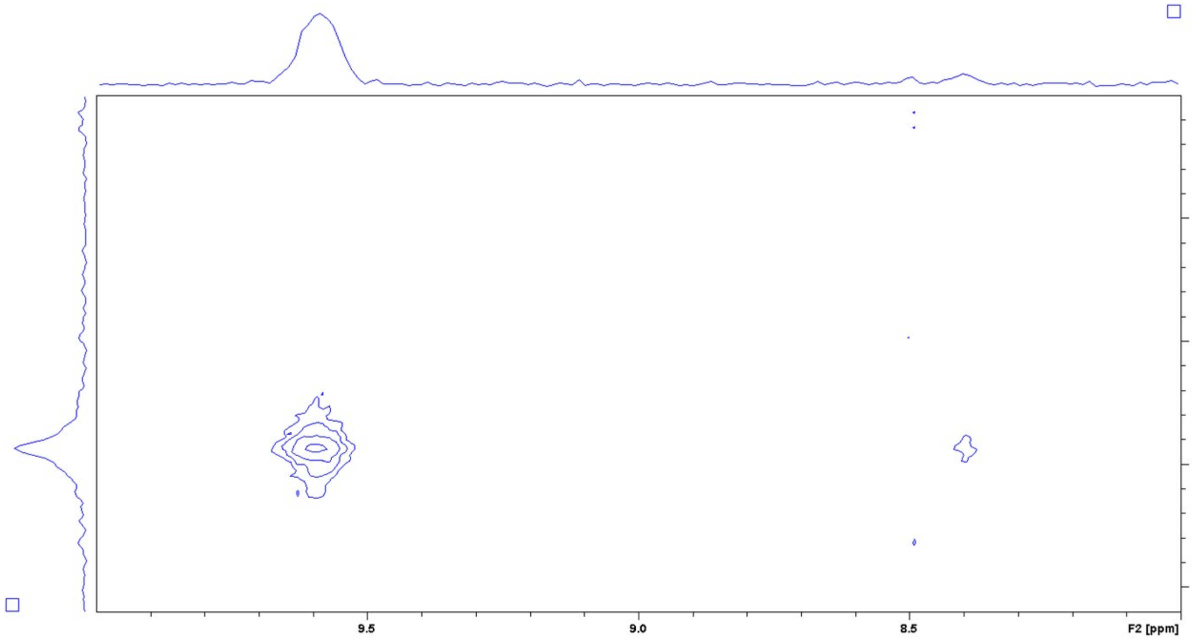

Figure B.16 ^{1}H-^{195}Pt HMQC NMR of **4** showing proton and platinum coupling resonances, in MeOD at 298 K.

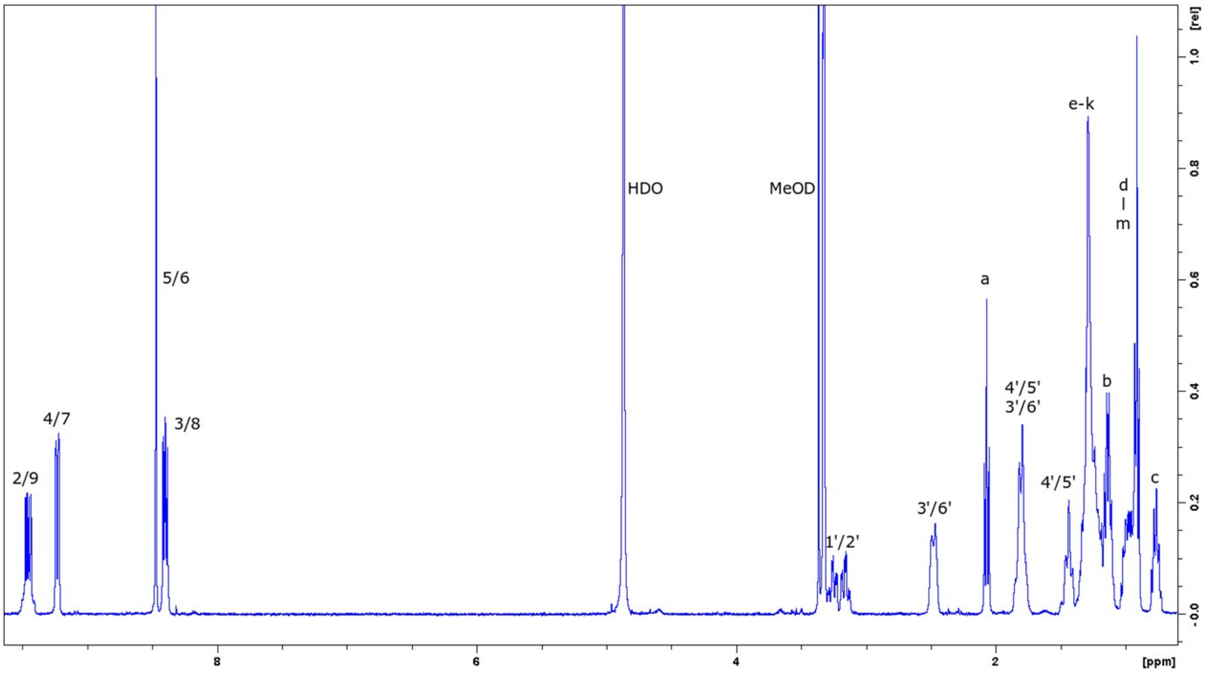

Figure B.17 ^{1}H NMR of **[Pt(PHEN)(SSDACH)(OH)(Tetradecanoate)]$(NO_3)_2$** (**5**) in MeOD at 298 K. Inset below: Structure and proton numbering scheme of **5**.

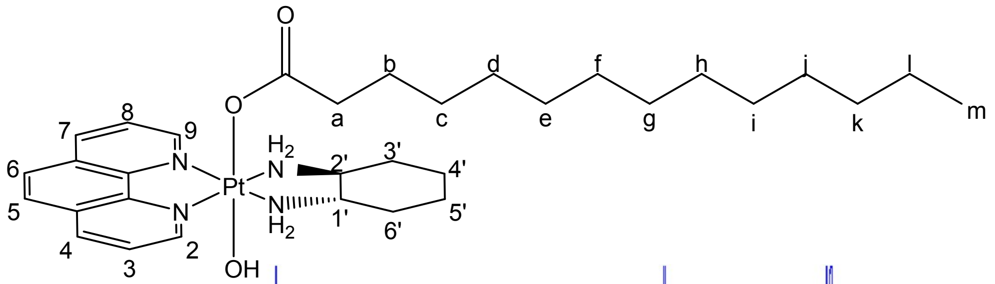

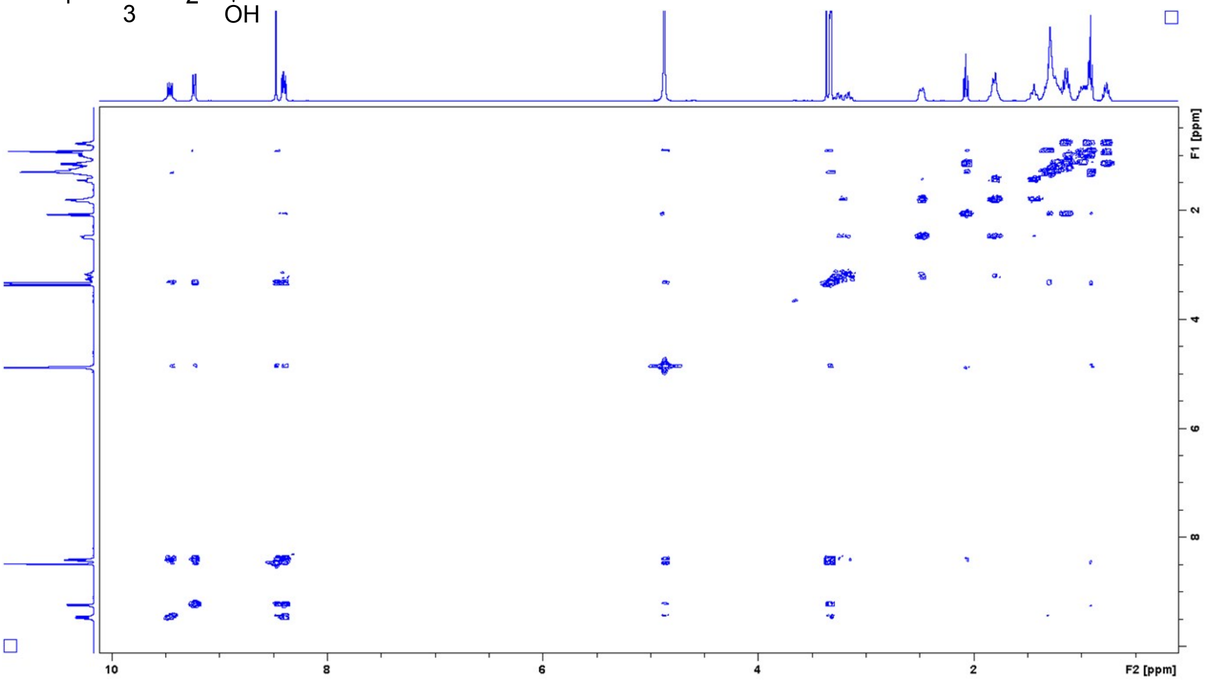

Figure B.18 COSY NMR of **5** in MeOD at 298 K.

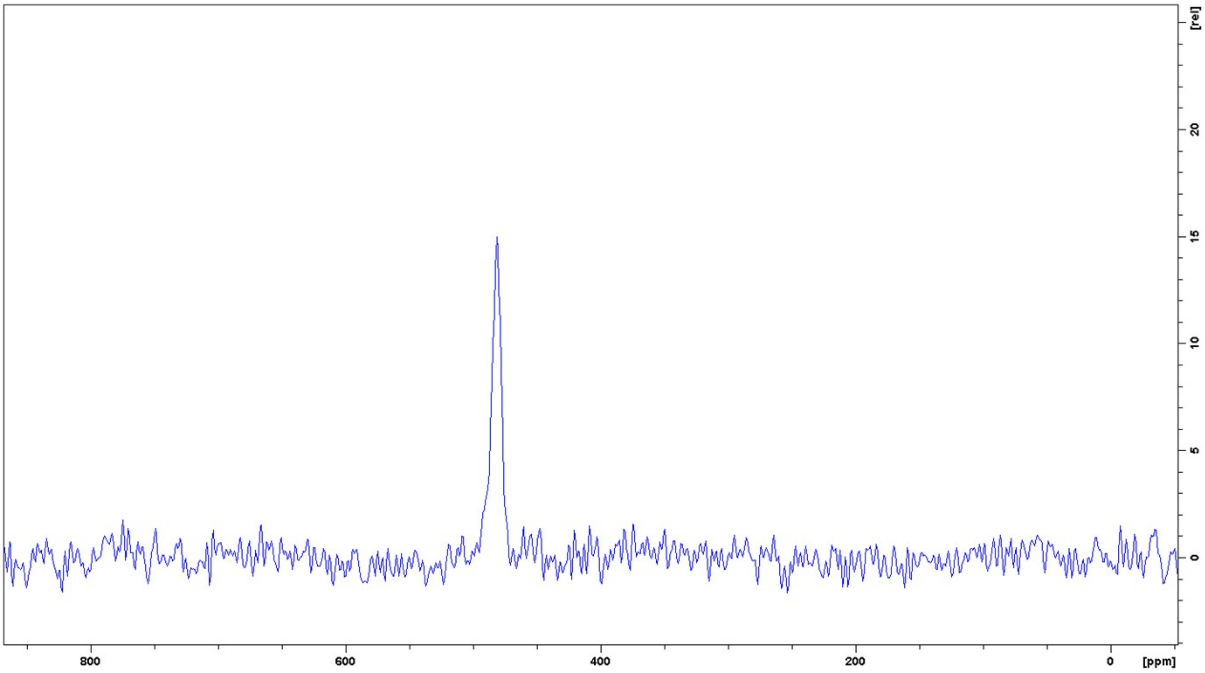

Figure B.19 ^{195}Pt NMR of **5** in MeOD at 298 K, showing a peak at 481 ppm.

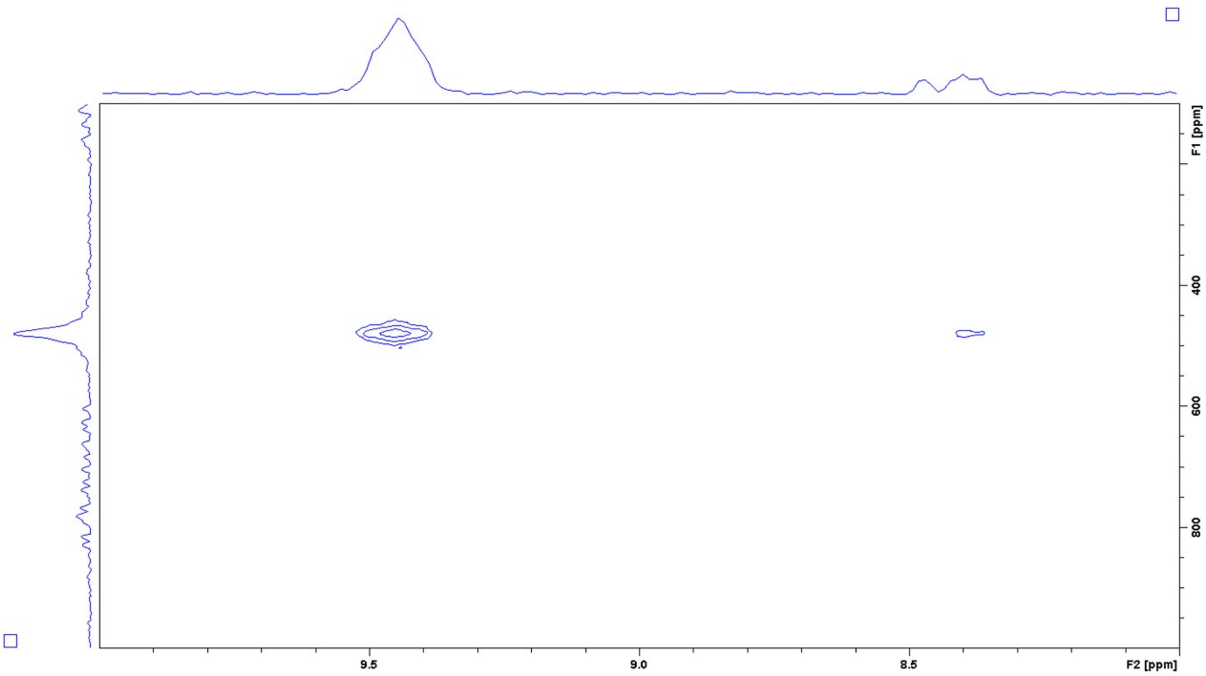

Figure B.20 ^{1}H-^{195}Pt HMQC NMR of **5** showing proton and platinum coupling resonances, in MeOD at 298 K.

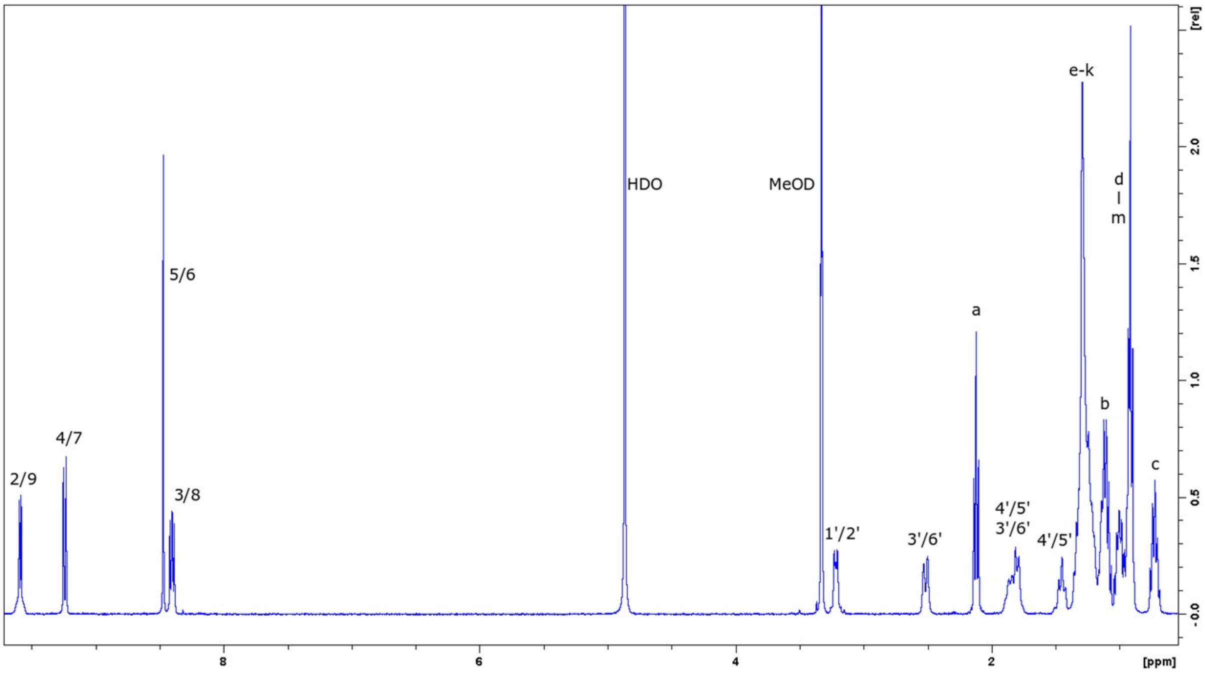

Figure B.21 ^{1}H NMR of **[Pt(PHEN)(SSDACH)(Tetradecanoate)$_2$](NO$_3$)$_2$** (**6**) in MeOD at 298 K. Inset: Structure and proton numbering scheme of **6**.

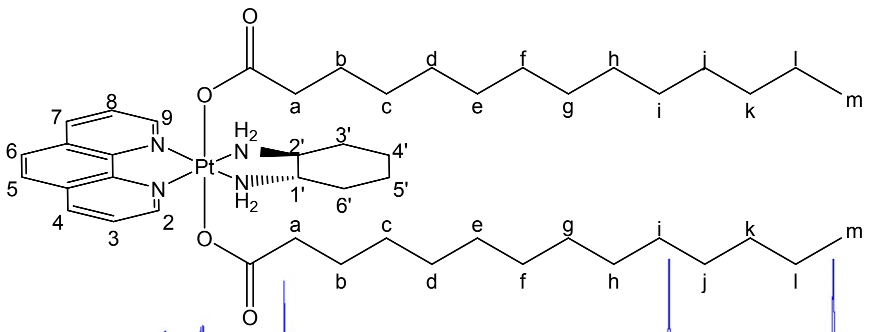

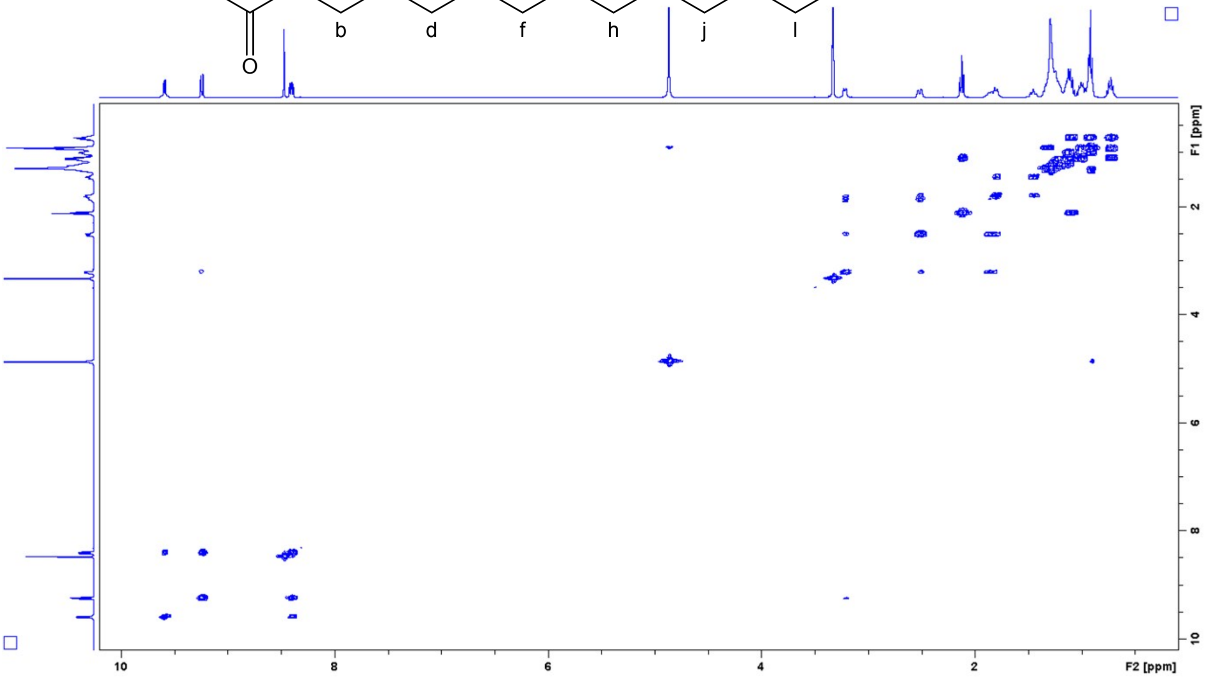

Figure B.22 COSY NMR of **6** in MeOD at 298 K.

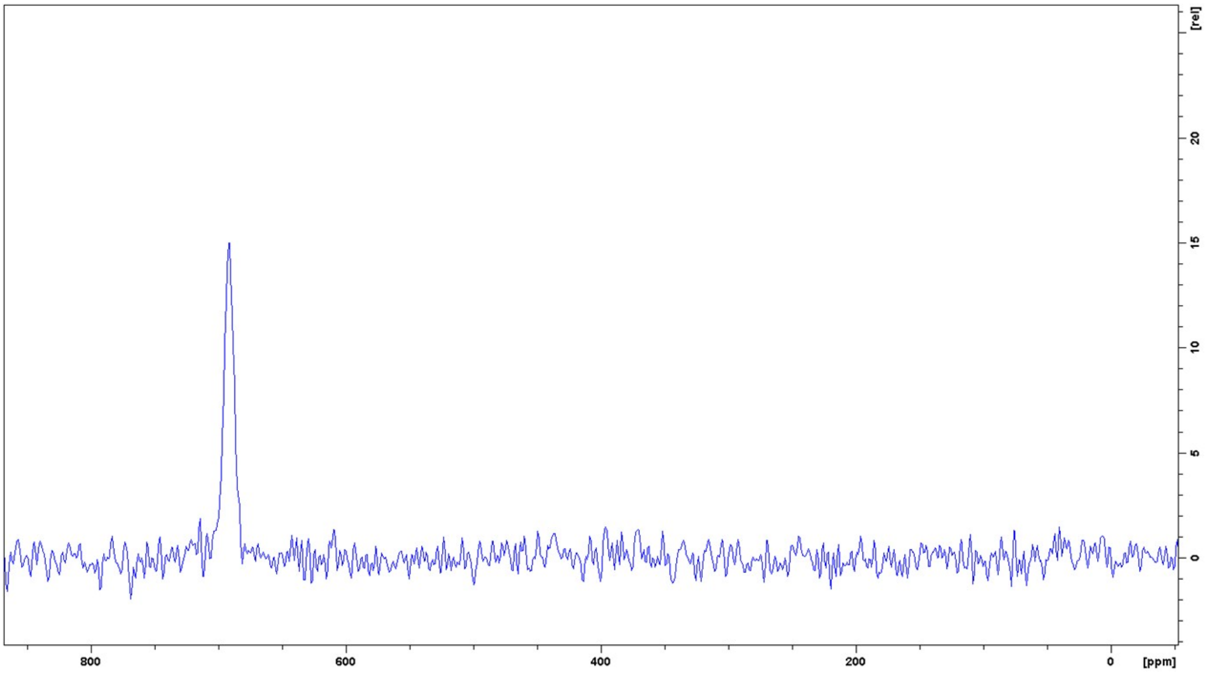

Figure B.23 ^{195}Pt NMR of **6** in MeOD at 298 K, showing a peak at 692 ppm.

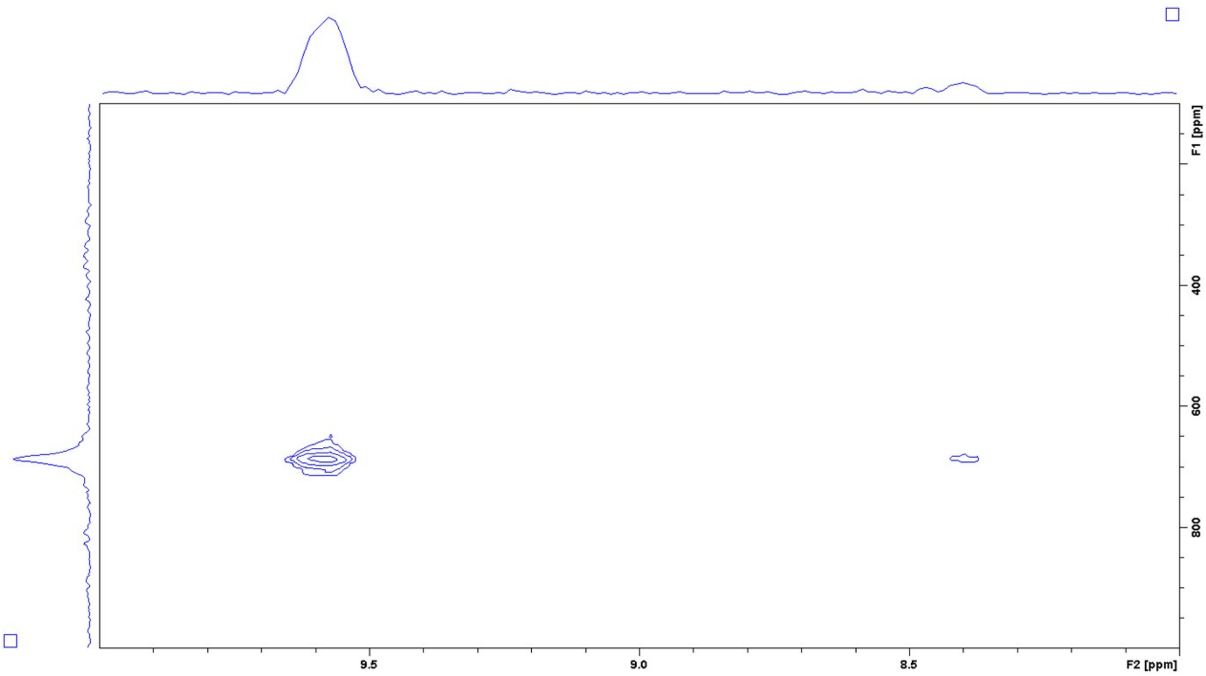

Figure B.24 ^{1}H-^{195}Pt HMQC NMR of **6** showing proton and platinum coupling resonances, in MeOD at 298 K.

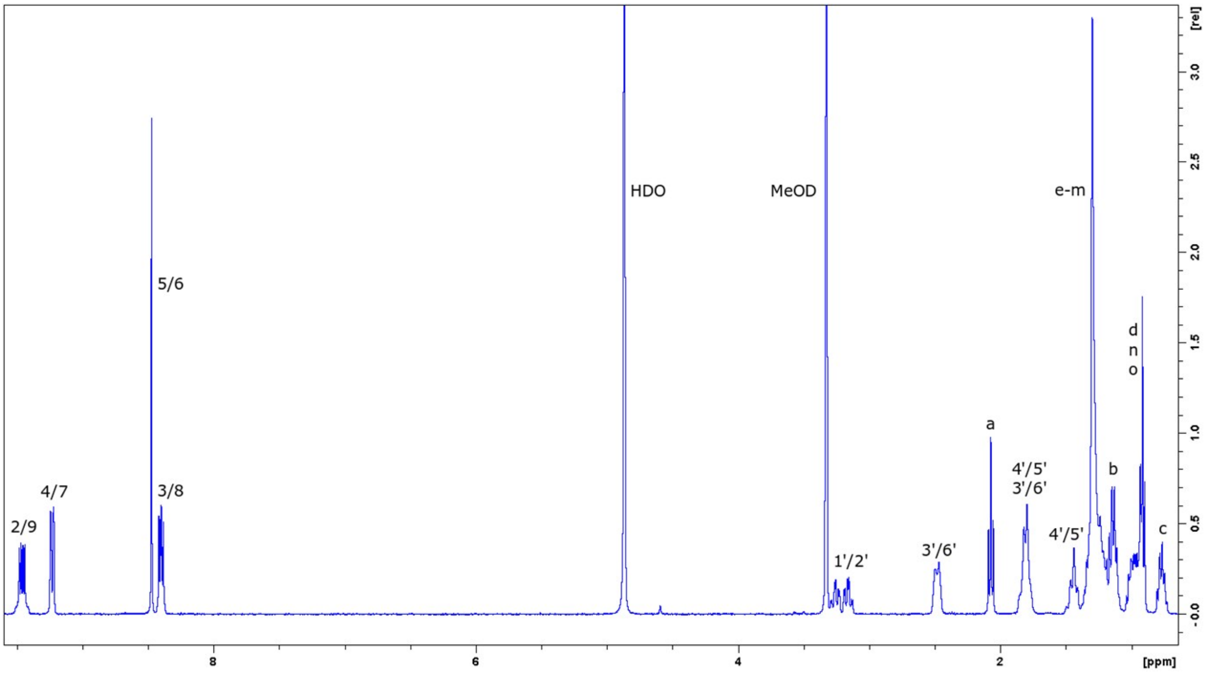

Figure B.25 ^{1}H NMR of **[Pt(PHEN)(SSDACH)(OH)(Hexadecanoate)]$(NO_3)_2$ (7)** in MeOD at 298 K. Inset below: Structure and proton numbering scheme of **7**.

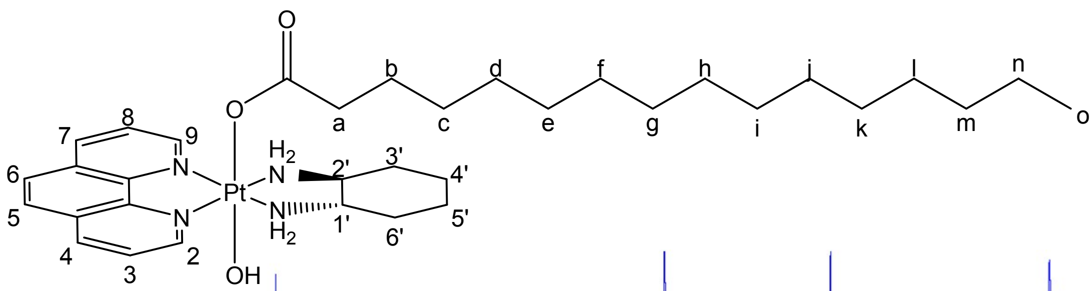

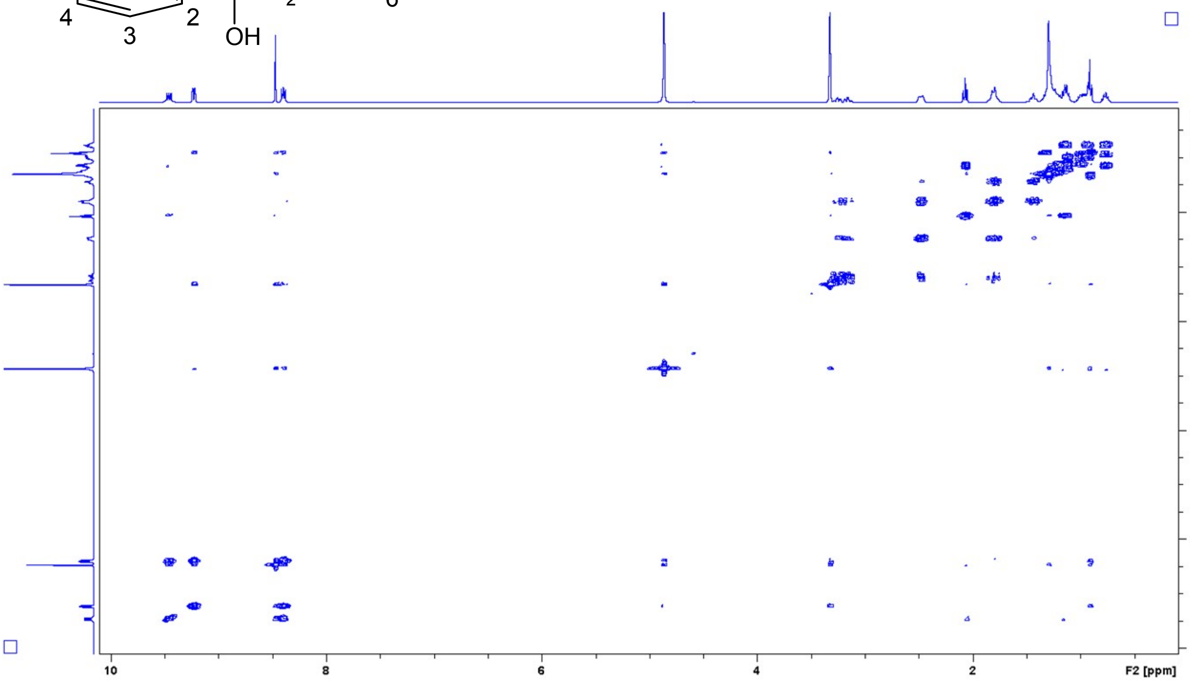

Figure B.26 COSY NMR of **7** in MeOD at 298 K.

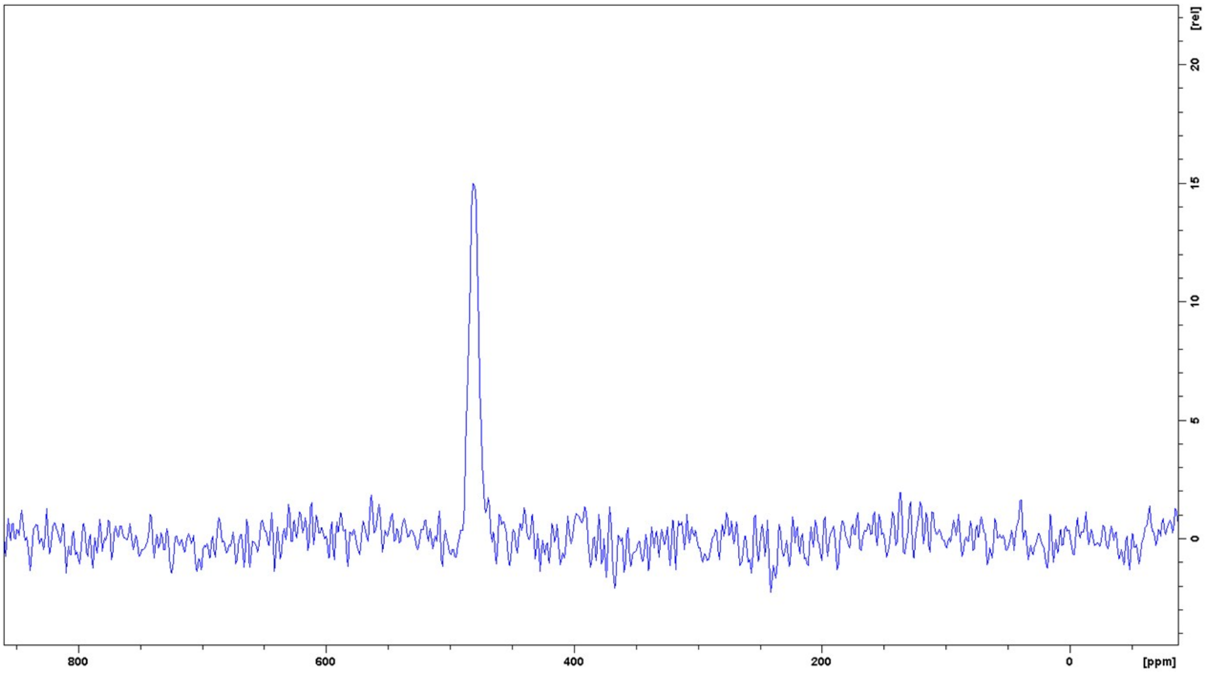

Figure B.27 ^{195}Pt NMR of **7** in MeOD at 298 K, showing a peak at 481 ppm.

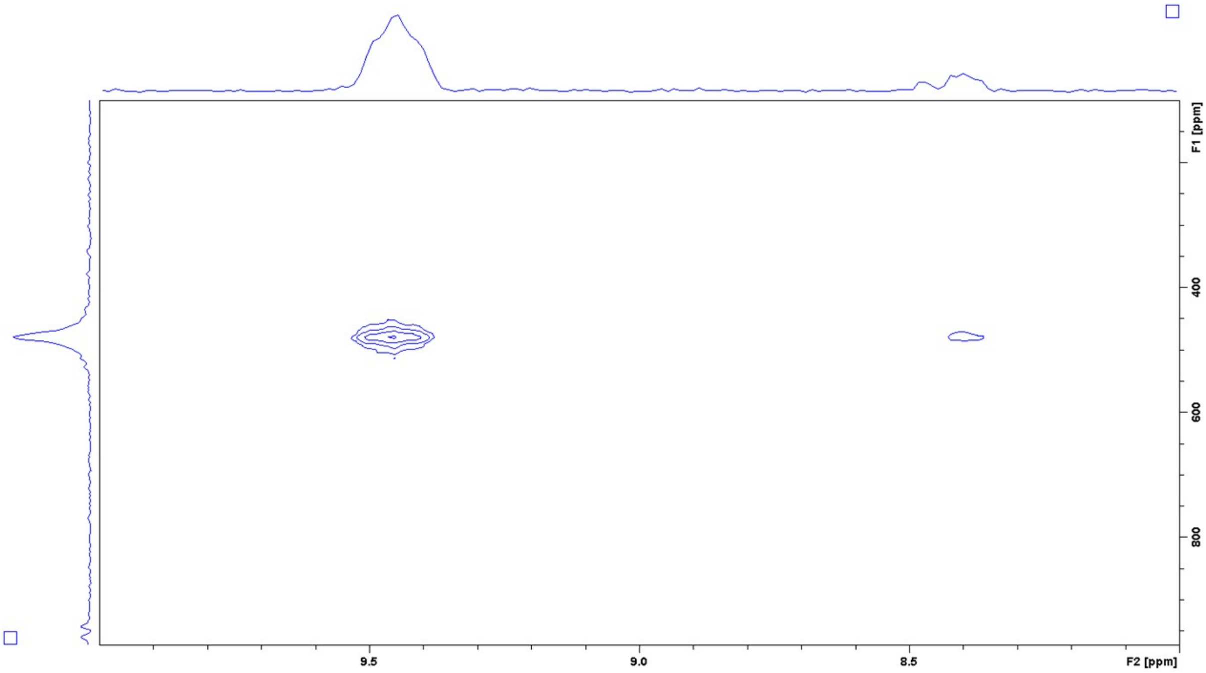

Figure B.28 ^{1}H-^{195}Pt HMQC NMR of **7** showing proton and platinum coupling resonances, in MeOD at 298 K.

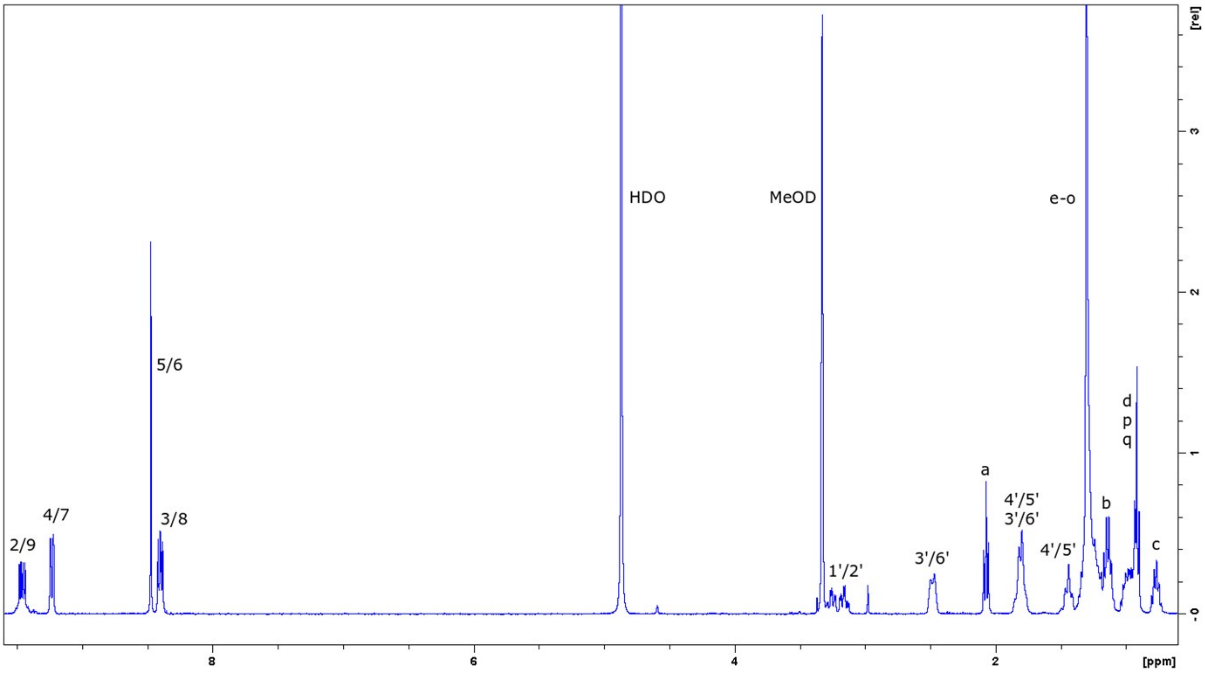

Figure B.29 [1]H NMR of **[Pt(PHEN)(SSDACH)(OH)(Octadecanoate)]$(NO_3)_2$** (**8**) in MeOD at 298 K. Inset below: Structure and proton numbering scheme of **8**.

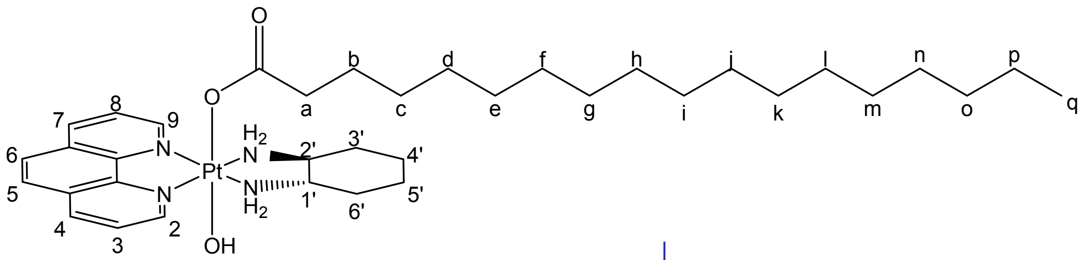

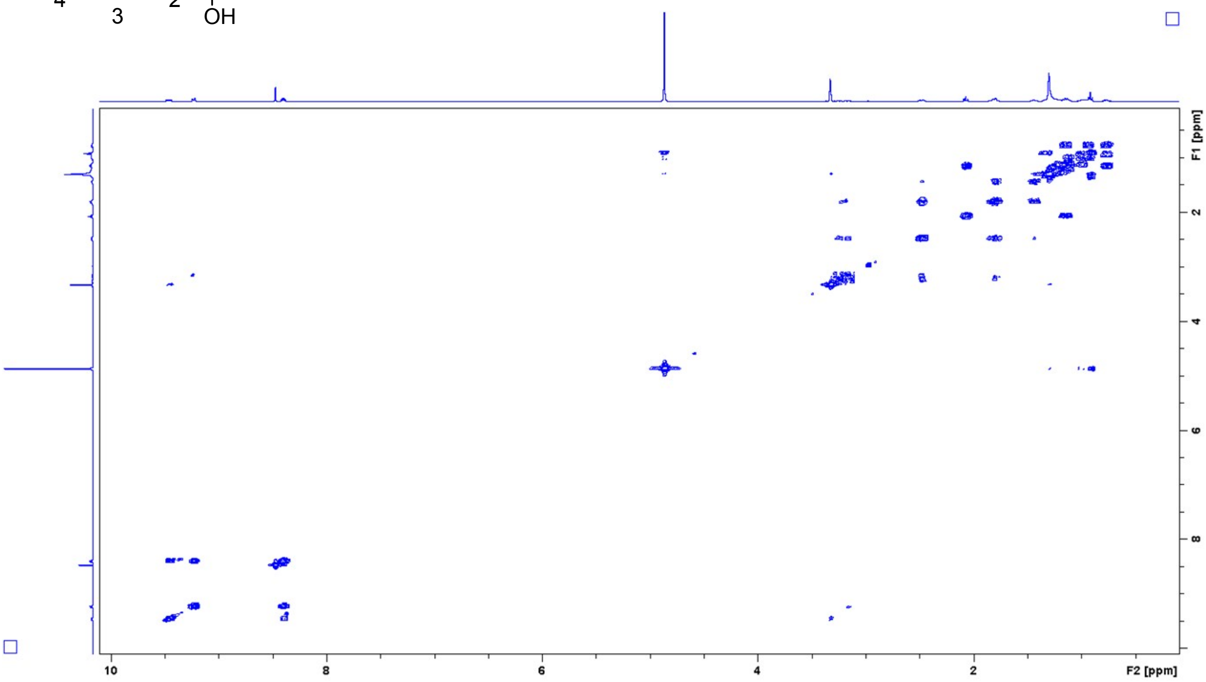

Figure B.30 COSY NMR of **8** in MeOD at 298 K.

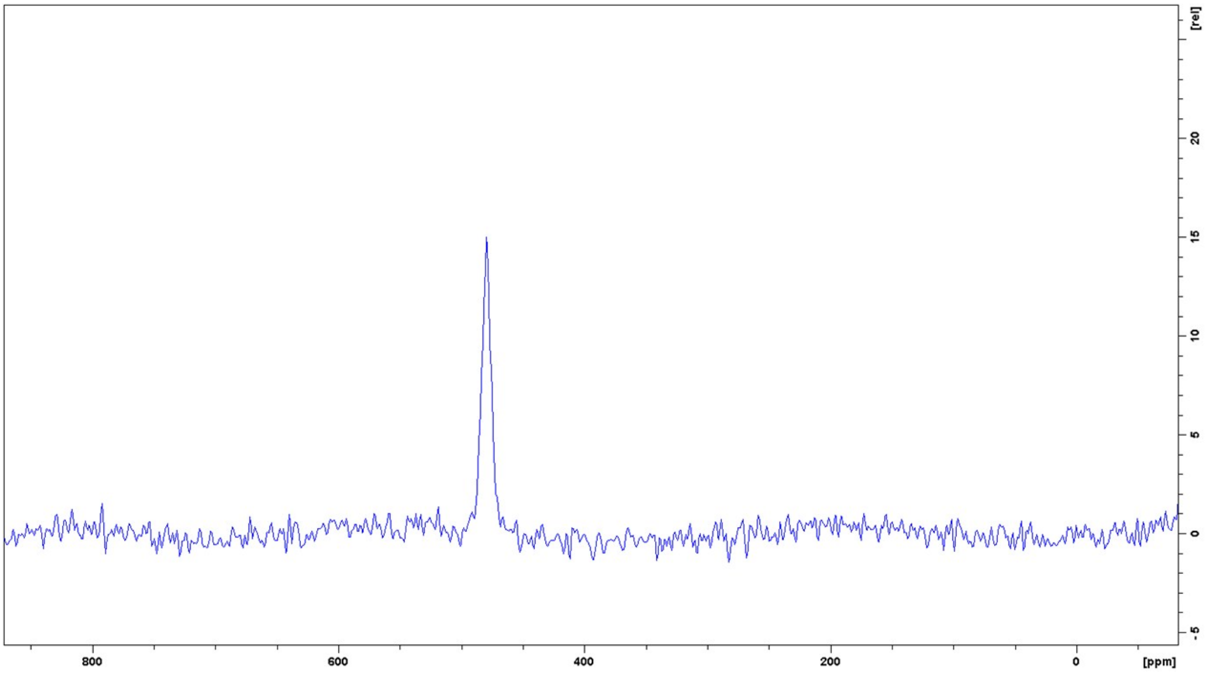

Figure B.31 ^{195}Pt NMR of **8** in MeOD at 298 K, showing a peak at 479 ppm.

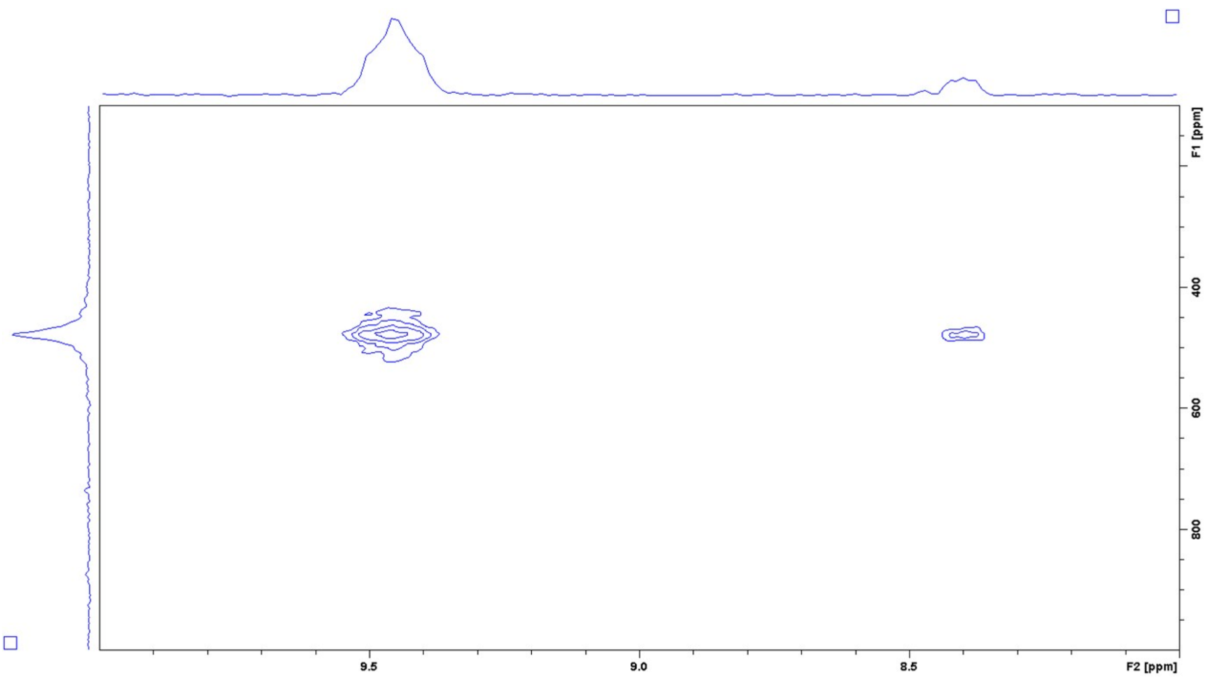

Figure B.32 ^{1}H-^{195}Pt HMQC NMR of **8** showing proton and platinum coupling resonances, in MeOD at 298 K.

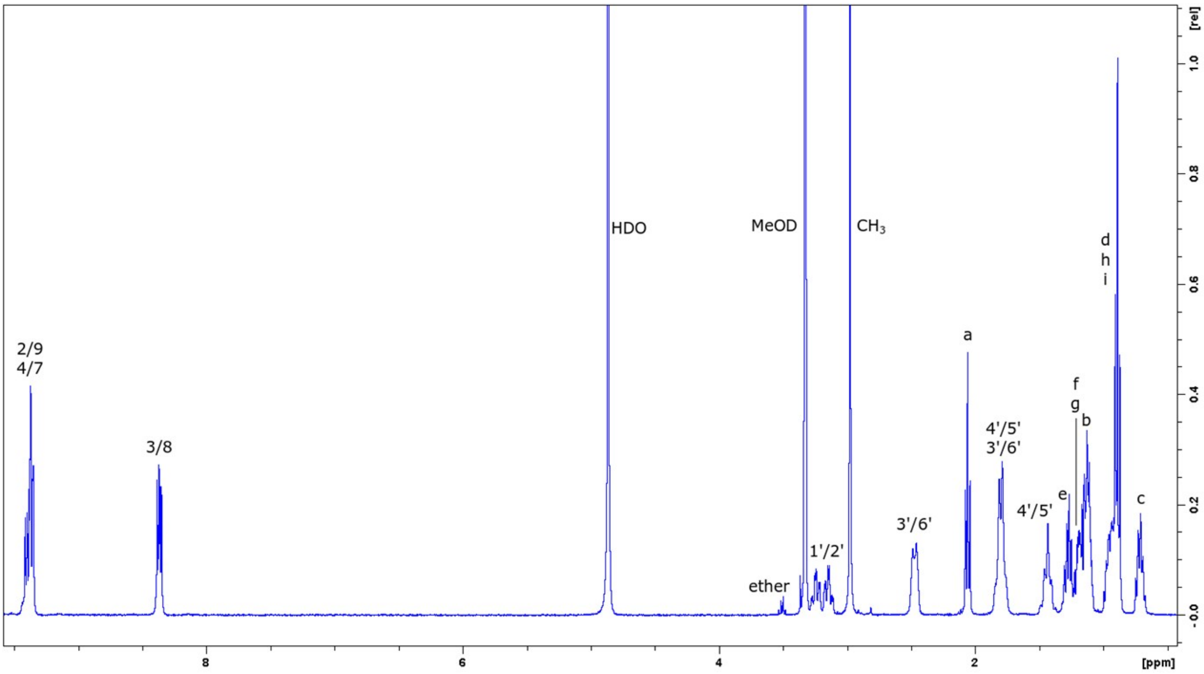

Figure B.33 ^{1}H NMR of **[Pt(56Me$_2$PHEN)(SSDACH)(OH)(Decanoate)](NO$_3$)$_2$ (9)** in MeOD at 298 K. Inset below: Structure and proton numbering scheme of **9**.

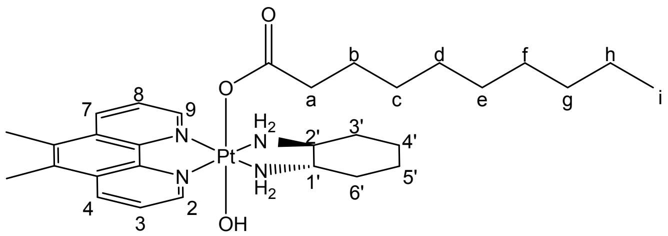

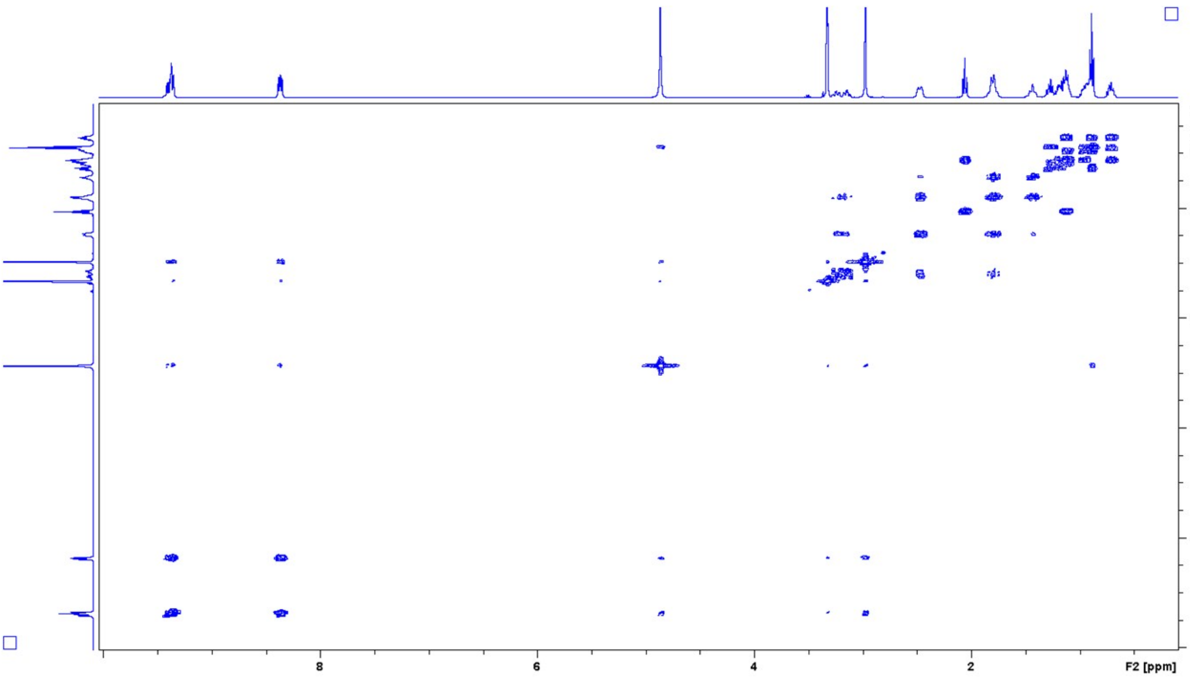

Figure B.34 COSY NMR of **9** in MeOD at 298 K.

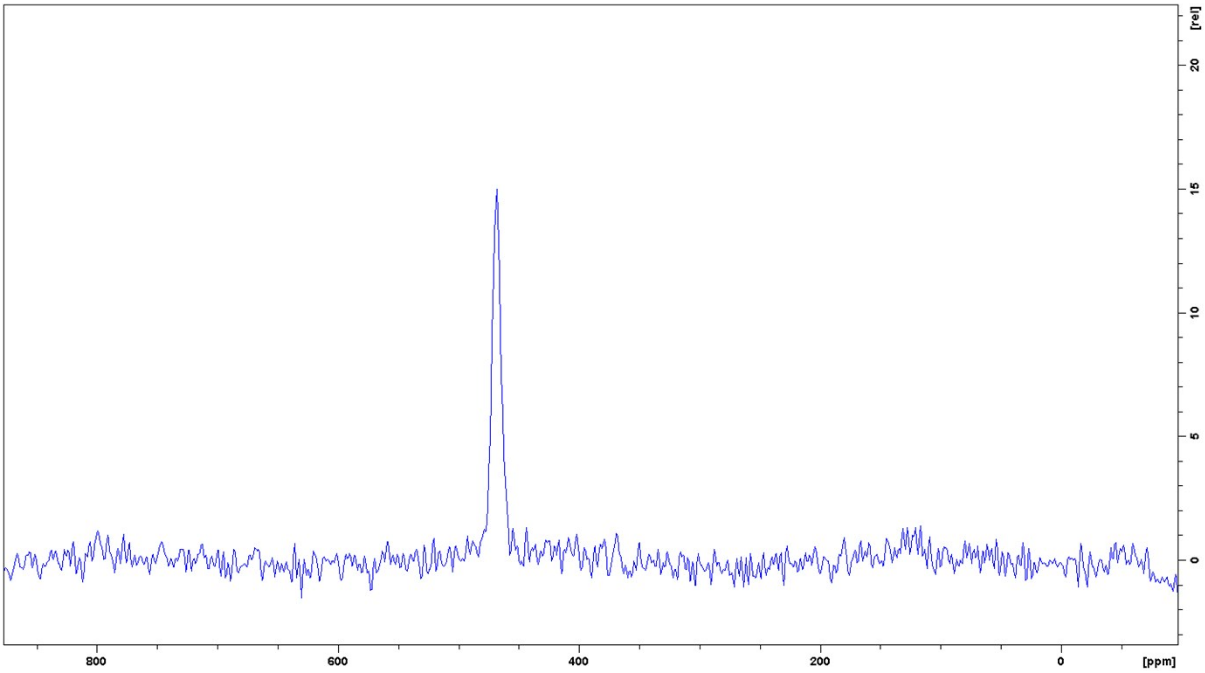

Figure B.35 ^{195}Pt NMR of **9** in MeOD at 298 K, showing a peak at 468 ppm.

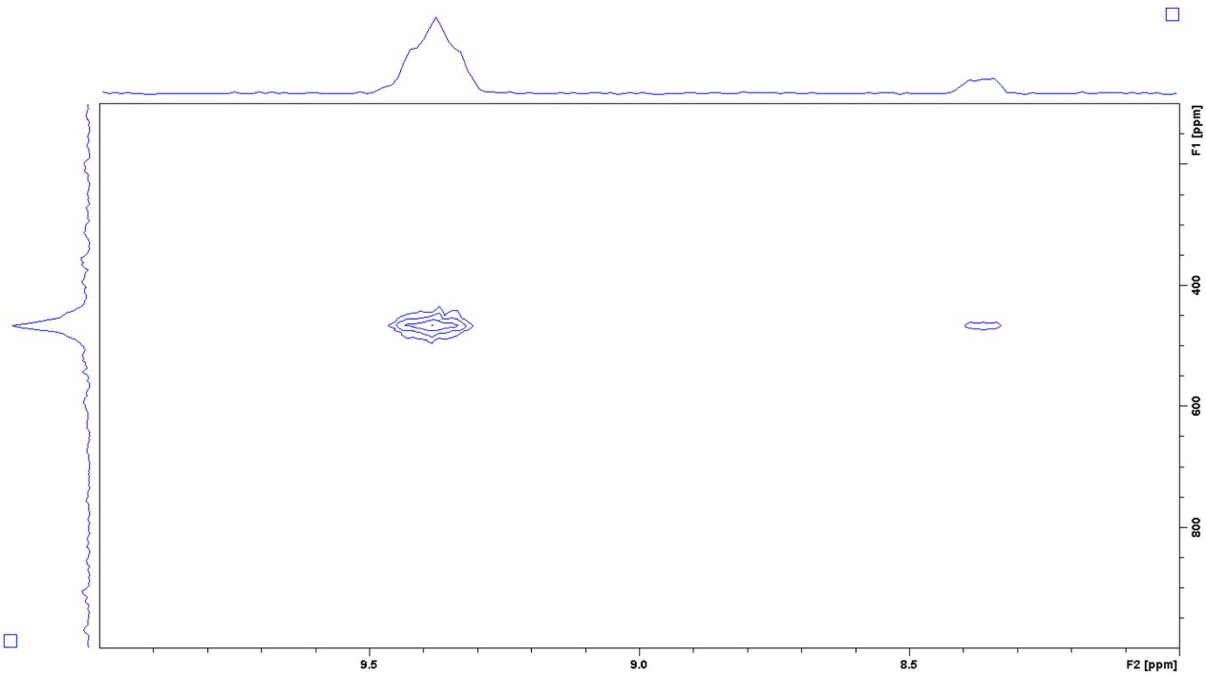

Figure B.36 ^{1}H-^{195}Pt HMQC NMR of **9** showing proton and platinum coupling resonances, in MeOD at 298 K.

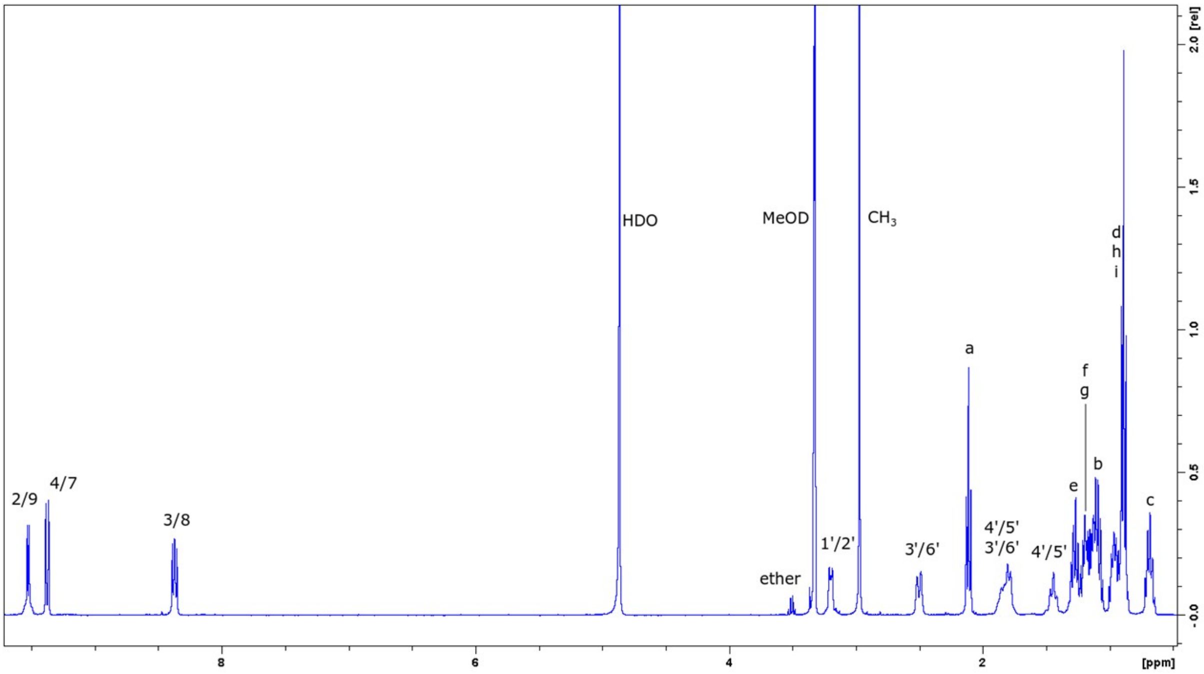

Figure B.37 ^{1}H NMR of **[Pt(56Me$_2$PHEN)(SSDACH)(Decanoate)$_2$](NO$_3$)$_2$** (**10**) in MeOD at 298 K. Inset below: Structure and proton numbering scheme of **10**.

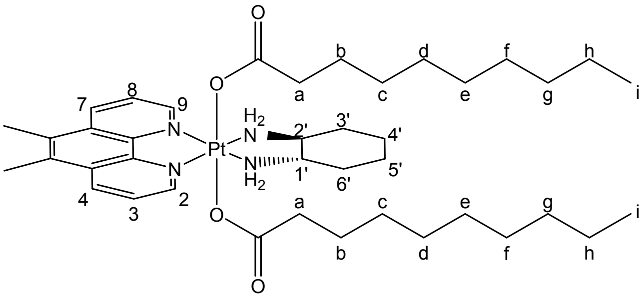

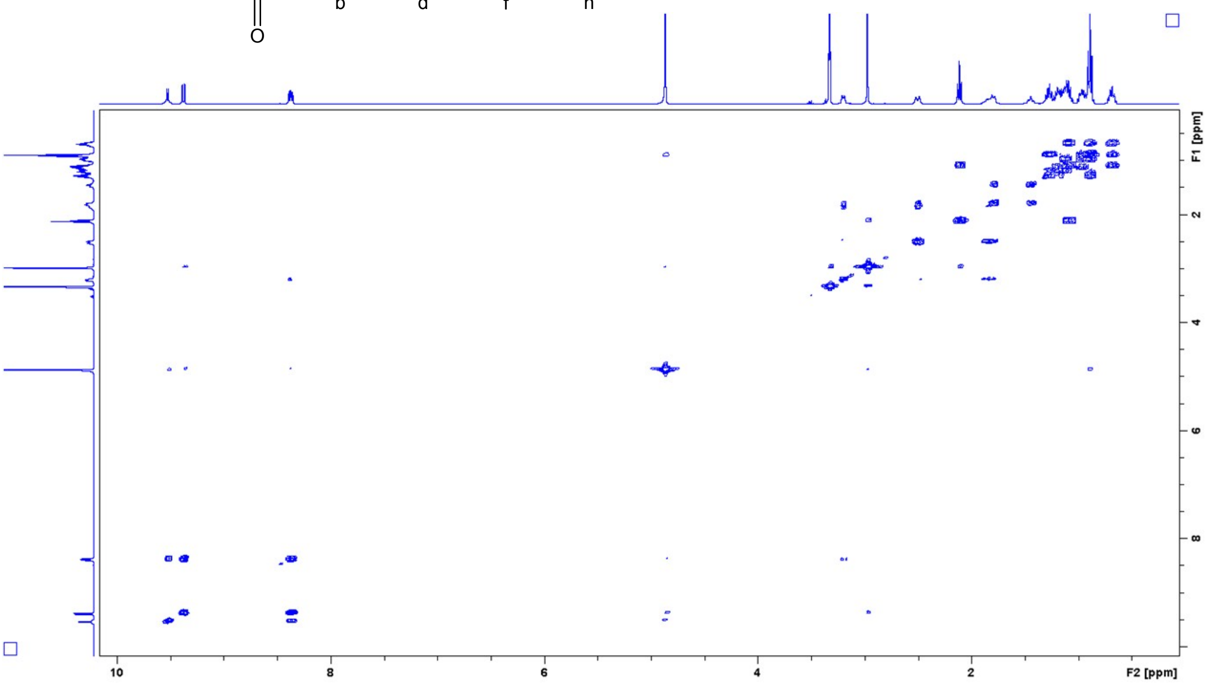

Figure B.38 COSY NMR of **10** in MeOD at 298 K.

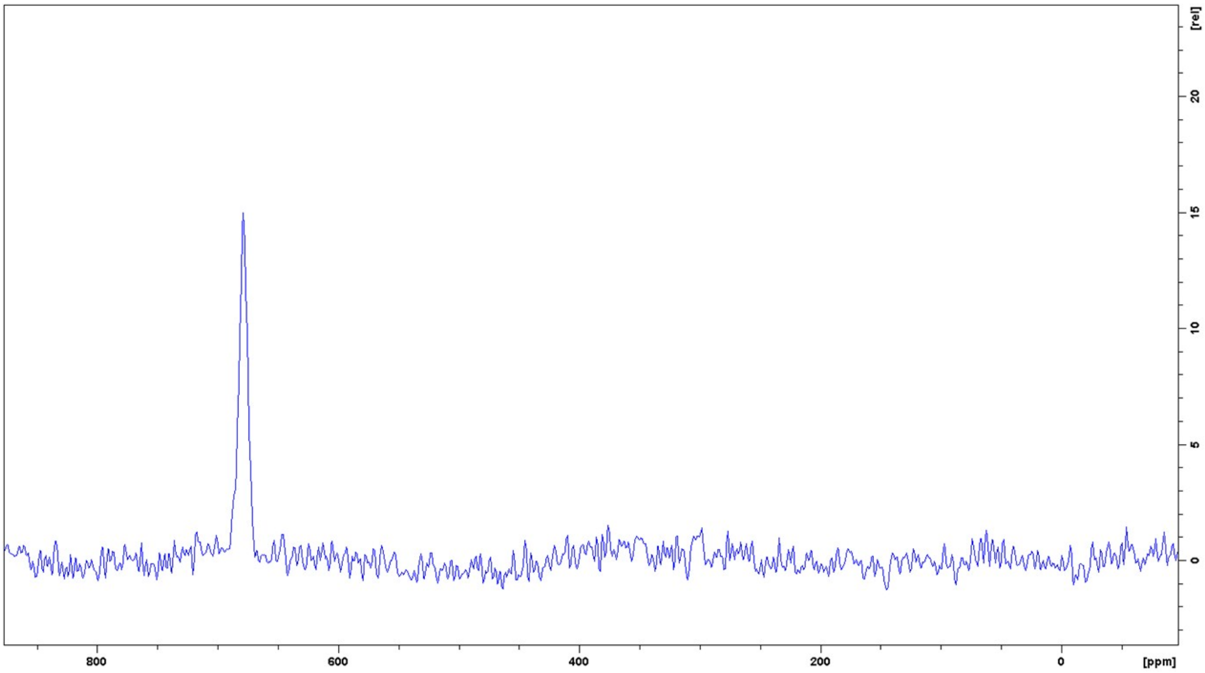

Figure B.39 ^{195}Pt NMR of **10** in MeOD at 298 K, showing a peak at 678 ppm.

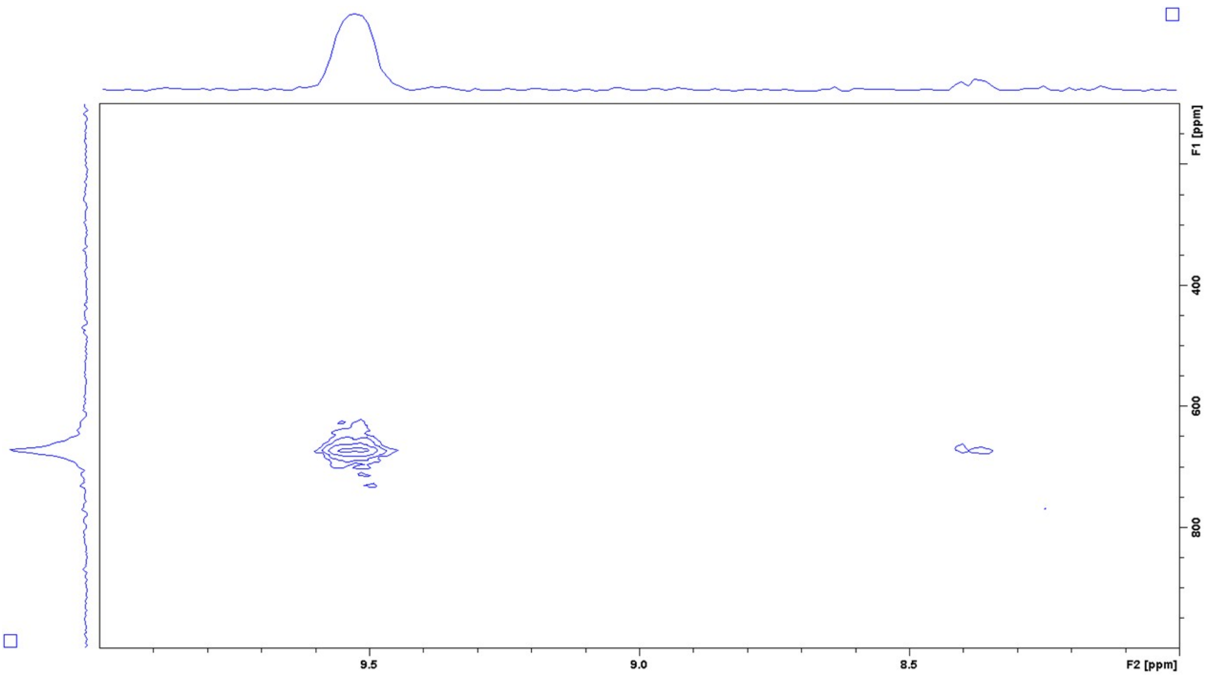

Figure B.40 ^{1}H-^{195}Pt HMQC NMR of **10** showing proton and platinum coupling resonances, in MeOD at 298 K.

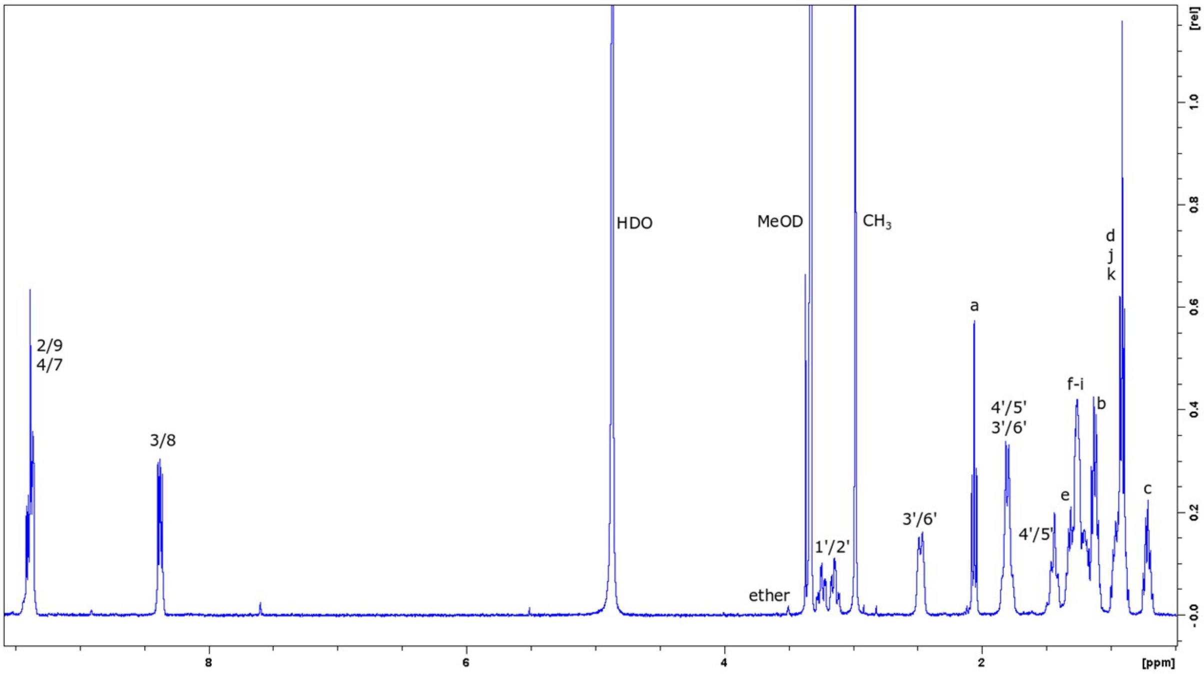

Figure B.41 ^{1}H NMR of **[Pt(56Me$_2$PHEN)(SSDACH)(OH)(Dodecanoate)](NO$_3$)$_2$** (**11**) in MeOD at 298 K. Inset below: Structure and proton numbering scheme of **11**.

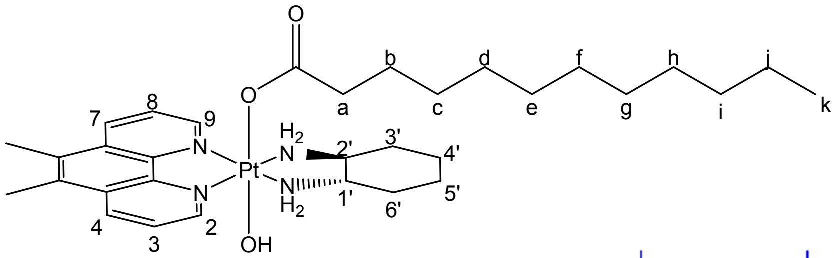

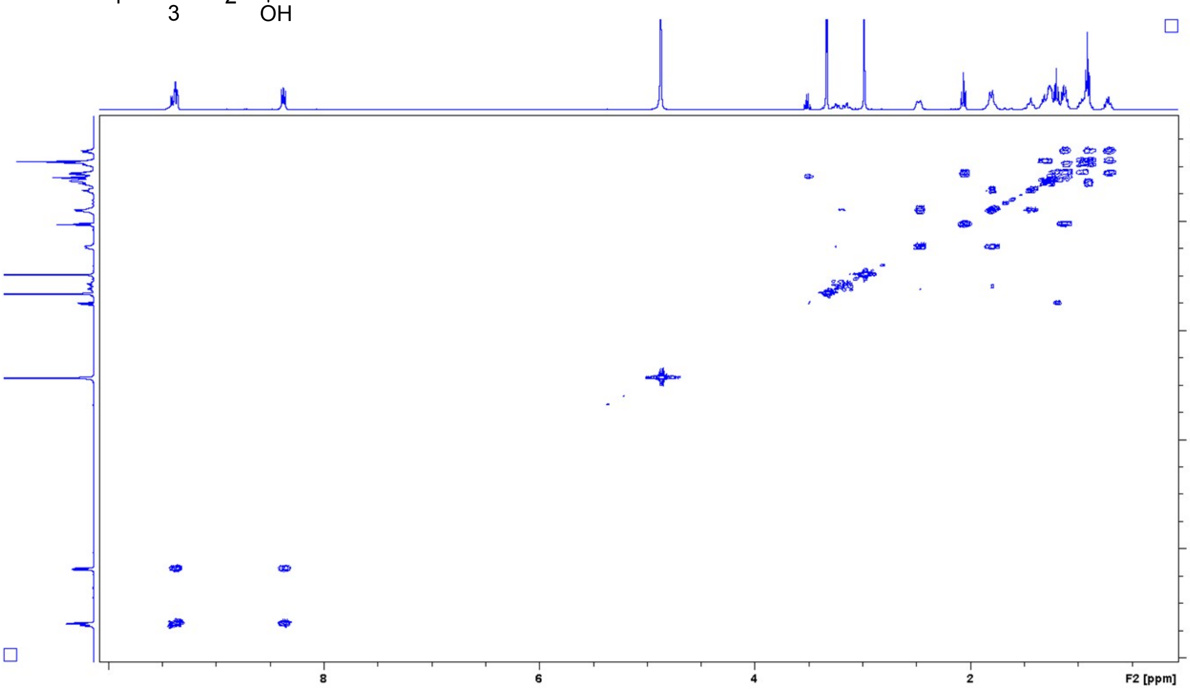

Figure B.42 COSY NMR of **11** in MeOD at 298 K.

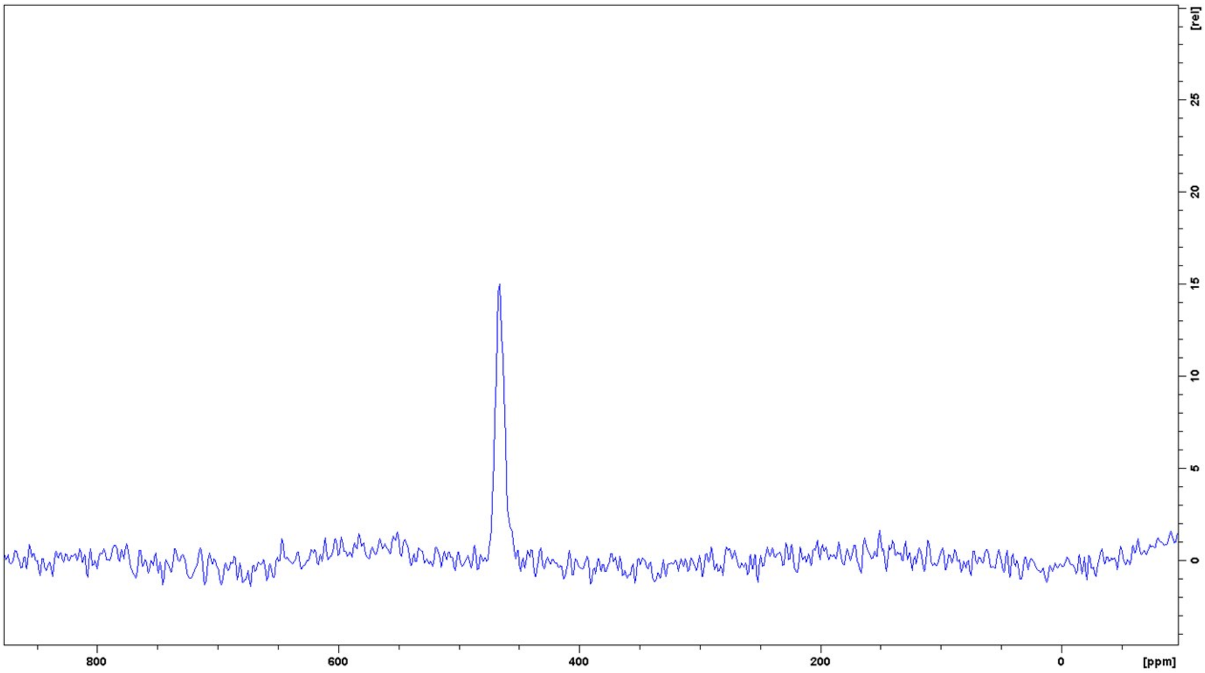

Figure B.43 ^{195}Pt NMR of **11** in MeOD at 298 K, showing a peak at 466 ppm.

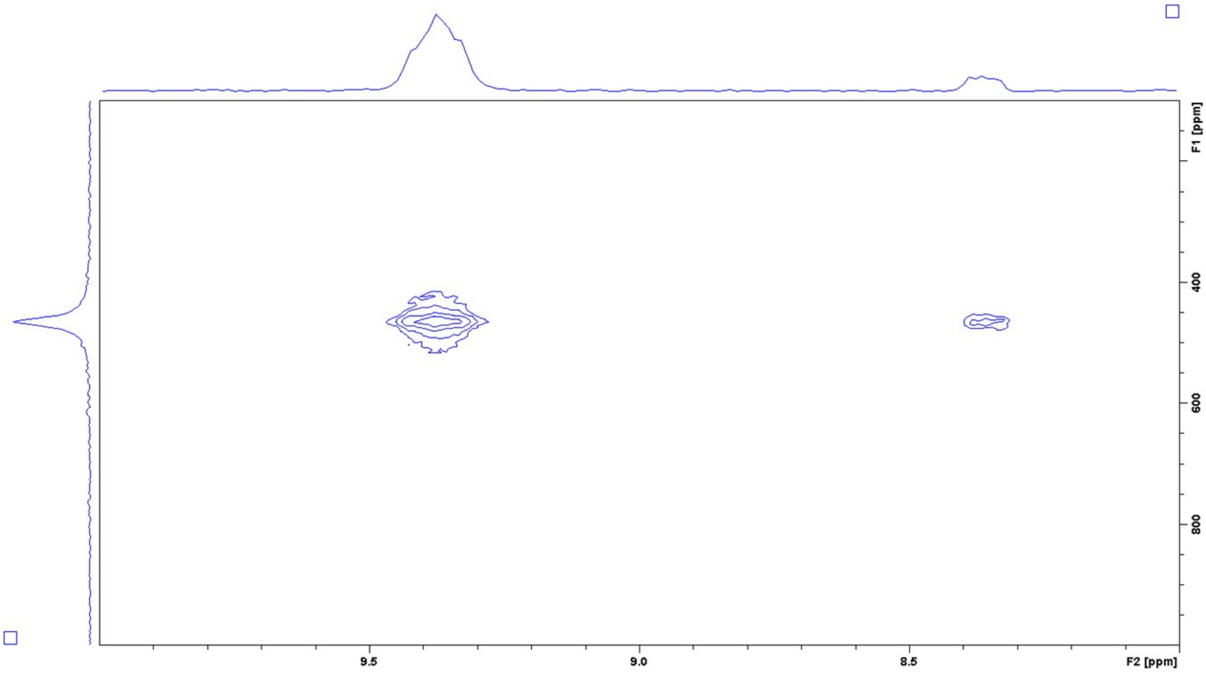

Figure B.44 ^{1}H-^{195}Pt HMQC NMR of **11** showing proton and platinum coupling resonances, in MeOD at 298 K.

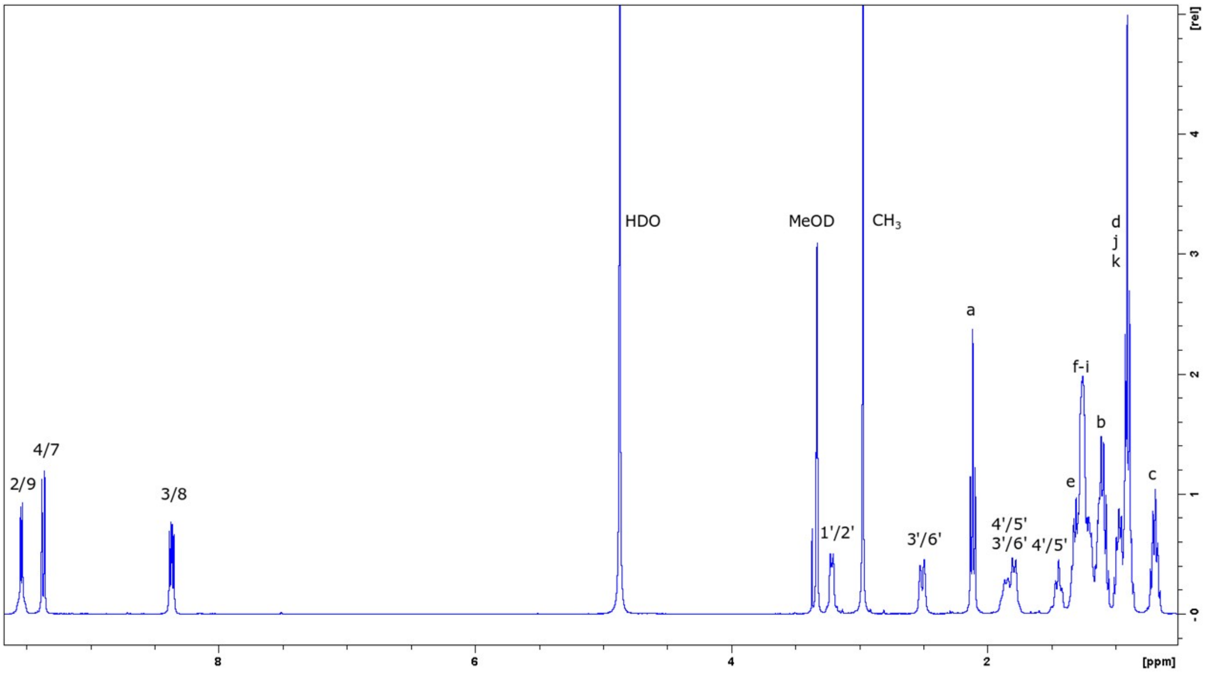

Figure B.45 ^{1}H NMR of **[Pt(56Me$_2$PHEN)(SSDACH)(Dodecanoate)$_2$](NO$_3$)$_2$** (**12**) in MeOD at 298 K. Inset below: Structure and proton numbering scheme of **12**.

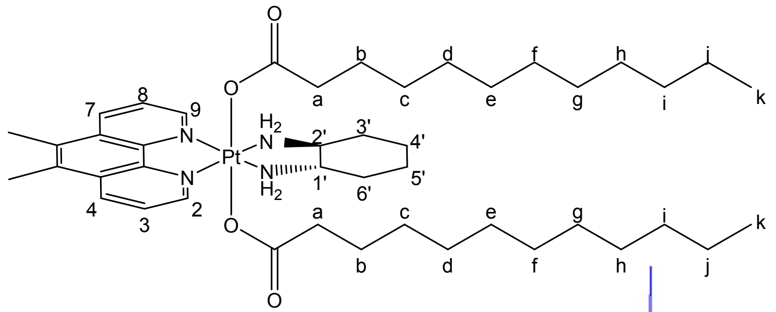

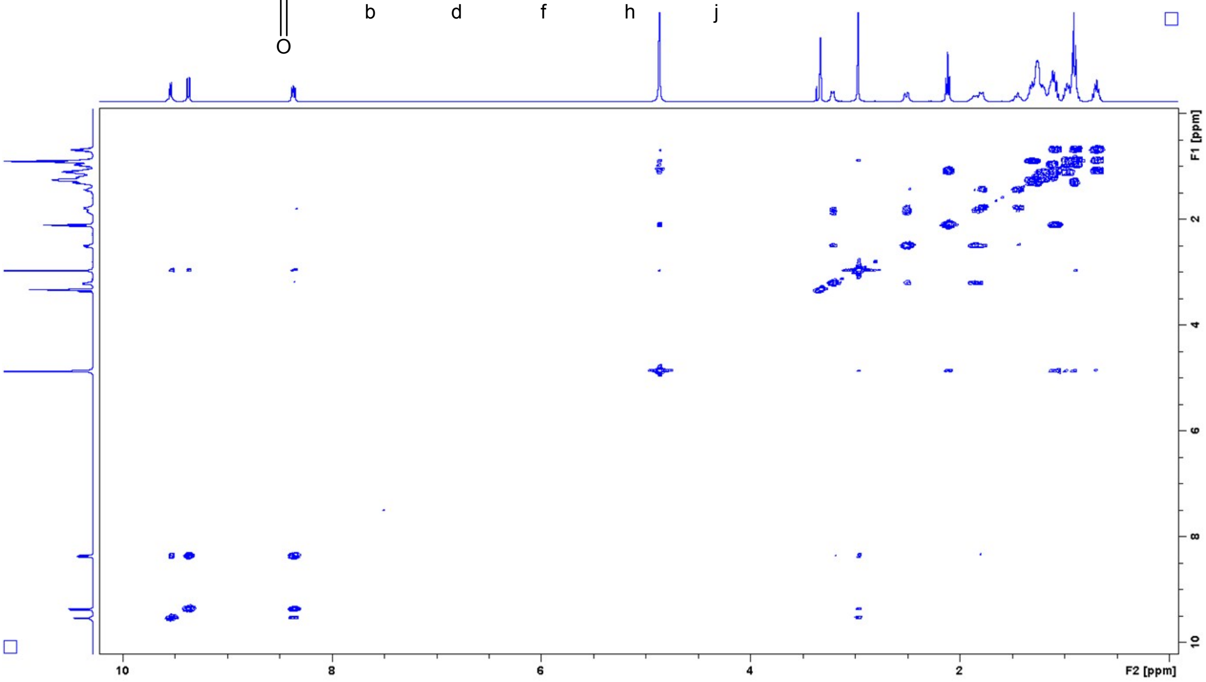

Figure B.46 COSY NMR of **12** in MeOD at 298 K.

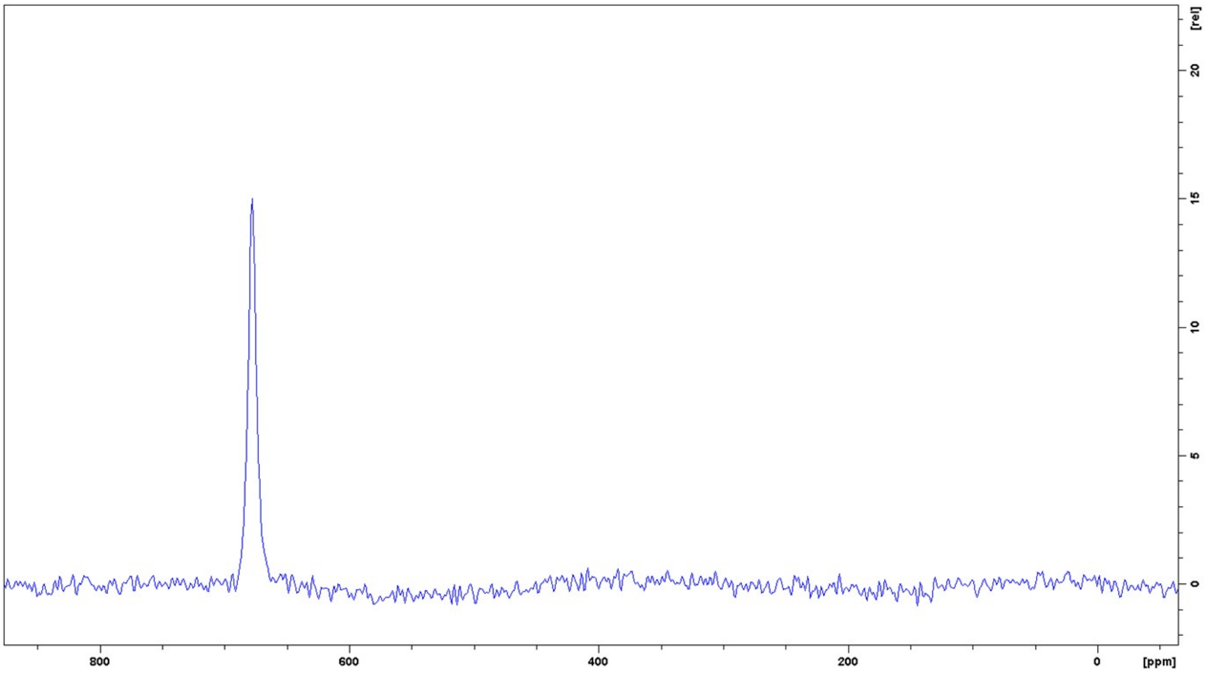

Figure B.47 ^{195}Pt NMR of **12** in MeOD at 298 K, showing a peak at 678 ppm.

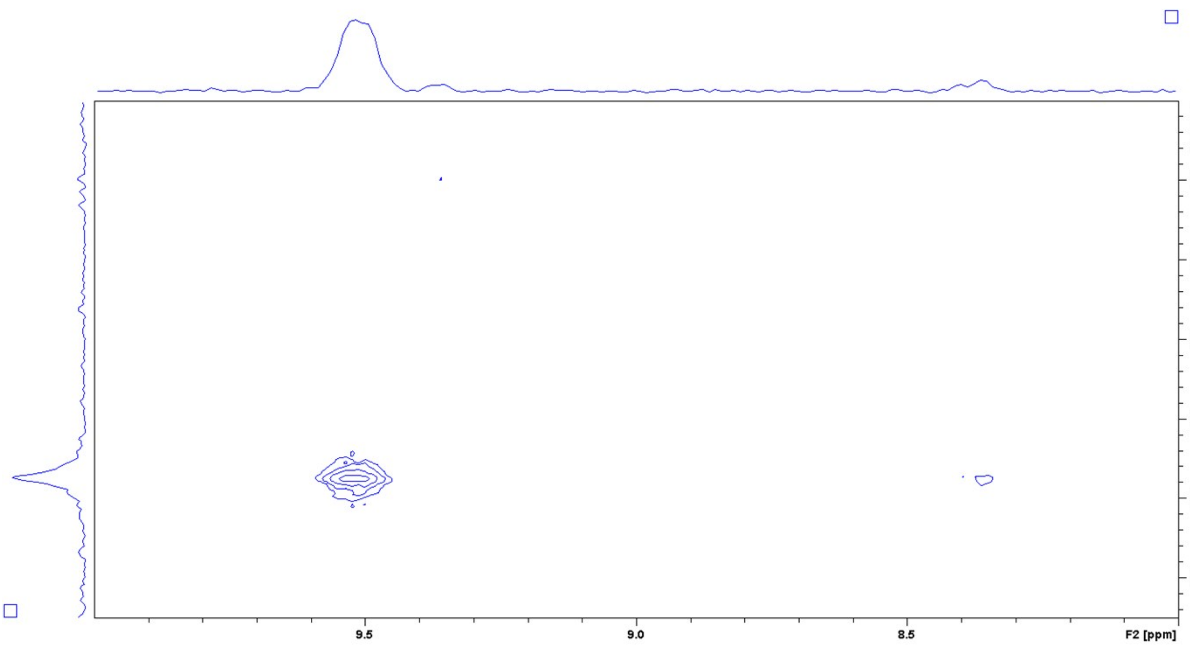

Figure B.48 ^{1}H-^{195}Pt HMQC NMR of **12** showing proton and platinum coupling resonances, in MeOD at 298 K.

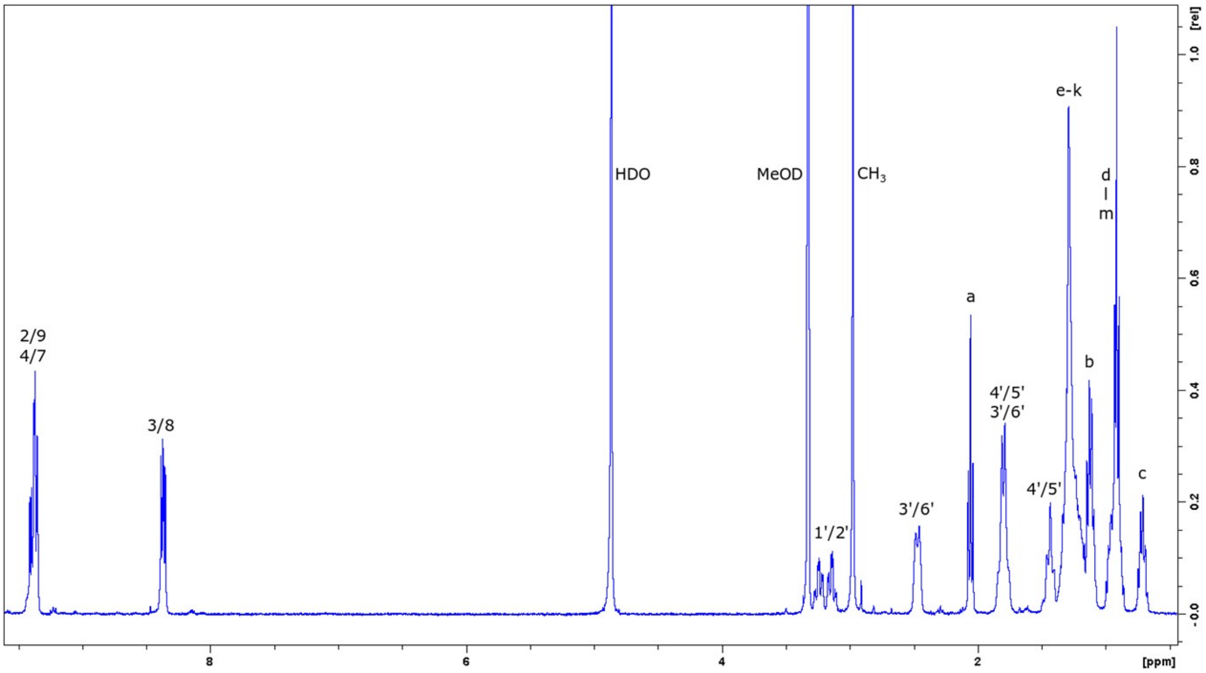

Figure B.49 [1]H NMR of **[Pt(56Me$_2$PHEN)(SSDACH)(OH)(Tetradecanoate)](NO$_3$)$_2$** (**13**) in MeOD at 298 K. Inset below: Structure and proton numbering scheme of **13**.

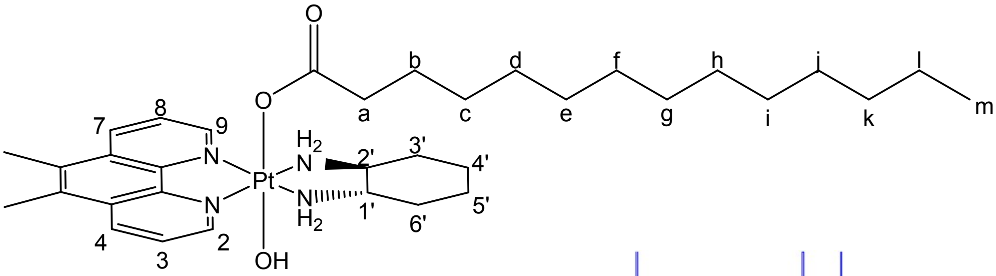

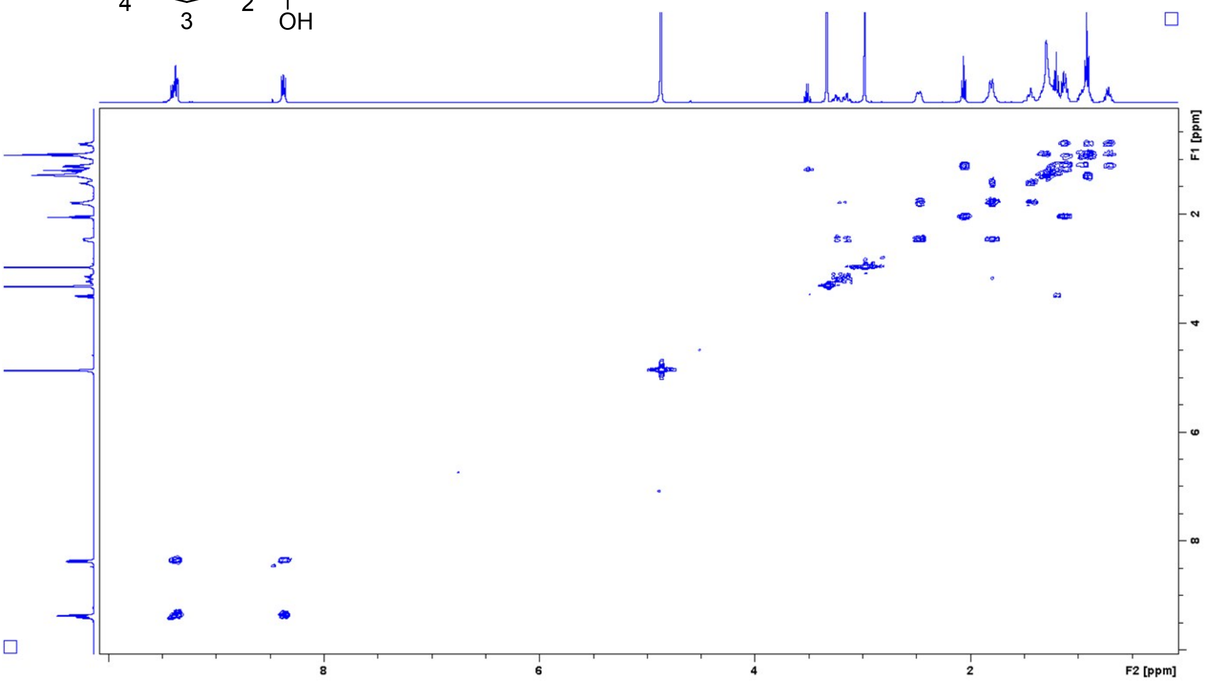

Figure B.50 COSY NMR of **13** in MeOD at 298 K.

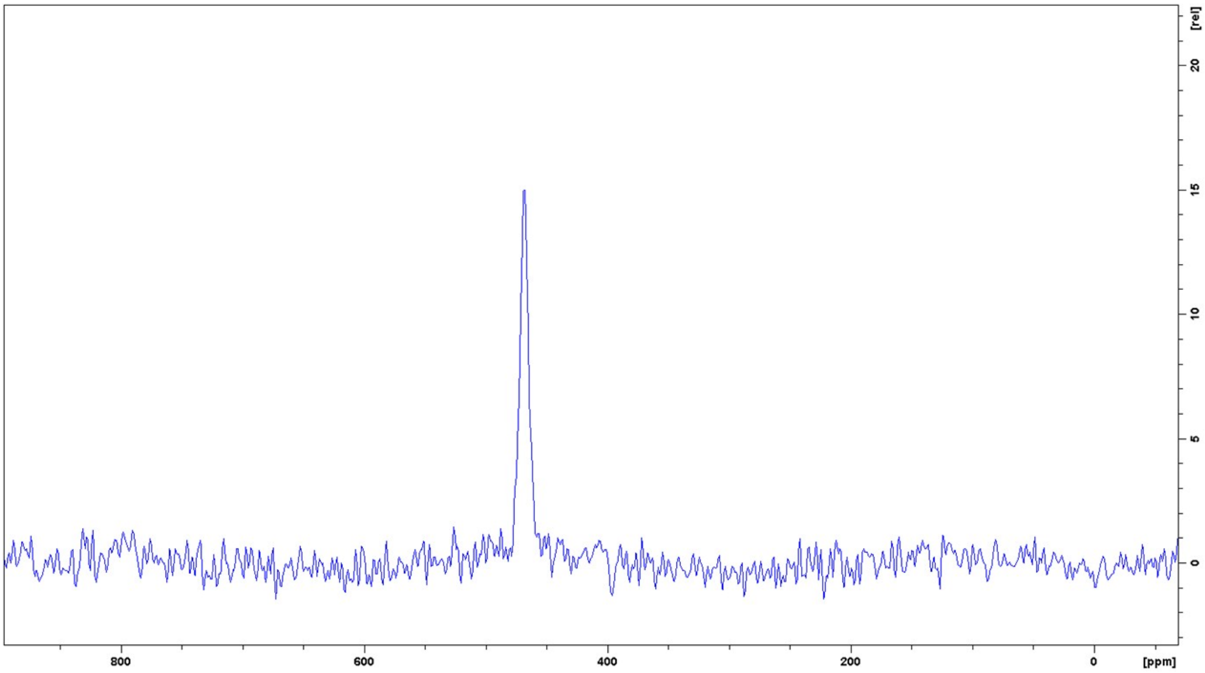

Figure B.51 ^{195}Pt NMR of **13** in MeOD at 298 K, showing a peak at 469 ppm.

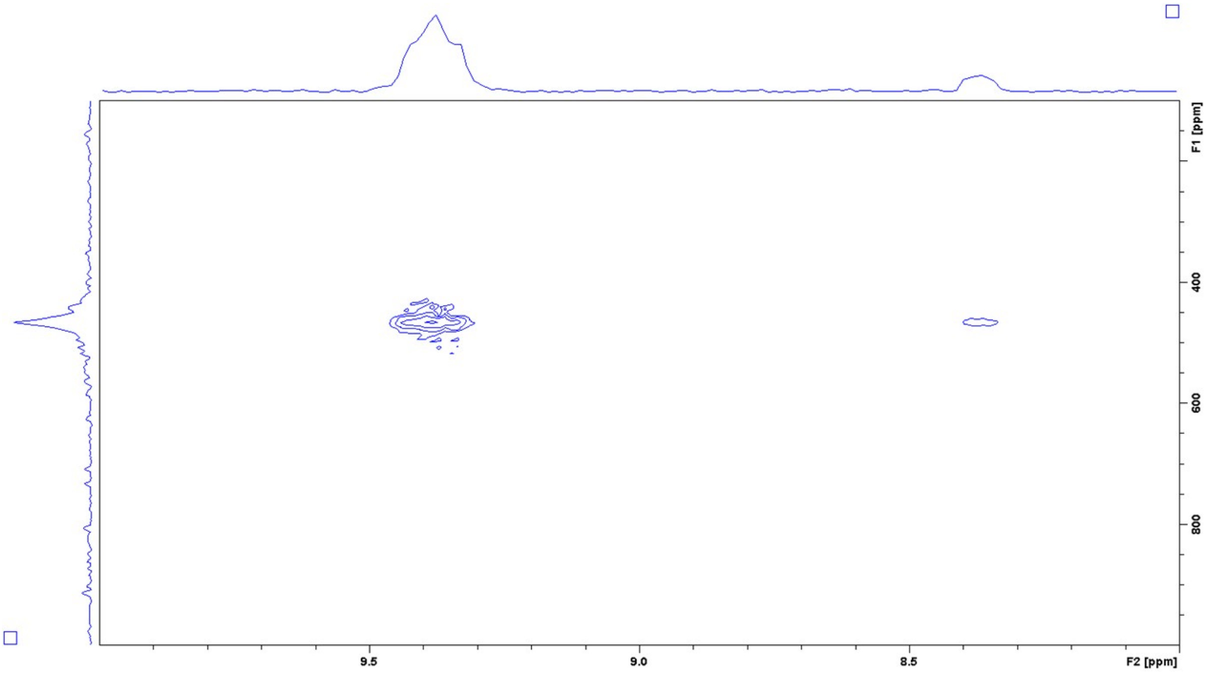

Figure B.52 ^{1}H-^{195}Pt HMQC NMR of **13** showing proton and platinum coupling resonances, in MeOD at 298 K.

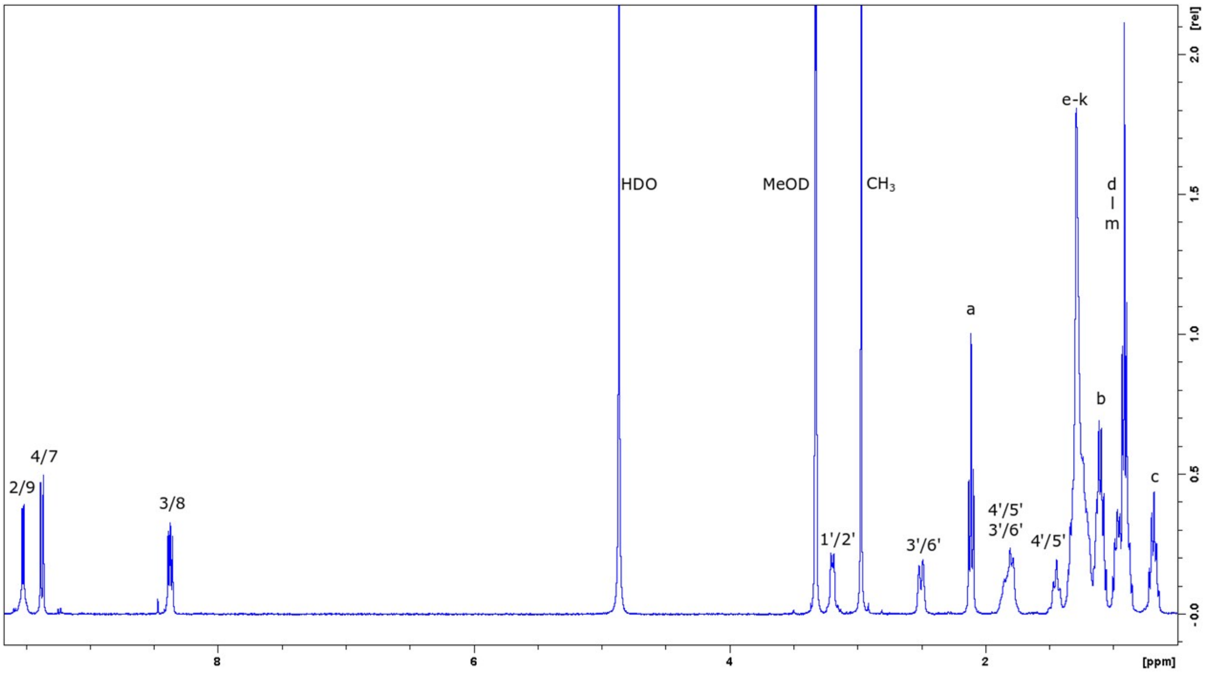

Figure B.53 ^{1}H NMR of **[Pt(56Me$_2$PHEN)(SSDACH)(Tetradecanoate)$_2$](NO$_3$)$_2$ (14)** in MeOD at 298 K. Inset below: Structure and proton numbering scheme of **14**.

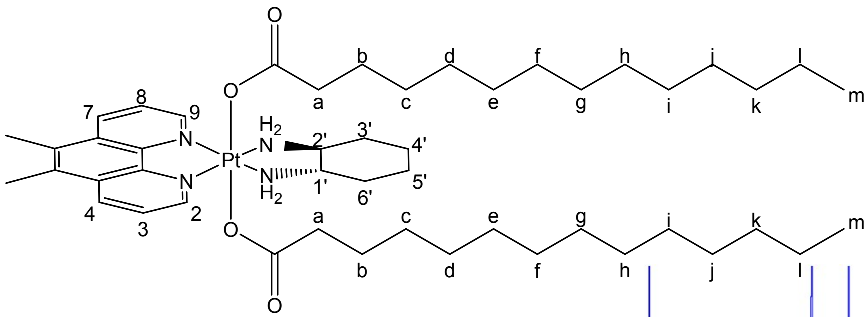

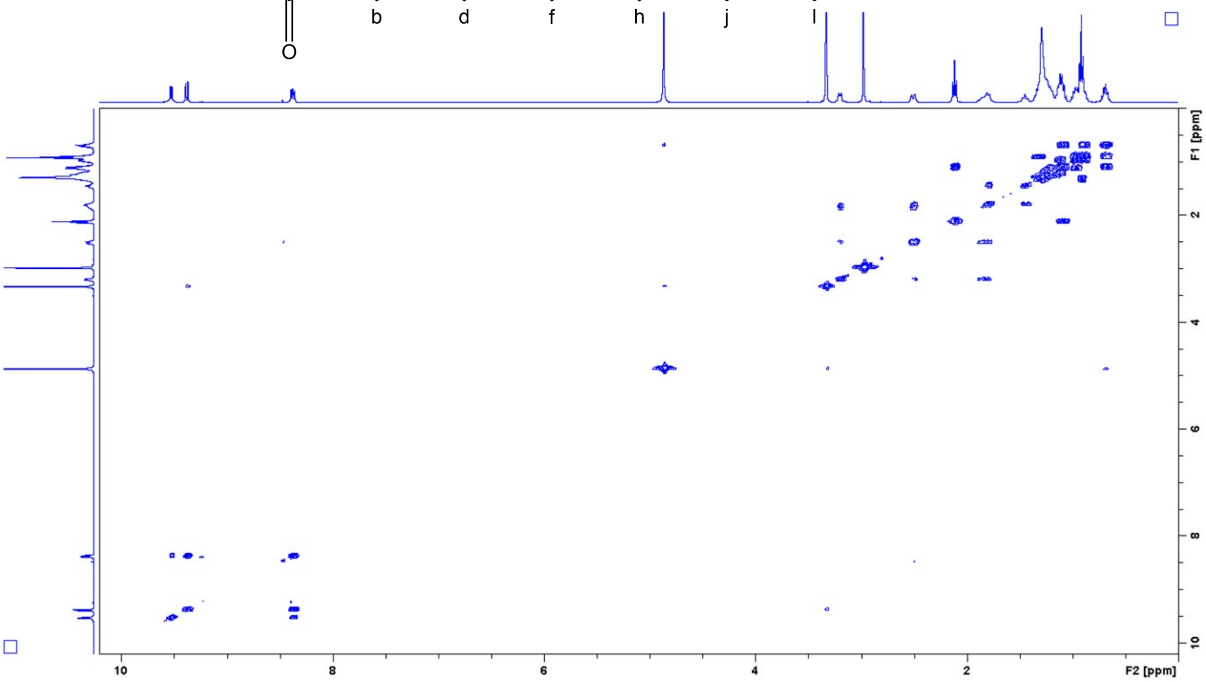

Figure B.54 COSY NMR of **14** in MeOD at 298 K.

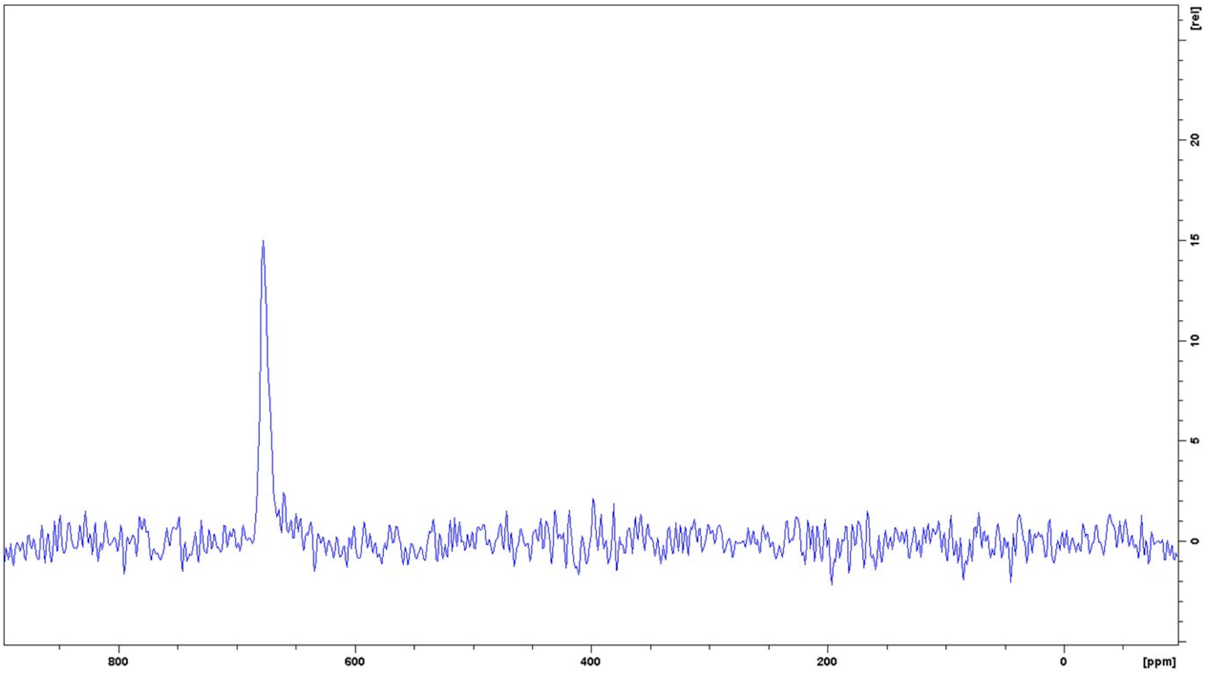

Figure B.55 ^{195}Pt NMR of **14** in MeOD at 298 K, showing a peak at 677 ppm.

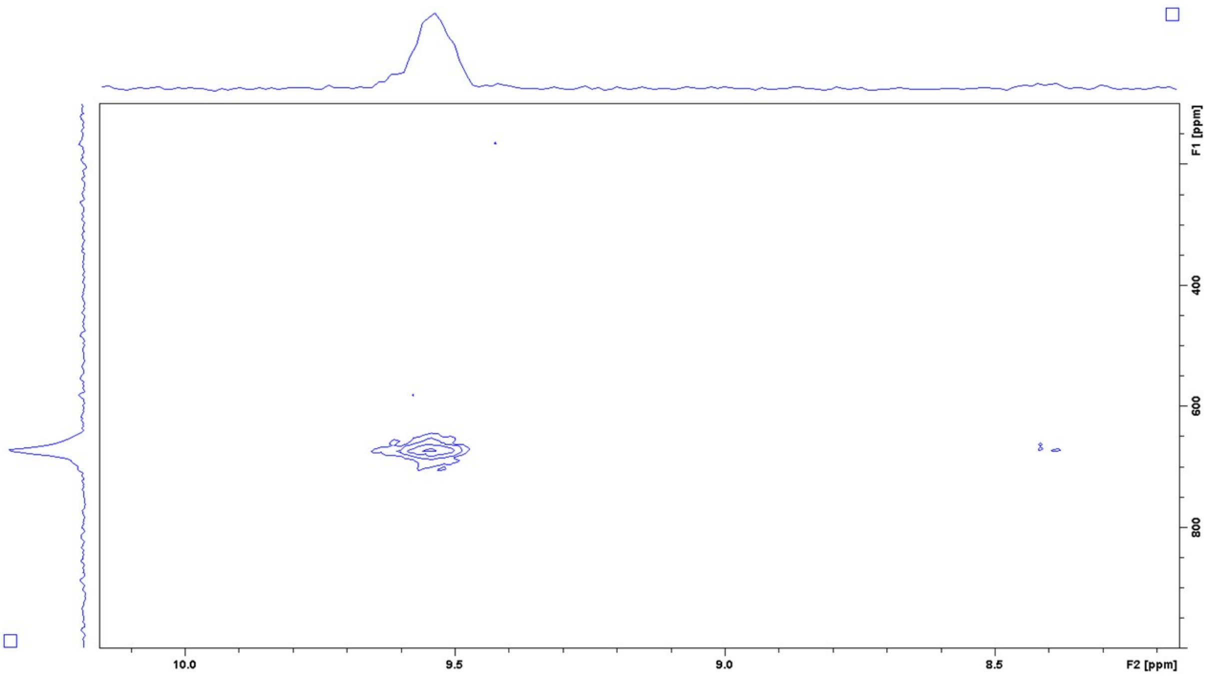

Figure B.56 ^{1}H-^{195}Pt HMQC NMR of **14** showing proton and platinum coupling resonances, in MeOD at 298 K.

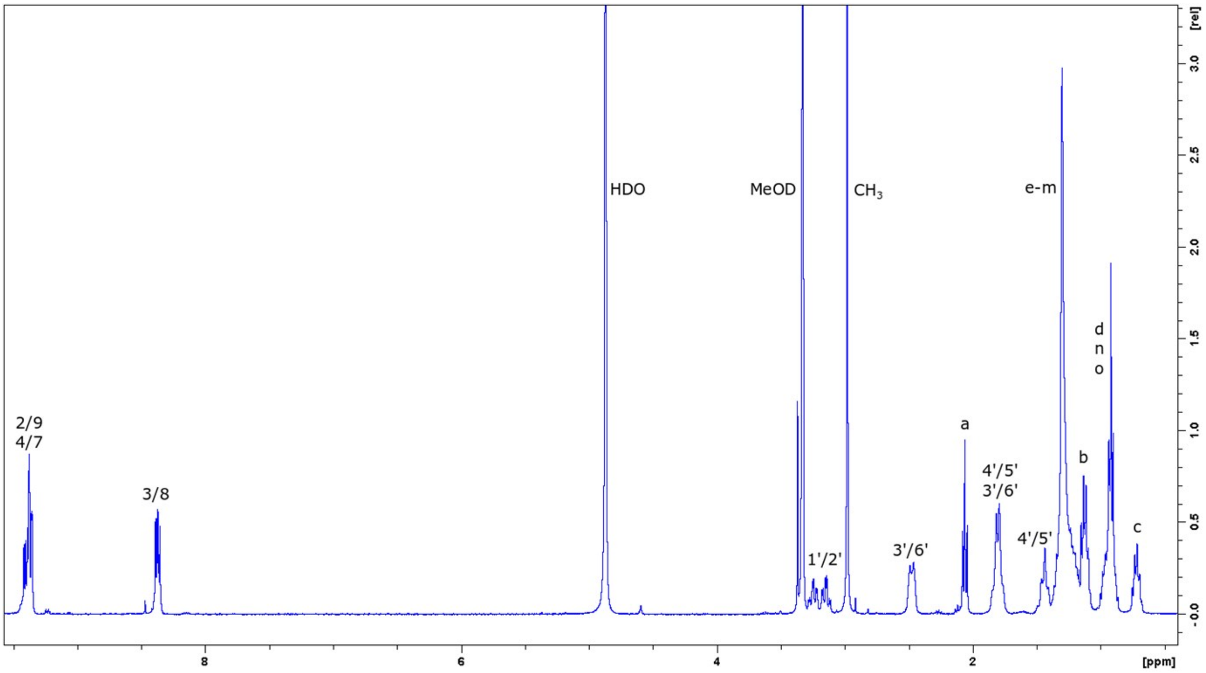

Figure B.57 [1]H NMR of **[Pt(56Me$_2$PHEN)(SSDACH)(OH)(Hexadecanoate)](NO$_3$)$_2$** (**15**) in MeOD at 298 K. Inset below: Structure and proton numbering scheme of **15**.

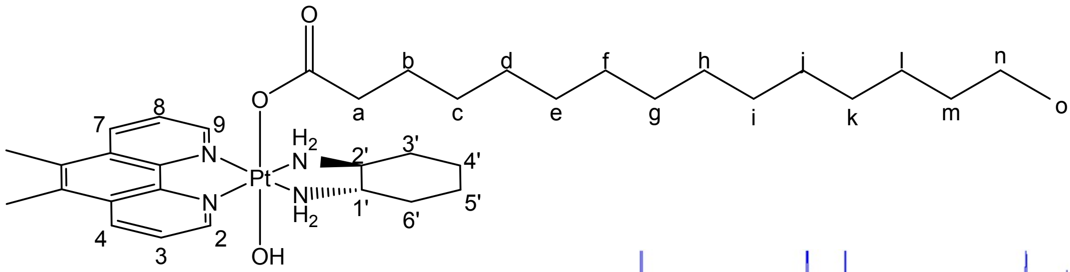

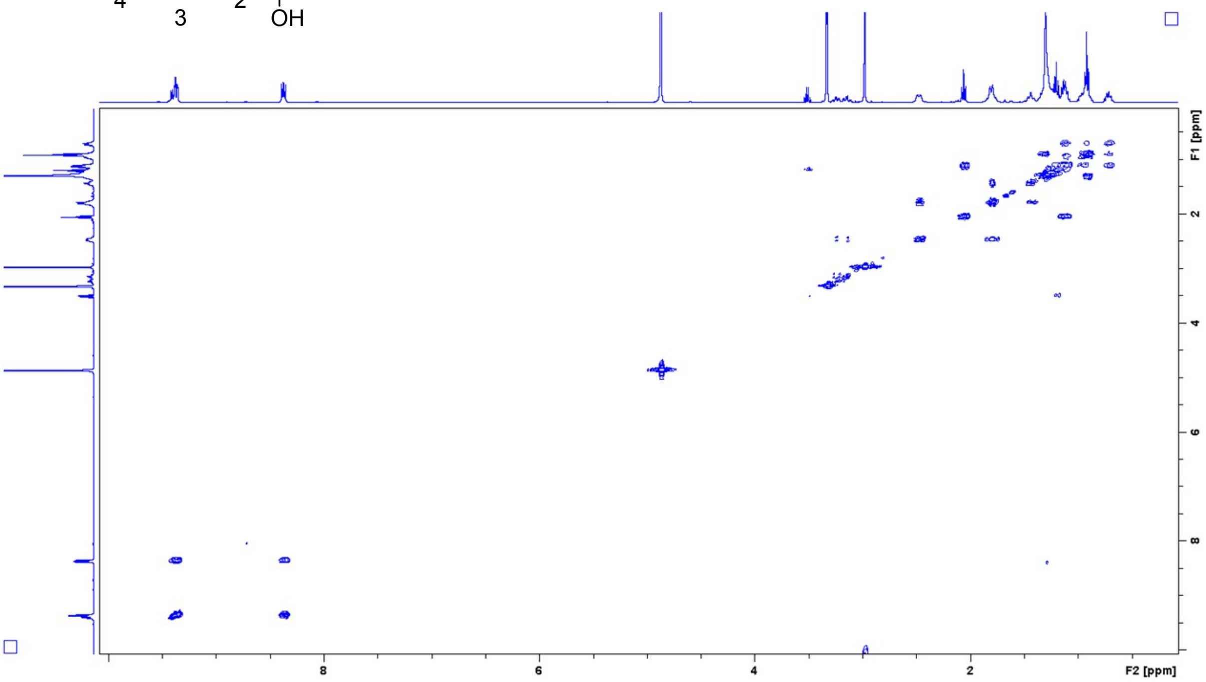

Figure B.58 COSY NMR of **15** in MeOD at 298 K.

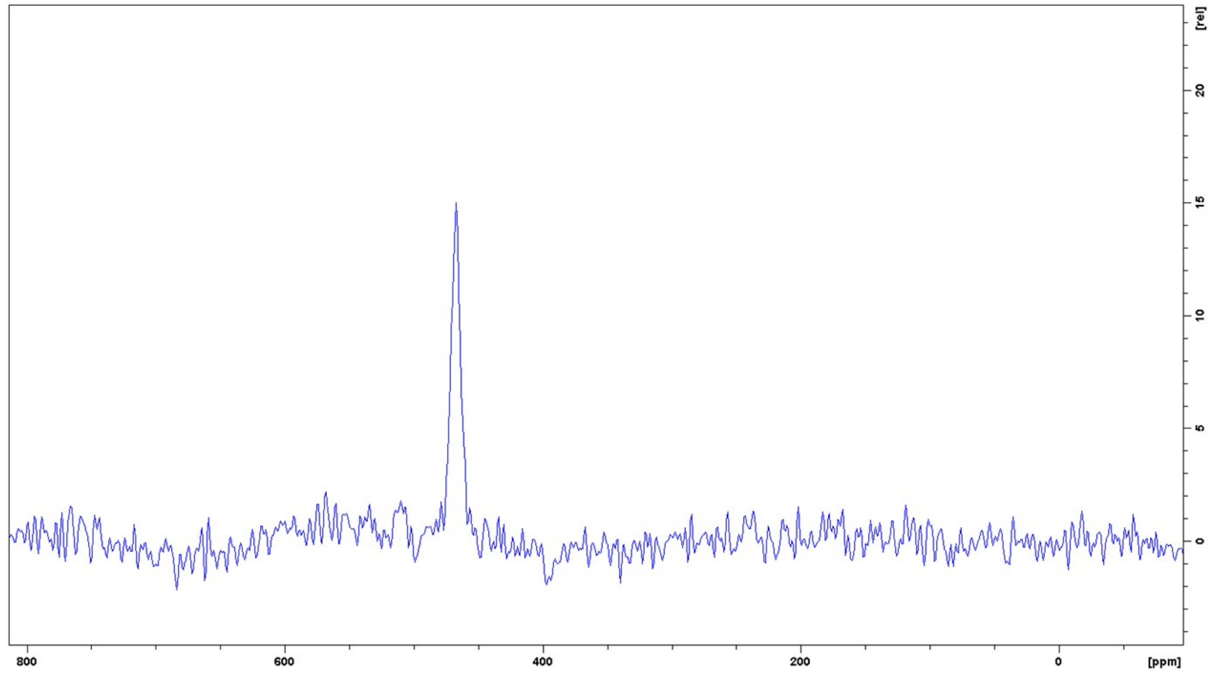

Figure B.59 ^{195}Pt NMR of **15** in MeOD at 298 K, showing a peak at 467 ppm.

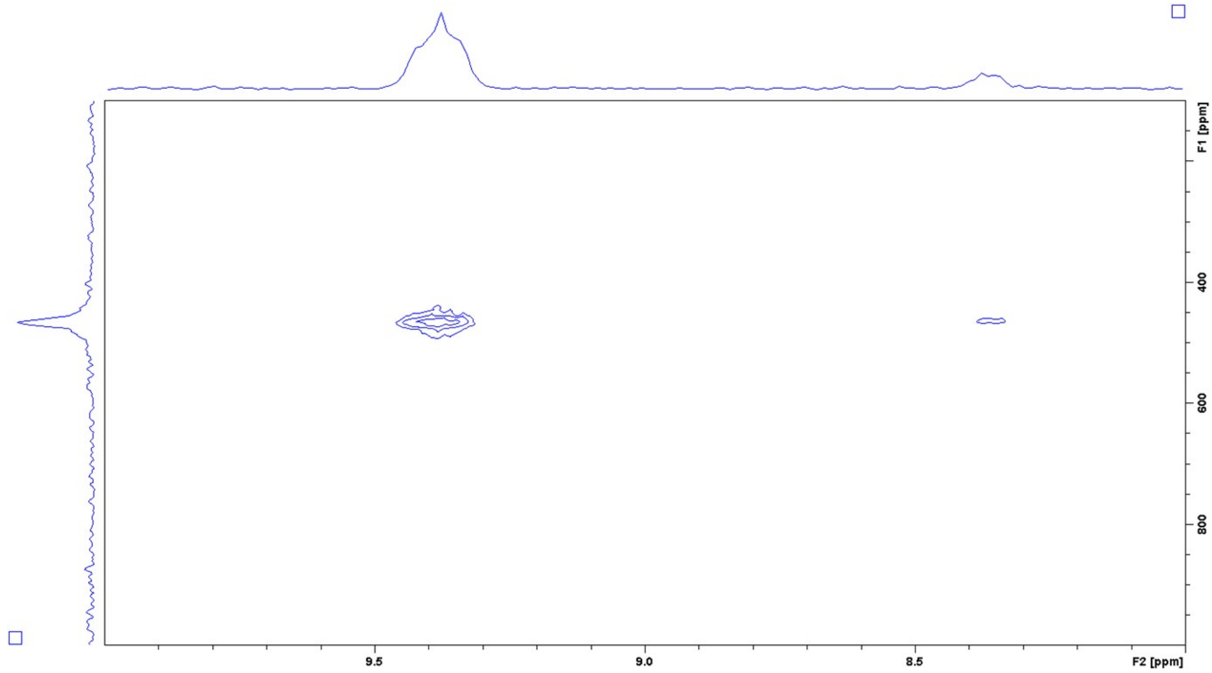

Figure B.60 ^{1}H-^{195}Pt HMQC NMR of **15** showing proton and platinum coupling resonances, in MeOD at 298 K.

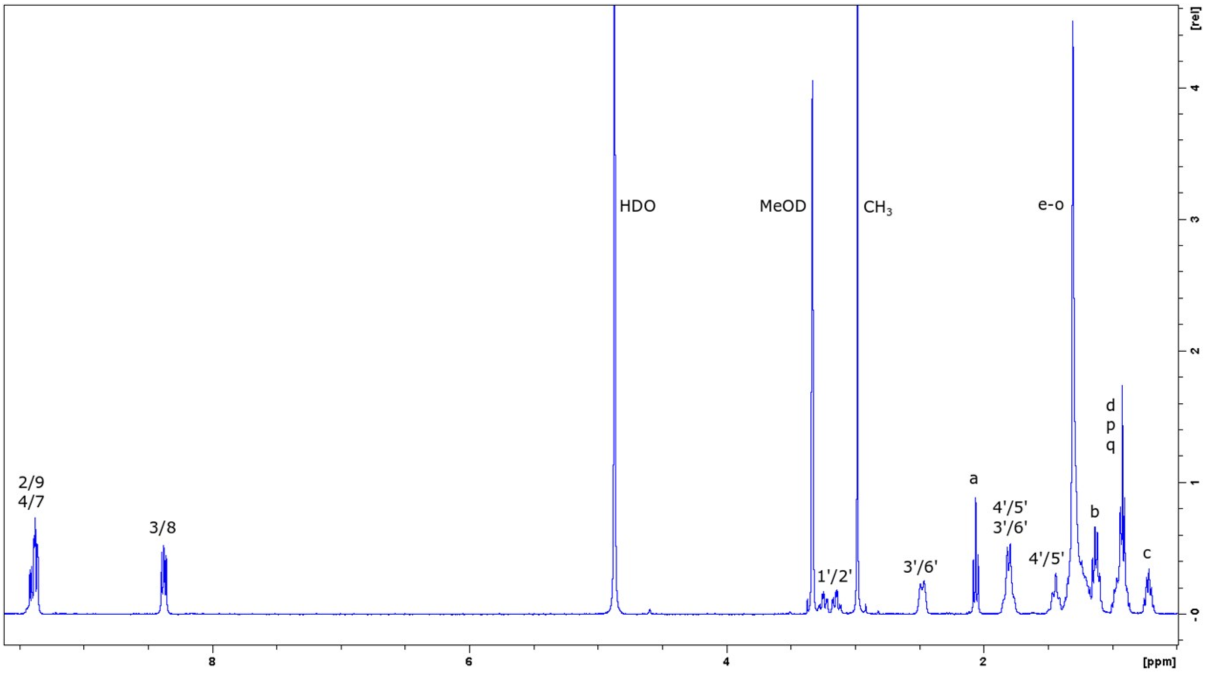

Figure B.61 [1]H NMR of **[Pt(56Me$_2$PHEN)(SSDACH)(OH)(Octadecanoate)](NO$_3$)$_2$** (**16**) in MeOD at 298 K. Inset below: Structure and proton numbering scheme of **16**.

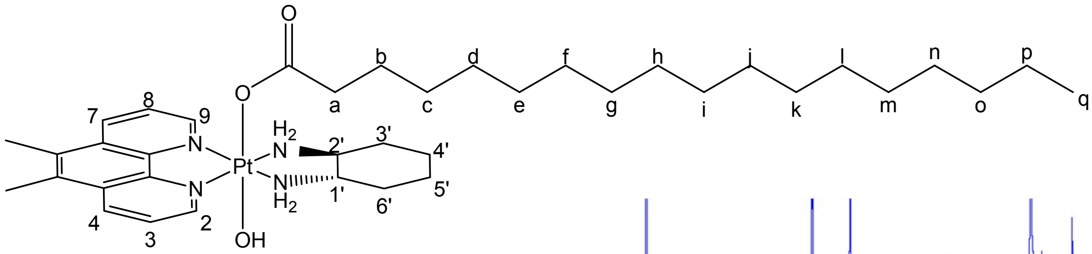

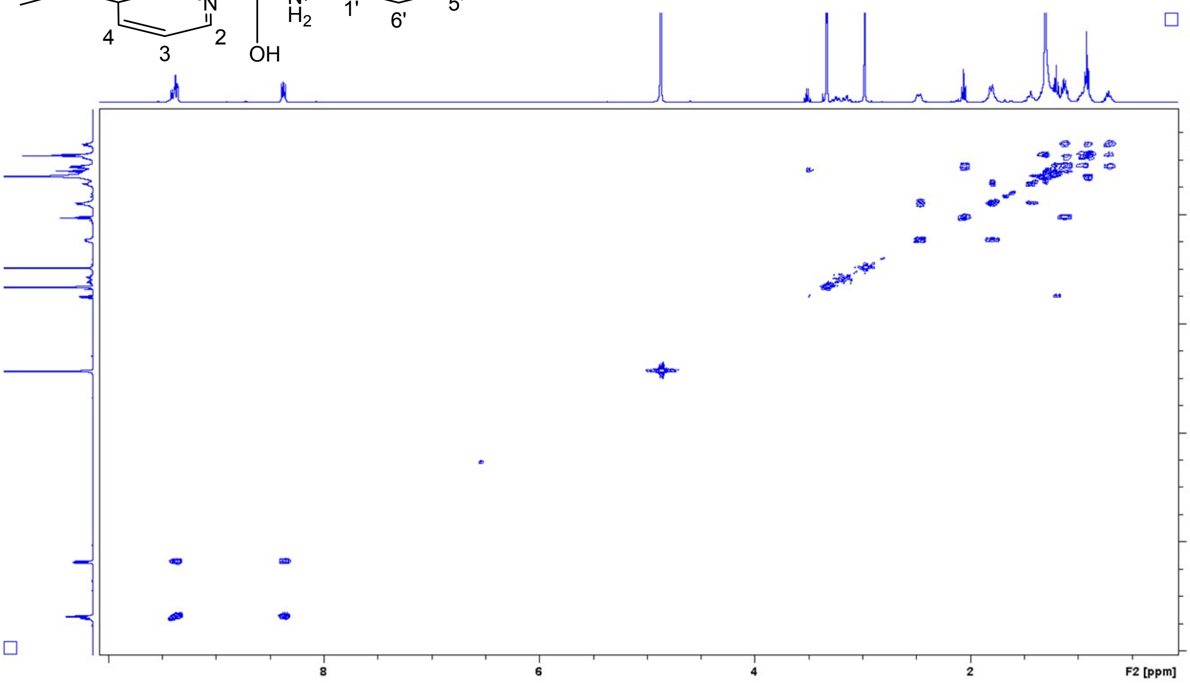

Figure B.62 COSY NMR of **16** in MeOD at 298 K.

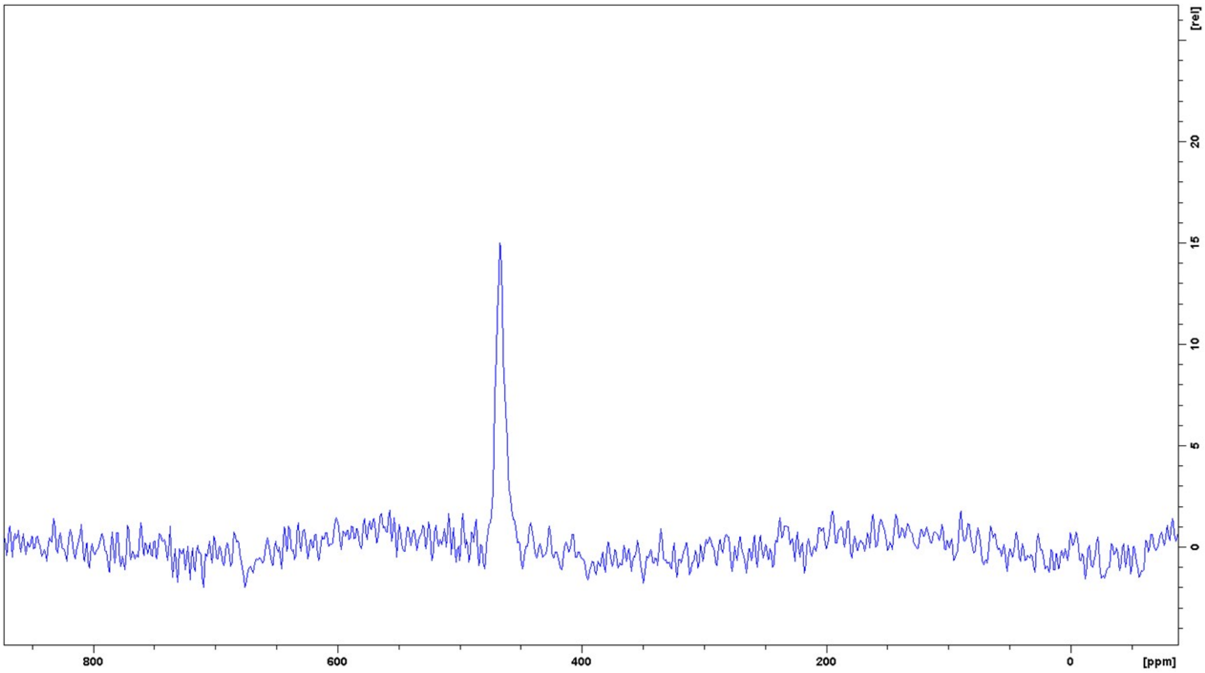

Figure B.63 ^{195}Pt NMR of **16** in MeOD at 298 K, showing a peak at 467 ppm.

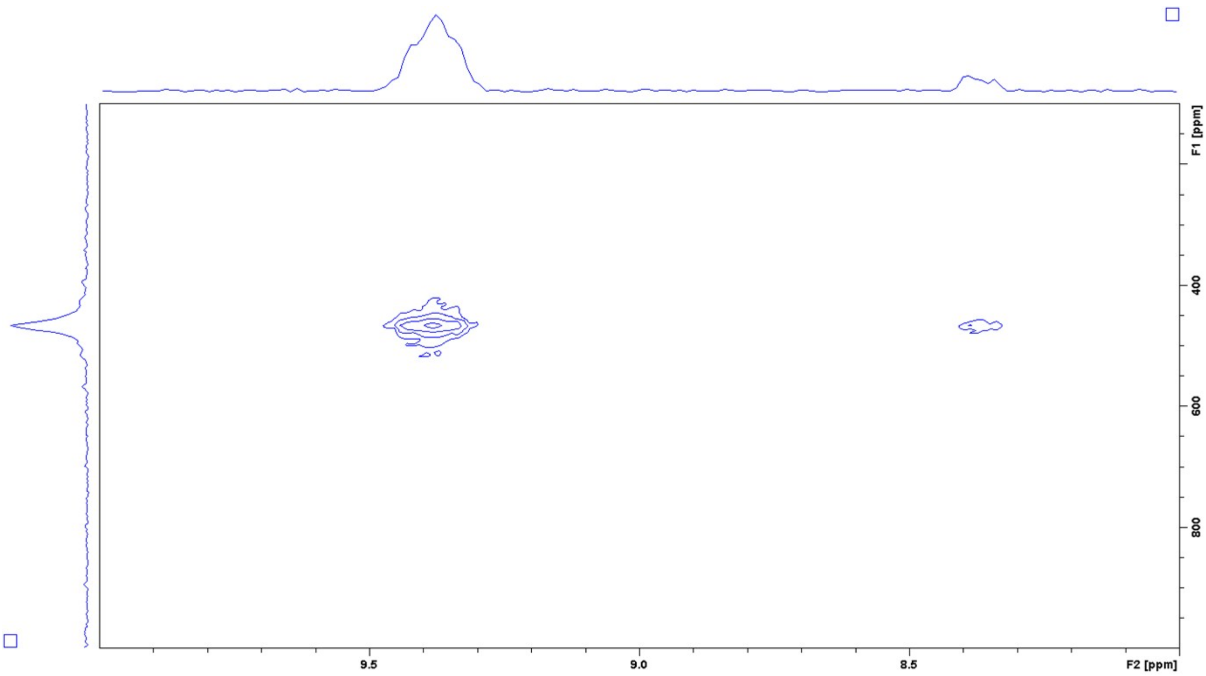

Figure B.64 ^{1}H-^{195}Pt HMQC NMR of **16** showing proton and platinum coupling resonances, in MeOD at 298 K.

Table B.1 Summary of NMR spectroscopy data of **1-8** in MeOD, showing chemical shift (ppm), integration, multiplicity and coupling constants.

	Complex							
Label	**1**	**2**	**3**	**4**	**5**	**6**	**7**	**8**
H2/9	9.46 (dd, J_1 = 11.82 Hz, J_2 = 5.30 Hz, 2 H)	9.59 (d, J = 5.52 Hz, 2 H)	9.46 (dd, J_1 = 12.74 Hz, J_2 = 5.58 Hz, 2 H)	9.59 (d, J = 5.52 Hz, 2 H)	9.45 (dd, J_1 = 12.76 Hz, J_2 = 5.58 Hz, 2 H)	9.59 (d, J = 5.52 Hz, 2 H)	9.46 (dd, J_1 = 11.88 Hz, J_2 = 5.56 Hz, 2 H)	9.46 (dd, J_1 = 11.82 Hz, J_2 = 5.54 Hz, 2 H)
H3/8	8.40 (dd, J_1 = 8.30 Hz, J_2 = 5.54 Hz, 2 H)	8.40 (d, J_1 = 8.26 Hz, J_2 = 5.58 Hz, 2 H)	8.40 (dd, J_1 = 8.30 Hz, J_2 = 5.54 Hz, 2 H)	8.40 (dd, J_1 = 8.28 Hz, J_2 = 5.60 Hz, 2 H)	8.40 (dd, J_1 = 8.30 Hz, J_2 = 5.54 Hz, 2 H)	8.40 (d, J_1 = 8.28 Hz, J_2 = 5.60 Hz, 2 H)	8.40 (dd, J_1 = 8.30 Hz, J_2 = 5.54 Hz, 2 H)	8.40 (dd, J_1 = 8.28 Hz, J_2 = 5.52 Hz, 2 H)
H4/7	9.23 (d, J = 8.28 Hz, 2 H)	9.24 (d, J = 8.24 Hz, 2 H)	9.24 (d, J = 8.32 Hz, 2 H)	9.24 (d, J = 8.24 Hz, 2 H)	9.24 (d, J = 8.28 Hz, 2 H)	9.24 (d, J = 8.28 Hz, 2 H)	9.23 (d, J = 8.36 Hz, 2 H)	9.23 (d, J = 8.32 Hz, 2 H)
H5/6	8.47 (s, 2 H)	8.47 (s, 2H)	8.47 (s, 2 H)	8.47 (s, 2 H)	8.47 (s, 2 H)	8.47 (s, 2 H)	8.47 (s, 2 H)	8.47 (s, 2 H)
H1′/2′	3.21 (m, 2H)	3.22 (m, 2H)	3.21 (m, 2H)	3.22 (m, 2 H)	3.21 (m, 2H)	3.22 (m, 2H)	3.21 (m, 2H)	3.21 (m, 2H)
H3′/6′	2.48 (m, 2 H)	2.51 (m, 2H)	2.48 (m, 2 H)	2.52 (m, 2 H)	2.48 (m, 2 H)	2.51 (m, 2H)	2.48 (m, 2 H)	2.48 (m, 2 H)
H4′/5′	1.81 (m, 4 H)	1.83 (m, 4 H)	1.81 (m, 4 H)	1.83 (m, 4 H)	1.81 (m, 4 H)	1.83 (m, 4 H)	1.81 (m, 4 H)	1.81 (m, 4 H)
H3′/6′	1.81 (m, 4 H)	1.83 (m, 4 H)	1.81 (m, 4 H)	1.83 (m, 4 H)	1.81 (m, 4 H)	1.83 (m, 4 H)	1.81 (m, 4 H)	1.81 (m, 4 H)
H4′/5′	1.44 (m, 2 H)	1.45 (m, 2 H)	1.43 (m, 2 H)	1.45 (m, 2 H)	1.44 (m, 2 H)	1.45 (m, 2 H)	1.44 (m, 2 H)	1.44 (m, 2 H)
a	2.07 (t, J = 7.32 Hz, 2 H)	2.12 (t, J = 7.28 Hz, 4 H)	2.07 (t, J = 7.34 Hz, 2 H)	2.12 (t, J = 7.28 Hz, 4 H)	2.07 (t, J = 7.32 Hz, 2 H)	2.12 (t, J = 7.30 Hz, 4 H)	2.07 (t, J = 7.34 Hz, 2 H)	2.07 (t, J = 7.32 Hz, 2 H)
b	1.31 – 1.10 (m, 8 H)	1.31 – 1.06 (m, 16 H)	1.35 – 1.09 (m, 12 H)	1.35 – 1.07 (m, 24 H)	1.35 – 1.11 (m, 16 H)	1.36 – 1.07 (m, 32 H)	1.36 – 1.11 (m, 20 H)	1.36 – 1.10 (m, 24 H)
c	0.76 (pnt, J = 7.70 Hz, 2 H)	0.72 (pnt, J = 7.43 Hz, 4 H)	0.77 (m (pnt, J = 7.70 Hz, 2 H)	0.73 (m (pnt, J = 7.48 Hz, 4 H)	0.77 (m (pnt, J = 7.34 Hz, 2 H)	0.72 (m (pnt, J = 7.48 Hz, 4 H)	0.77 (m (pnt, J = 7.29 Hz, 2 H)	0.77 (m (pnt, J = 7.30 Hz, 2 H)
d	1.03 – 0.88 (m, 7 H)	1.03 – 0.88 (m, 14 H)	1.04 – 0.89 (m, 7 H)	1.03 – 0.89 (m, 14 H)	1.04 – 0.90 (m, 7 H)	1.04 – 0.90 (m, 14 H)	1.04 – 0.90 (m, 7 H)	1.04 – 0.90 (m, 7 H)
e	Merged with b	Merged with b	Merged with b	Merged with b	Merged with b	Merged with b	Merged with b	Merged with b
f	″	″	″	″	″	″	″	″
g	″	″	″	″	″	″	″	″
h	Merged with d	Merged with d	″	″	″	″	″	″
i	″	″	″	″	″	″	″	″
j	-	-	Merged with d	Merged with d	″	″	″	″
k	-	-	″	″	″	″	″	″

l	-	-	-	-	Merged with d	Merged with d	″	″
m	-	-	-	-	″	″	″	″
n	-	-	-	-	-	-	Merged with d	″
o	-	-	-	-	-	-	″	″
p	-	-	-	-	-	-	-	Merged with d
q	-	-	-	-	-	-	-	″
$^{1}H/^{195}Pt$	9.45, 8.39/480	9.59, 8.40/688	9.45, 8.40/479	9.59, 8.40/686	9.45, 8.39/480	9.58, 8.40/688	9.45, 8.40/480	9.45, 8.40/478

Table B.2 Summary of NMR spectroscopy data of **9-16** in MeOD, showing chemical shift (ppm), integration, multiplicity and coupling constants.

	Complex							
Label	**9**	**10**	**11**	**12**	**13**	**14**	**15**	**16**
H2/9	9.38 (m, 4 H)	9.53 (d, *J* = 5.52 Hz, 2 H)	9.38 (m, 4 H)	9.54 (d, *J* = 5.48 Hz, 2 H)	9.38 (m, 4 H)	9.53 (d, *J* = 5.24 Hz, 2 H)	9.38 (m, 4 H)	9.38 (m, 4 H)
H3/8	8.37 (d, J_1 = 8.56 Hz, J_2 = 5.48 Hz, 2 H)	8.37 (d, J_1 = 8.58 Hz, J_2 = 5.54 Hz, 2 H)	8.37 (d, J_1 = 8.56 Hz, J_2 = 5.48 Hz, 2 H)	8.37 (d, J_1 = 8.58 Hz, J_2 = 5.54 Hz, 2 H)	8.37 (d, J_1 = 8.54 Hz, J_2 = 5.54 Hz, 2 H)	8.37 (d, J_1 = 8.56 Hz, J_2 = 5.56 Hz, 2 H)	8.36 (d, J_1 = 8.60 Hz, J_2 = 5.52 Hz, 2 H)	8.37 (d, J_1 = 8.56 Hz, J_2 = 5.52 Hz, 2 H)
H4/7	9.38 (m, 4 H)	9.38 (d, *J* = 8.36 Hz, 2 H)	9.38 (m, 4 H)	9.37 (d, *J* = 8.52 Hz, 2 H)	9.38 (m, 4 H)	9.37 (d, *J* = 8.48 Hz, 2 H)	9.38 (m, 4 H)	9.38 (m, 4 H)
CH_3	2.98 (s, 6 H)	2.97 (s, 6 H)	2.98 (s, 6 H)	2.97 (s, 6 H)	2.98 (s, 6 H)	2.97 (s, 6 H)	2.98 (s, 6 H)	2.98 (s, 6 H)
H1′/2′	3.20 (m, 2H)	3.20 (m, 2H)	3.19 (m, 2H)	3.21 (m, 2H)	3.19 (m, 2H)	3.20 (m, 2H)	3.20 (m, 2H)	3.19 (m, 2H)
H3′/6′	2.47 (m, 2H)	2.51 (m, 2H)	2.47 (m, 2H)	2.51 (m, 2H)	2.47 (m, 2H)	2.51 (m, 2H)	2.47 (m, 2H)	2.47 (m, 2H)
H4′/5′	1.80 (m, 4 H)	1.82 (m, 4 H)	1.80 (m, 4 H)	1.82 (m, 4 H)	1.80 (m, 4 H)	1.83 (m, 4 H)	1.80 (m, 4 H)	1.80 (m, 4 H)
H3′/6′	1.80 (m, 4 H)	1.82 (m, 4 H)	1.80 (m, 4 H)	1.82 (m, 4 H)	1.80 (m, 4 H)	1.83 (m, 4 H)	1.80 (m, 4 H)	1.80 (m, 4 H)
H4′/5′	1.43 (m, 2 H)	1.44 (m, 2 H)	1.44 (m, 2 H)	1.44 (m, 2 H)	1.44 (m, 2 H)	1.45 (m, 2 H)	1.43 (m, 2 H)	1.43 (m, 2 H)
a	2.06 (t, *J* = 7.26 Hz, 2 H)	2.11 (t, *J* = 7.26 Hz, 4 H)	2.06 (t, *J* = 7.26 Hz, 2 H)	2.11 (t, *J* = 7.26 Hz, 4 H)	2.06 (t, *J* = 7.24 Hz, 2 H)	2.11 (t, *J* = 7.24 Hz, 4 H)	2.06 (t, *J* = 7.26 Hz, 2 H)	2.06 (t, *J* = 7.26 Hz, 2 H)
b	1.30 – 1.09 (m, 8 H)	1.30 – 1.06 (m, 16 H)	1.34 – 1.08 (m, 12 H)	1.34 – 1.05 (m, 24 H)	1.36 – 1.08 (m, 16 H)	1.35 – 1.06 (m, 32 H)	1.36 – 1.08 (m, 20 H)	1.36 – 1.08 (m, 24 H)
c	0.71 (pnt, *J* = 7.36 Hz, 2 H)	0.68 (pnt, *J* = 7.47 Hz, 4 H)	0.71 (pnt, *J* = 7.42 Hz, 2 H)	0.69 (pnt, *J* = 7.46 Hz, 4 H)	0.71 (pnt, *J* = 7.43 Hz, 2 H)	0.68 (pnt, *J* = 7.50 Hz, 4 H)	0.71 (pnt, *J* = 7.46 Hz, 2 H)	0.71 (pnt, *J* = 7.31 Hz, 2 H)
d	1.00 – 0.87 (m, 7 H)	1.01 – 0.86 (m, 14 H)	1.00 – 0.86 (m, 7 H)	1.01 – 0.86 (m, 14 H)	1.00 – 0.86 (m, 7 H)	1.01 – 0.86 (m, 14 H)	1.00 – 0.86 (m, 7 H)	1.00 – 0.86 (m, 7 H)
e	Merged with b	Merged with b	Merged with b	Merged with b	Merged with b	Merged with b	Merged with b	Merged with b
f	″	″	″	″	″	″	″	″
g	″	″	″	″	″	″	″	″
h	Merged with d	Merged with d	″	″	″	″	″	″
i	″	″	″	″	″	″	″	″
j	-	-	Merged with d	Merged with d	″	″	″	″
k	-	-	″	″	″	″	″	″

l	-	-	-	-	Merged with d	Merged with d	″	″
m	-	-	-	-	″	″	″	″
n	-	-	-	-	-	-	Merged with d	″
o	-	-	-	-	-	-	″	″
p	-	-	-	-	-	-	-	Merged with d
q	-	-	-	-	-	-	-	″
$^{1}H/^{195}Pt$	9.38, 8.36/468	9.53, 8.37/674	9.37, 8.36/465	9.52, 8.36/673	9.38, 8.37/467	9.54, 8.40/672	9.38, 8.36/467	9.38, 8.37/467

C. HPLC Traces

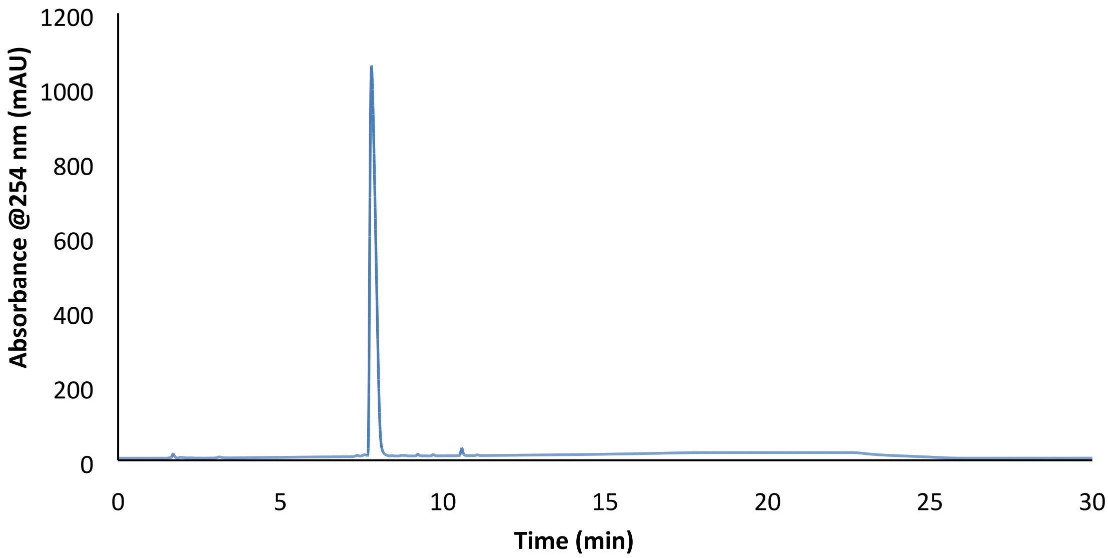

Figure C.1 HPLC trace of **[Pt(PHEN)(SSDACH)(OH)(Decanoate)]$(NO_3)_2$** (**1**) using a gradient of 10–100 % (H_2O:ACN/H_2O) over 15 min, T_R = 7.8 min.

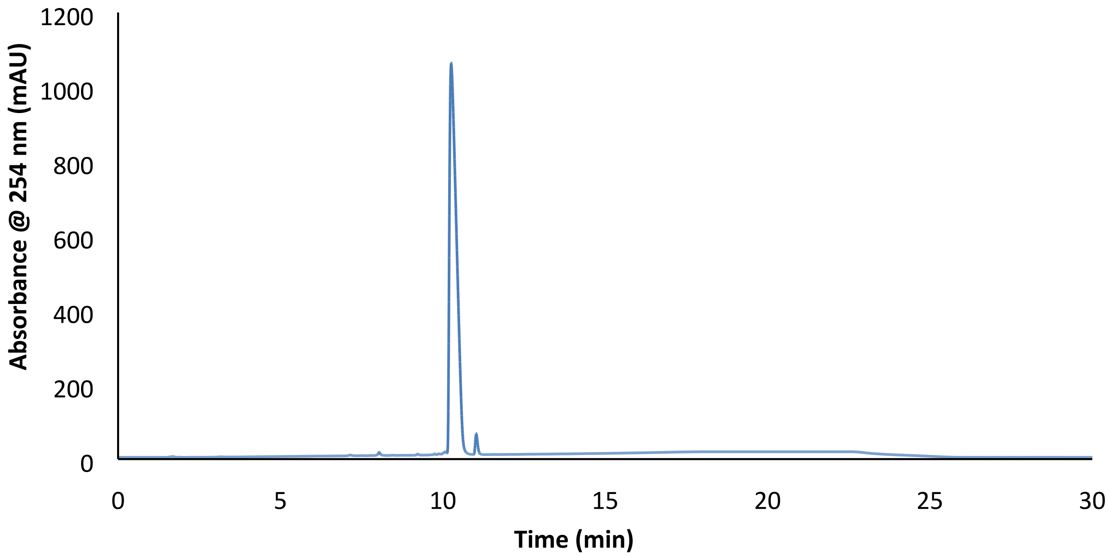

Figure C.2 HPLC trace of **[Pt(PHEN)(SSDACH)(Decanoate)$_2$]$(NO_3)_2$** (**2**) using a gradient of 10–100 % (H_2O:ACN/H_2O) over 15 min, T_R = 10.3 min.

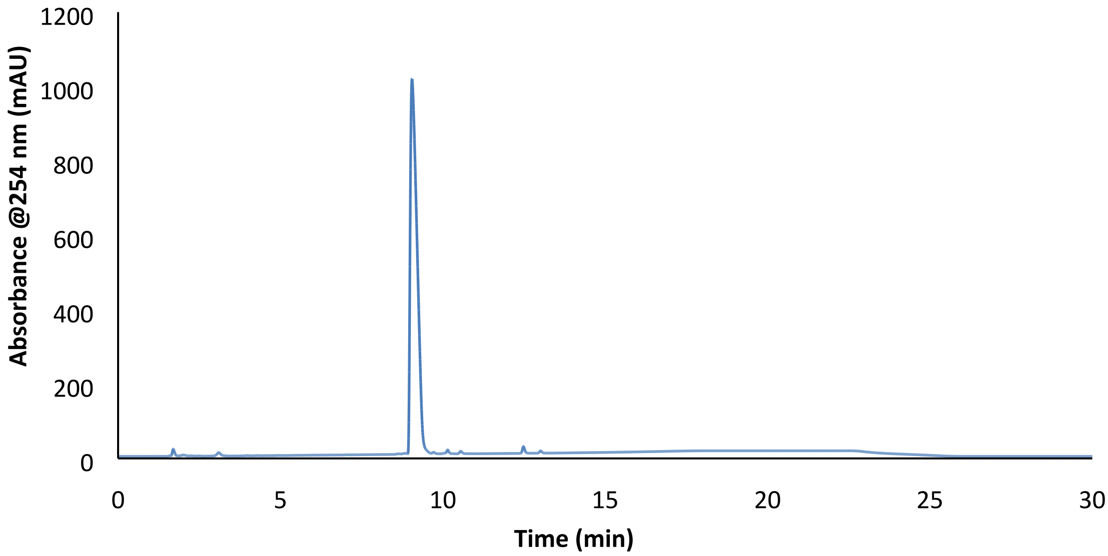

Figure C.3 HPLC trace of **[Pt(PHEN)(SSDACH)(OH)(Dodecanoate)]$(NO_3)_2$** (**3**) using a gradient of 10–100 % (H_2O:ACN/H_2O) over 15 min, T_R = 9.1 min.

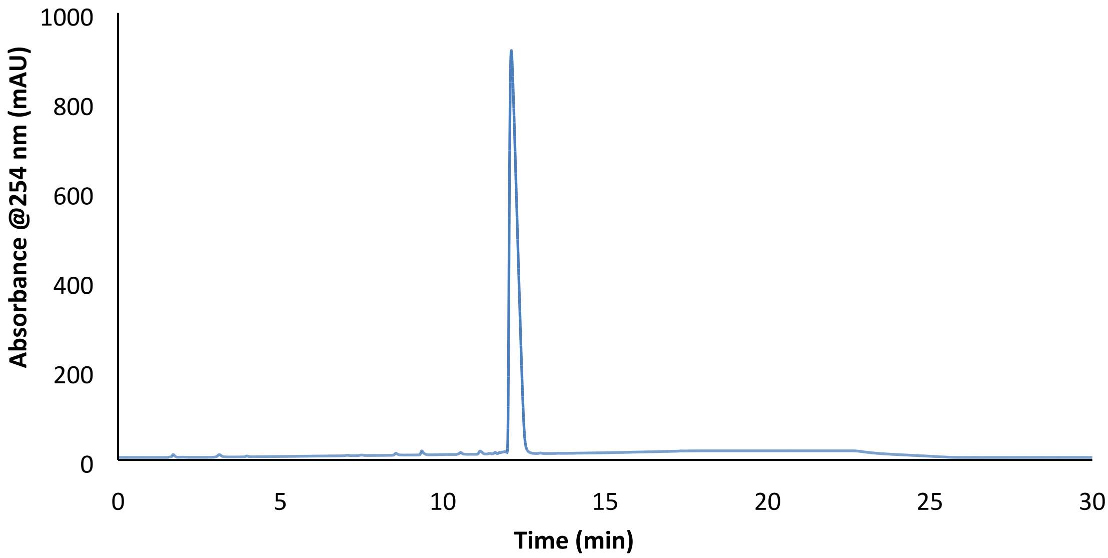

Figure C.4 HPLC trace of **[Pt(PHEN)(SSDACH)$(Dodecanoate)_2$]$(NO_3)_2$** (**4**) using a gradient of 10–100 % (H_2O:ACN/H_2O) over 15 min, T_R = 12.1 min.

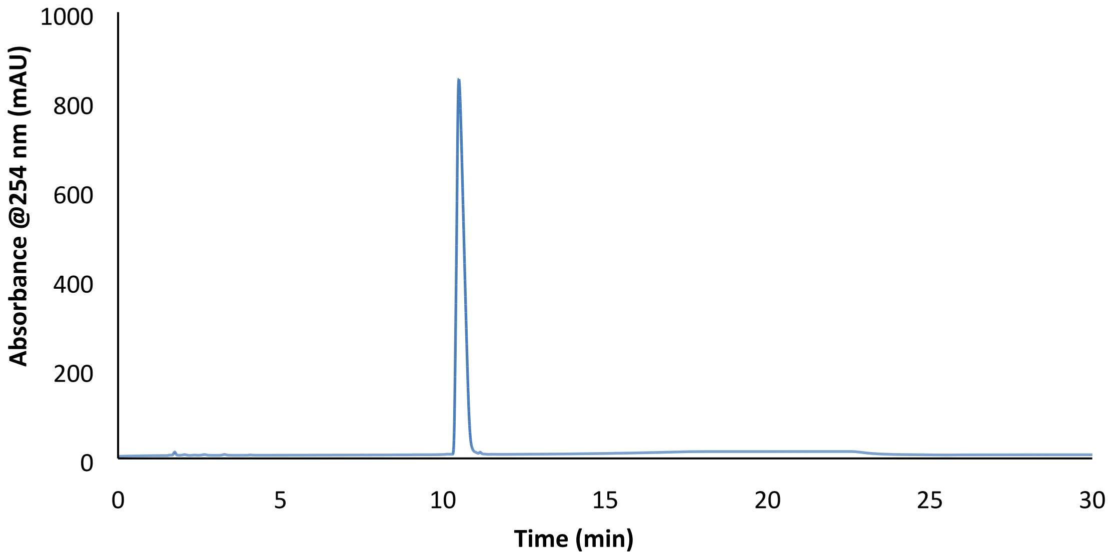

Figure C.5 HPLC trace of **[Pt(PHEN)(SSDACH)(OH)(Tetradecanoate)](NO_3)$_2$ (5)** using a gradient of 10–100 % (H_2O:ACN/H_2O) over 15 min, T_R = 10.3 min.

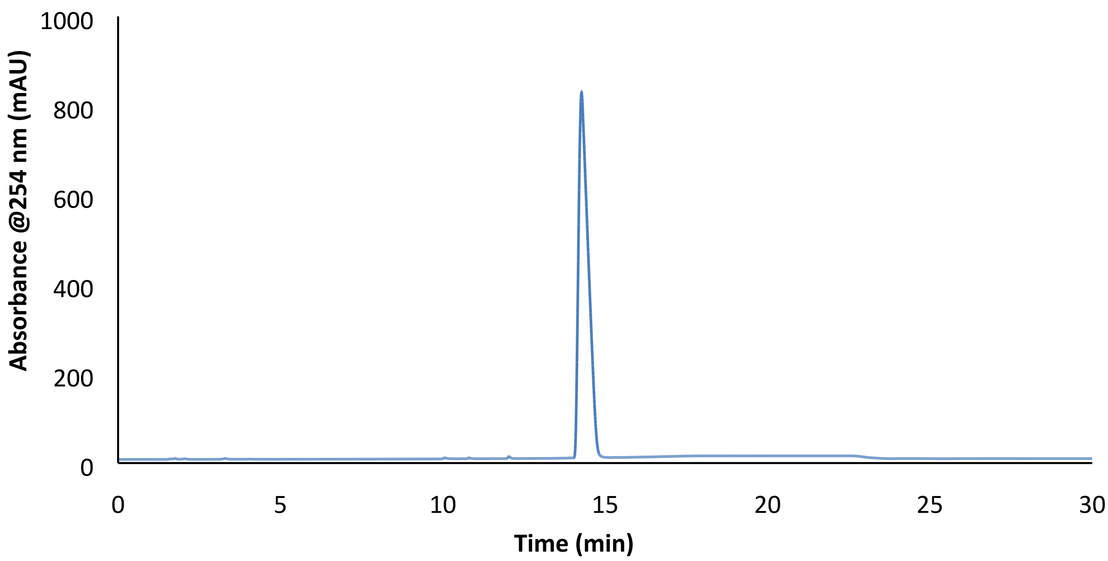

Figure C.6 HPLC trace of **[Pt(PHEN)(SSDACH)(Tetradecanoate)$_2$](NO_3)$_2$ (6)** using a gradient of 10–100 % (H_2O:ACN/H_2O) over 15 min, T_R = 14.1 min.

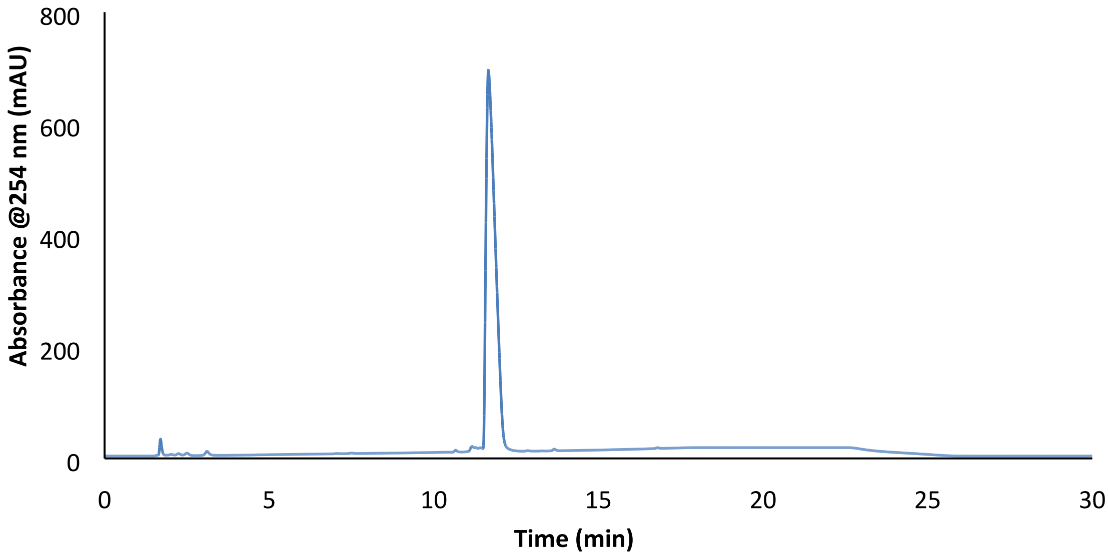

Figure C.7 HPLC trace of **[Pt(PHEN)(SSDACH)(OH)(Hexadecanoate)]$(NO_3)_2$** (**7**) using a gradient of 10–100 % (H_2O:ACN/H_2O) over 15 min, T_R = 11.7 min.

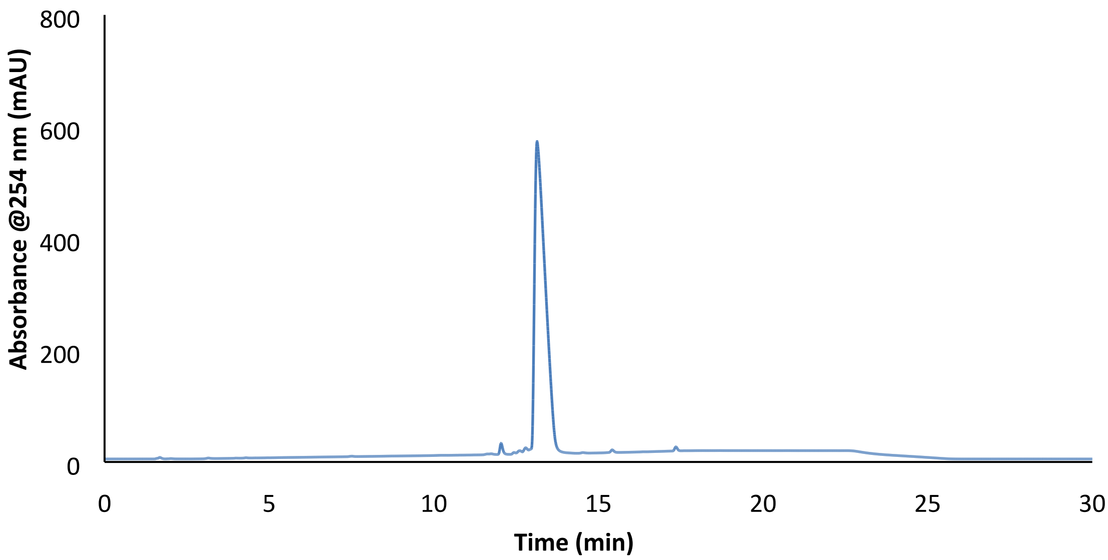

Figure C.8 HPLC trace of **[Pt(PHEN)(SSDACH)(OH)(Octadecanoate)]$(NO_3)_2$** (**8**) using a gradient of 10–100 % (H_2O:ACN/H_2O) over 15 min, T_R = 13.1 min.

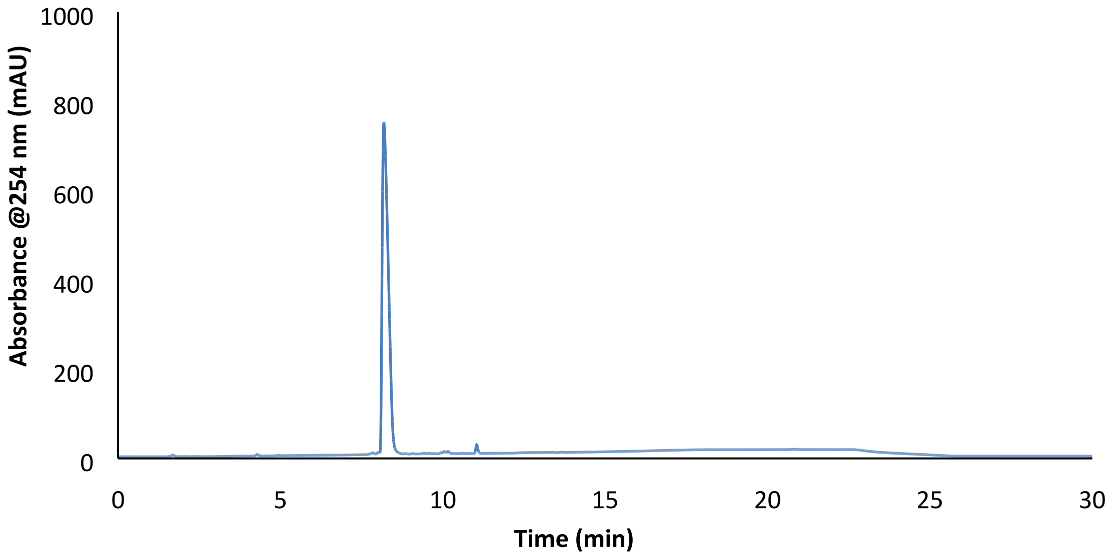

Figure C.9 HPLC trace of **[Pt(56Me$_2$PHEN)(SSDACH)(OH)(Decanoate)](NO$_3$)$_2$** (**9**) using a gradient of 10–100 % (H_2O:ACN/H_2O) over 15 min, T_R = 8.2 min.

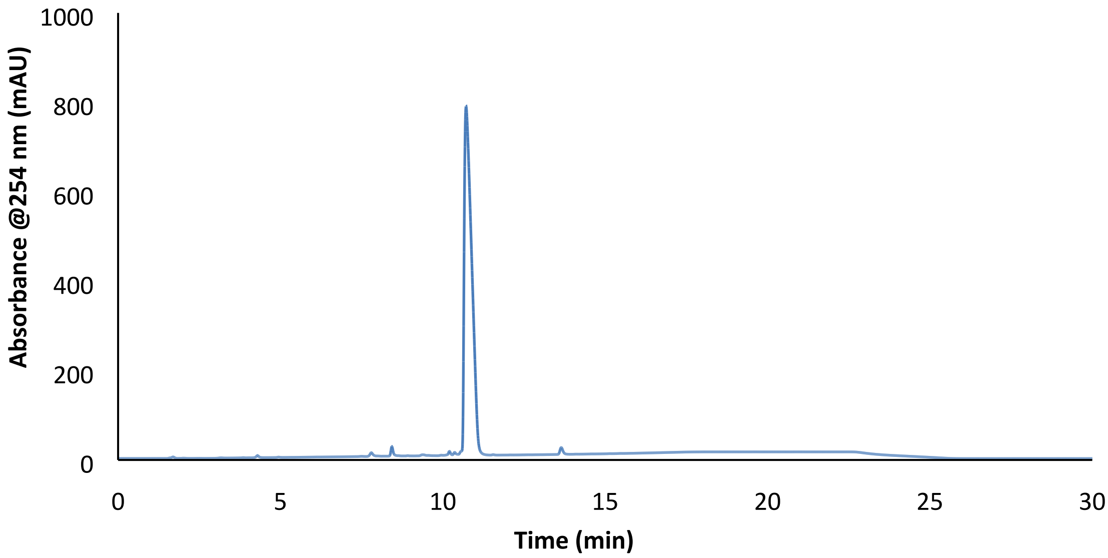

Figure C.10 HPLC trace of **[Pt(56Me$_2$PHEN)(SSDACH)(Decanoate)$_2$](NO$_3$)$_2$** (**10**) using a gradient of 10–100 % (H_2O:ACN/H_2O) over 15 min, T_R = 10.7 min.

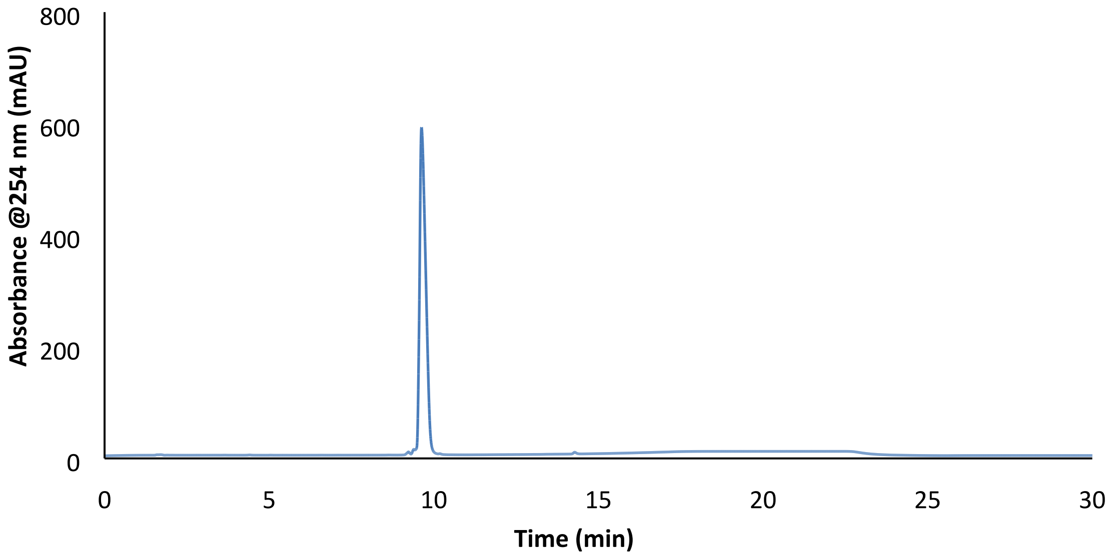

Figure C.11 HPLC trace of **[Pt(56Me$_2$PHEN)(SSDACH)(OH)(Dodecanoate)](NO$_3$)$_2$** (**11**) using a gradient of 10–100 % (H_2O:ACN/H_2O) over 15 min, T_R = 9.4 min.

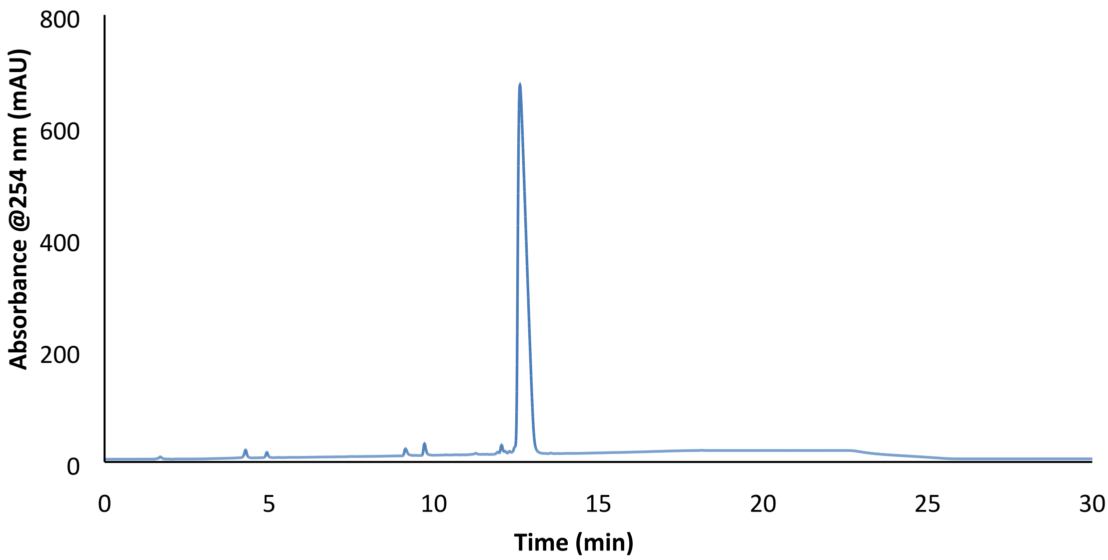

Figure C.12 HPLC trace of **[Pt(56Me$_2$PHEN)(SSDACH)(Dodecanoate)$_2$](NO$_3$)$_2$** (**12**) using a gradient of 10–100 % (H_2O:ACN/H_2O) over 15 min, T_R = 12.6 min.

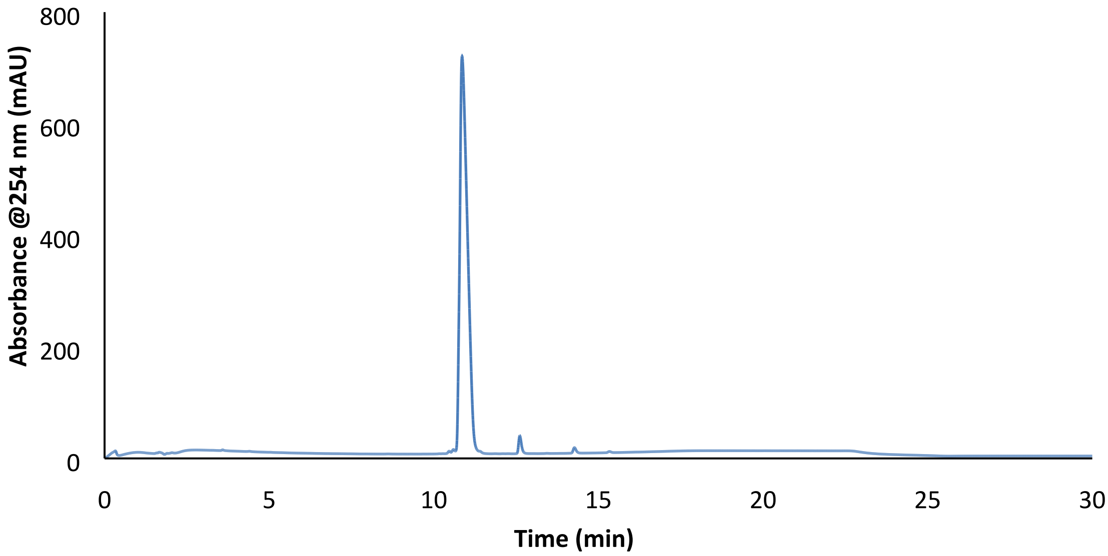

Figure C.13 HPLC trace of **[Pt(56Me$_2$PHEN)(SSDACH)(OH)(Tetradecanoate)](NO$_3$)$_2$** (**13**) using a gradient of 10–100 % (H_2O:ACN/H_2O) over 15 min, T_R = 10.7 min.

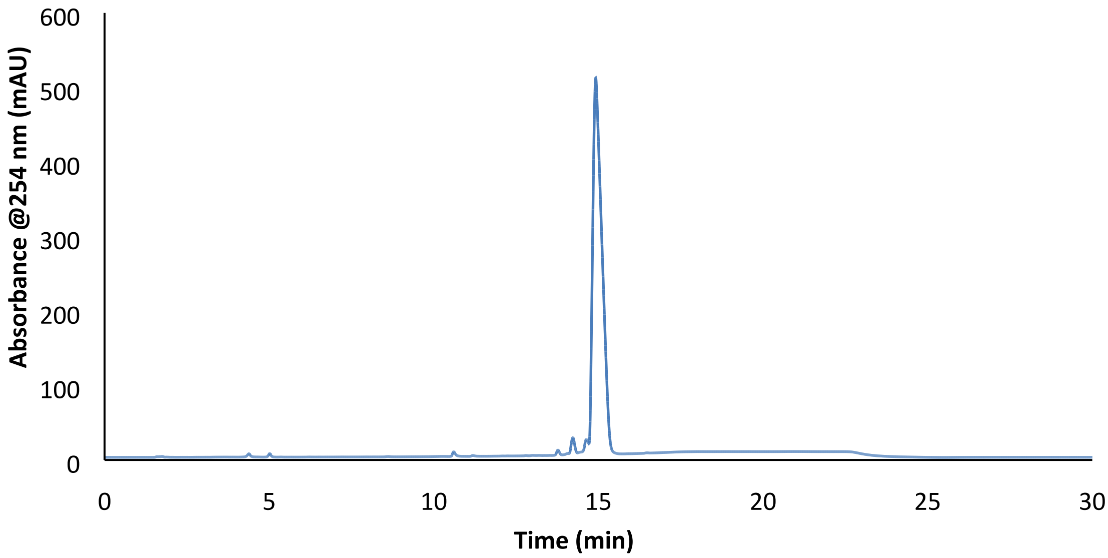

Figure C.14 HPLC trace of **[Pt(56Me$_2$PHEN)(SSDACH)(Tetradecanoate)$_2$](NO$_3$)$_2$** (**14**) using a gradient of 10–100 % (H_2O:ACN/H_2O) over 15 min, T_R = 14.7 min.

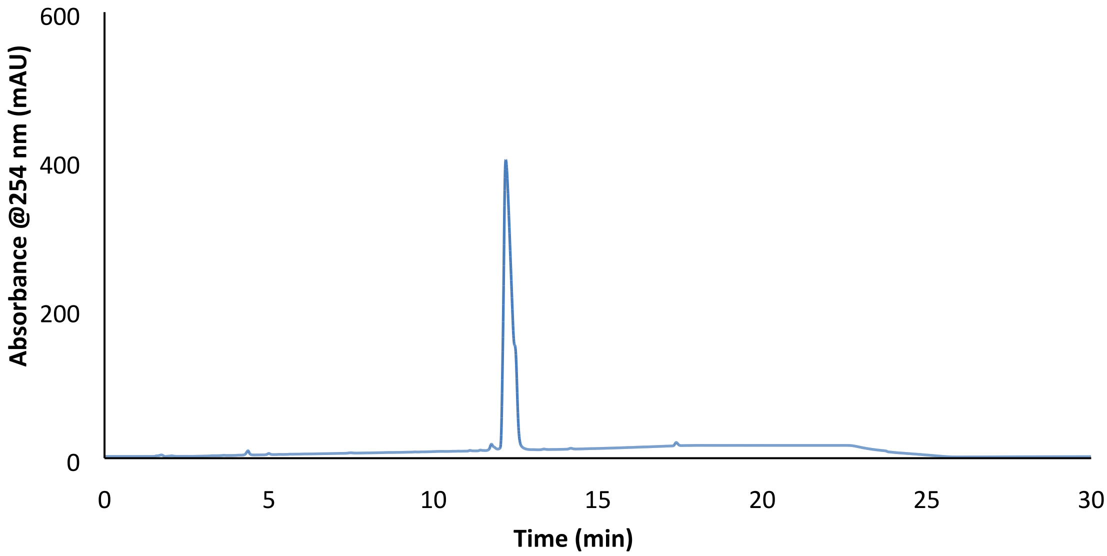

Figure C.15 HPLC trace of **[Pt(56Me$_2$PHEN)(SSDACH)(OH)(Hexadecanoate)](NO$_3$)$_2$** (**15**) using a gradient of 10–100 % (H_2O:ACN/H_2O) over 15 min, T_R = 12.1 min.

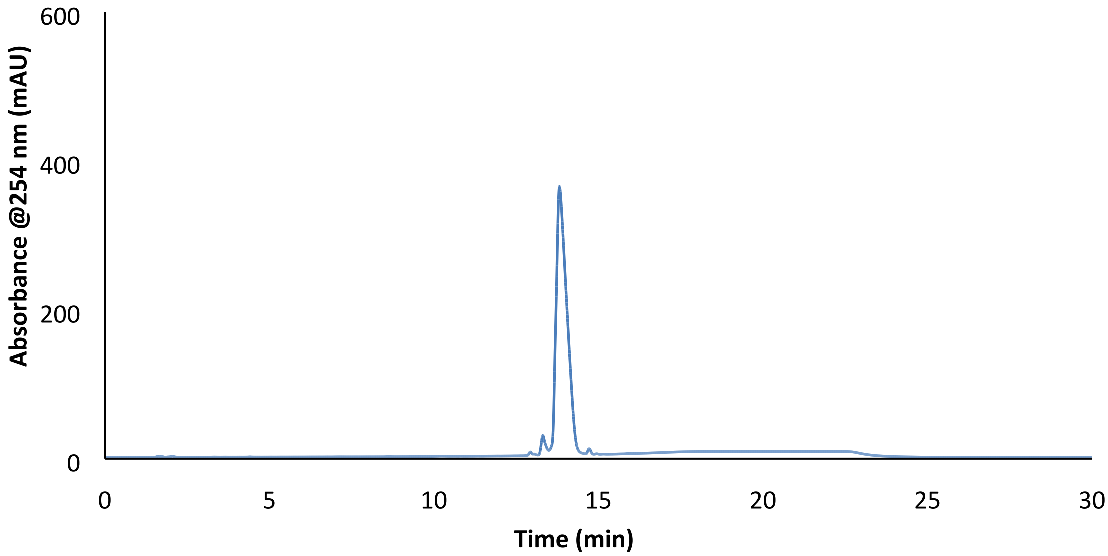

Figure C.16 HPLC trace of **[Pt(56Me$_2$PHEN)(SSDACH)(OH)(Octadecanoate)](NO$_3$)$_2$** (**16**) using a gradient of 10–100 % (H_2O:ACN/H_2O) over 15 min, T_R = 13.7 min.

D. ESI-MS

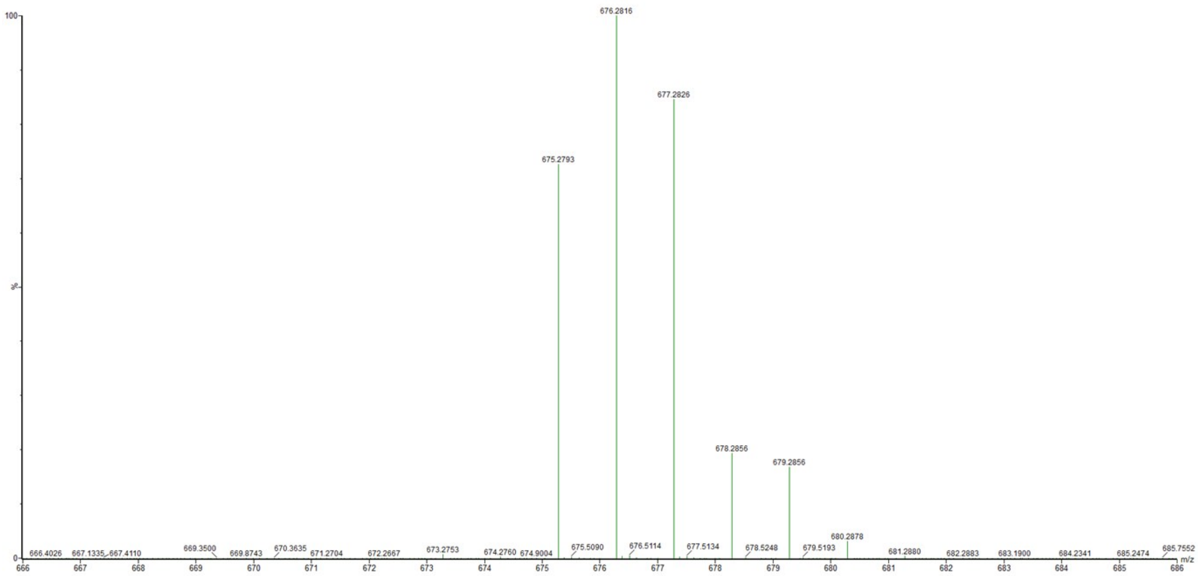

Figure D.1 ESI-MS spectrum of **[Pt(PHEN)(SSDACH)(OH)(Decanoate)](NO_3)$_2$** (**1**).

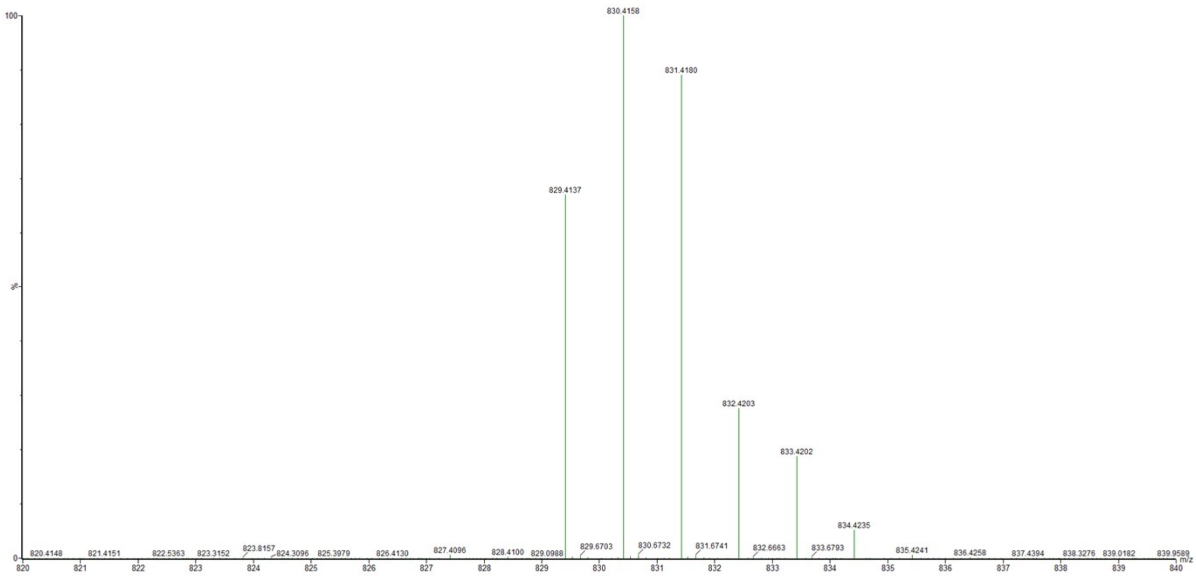

Figure D.2 ESI-MS spectrum of **[Pt(PHEN)(SSDACH)(Decanoate)$_2$](NO_3)$_2$** (**2**).

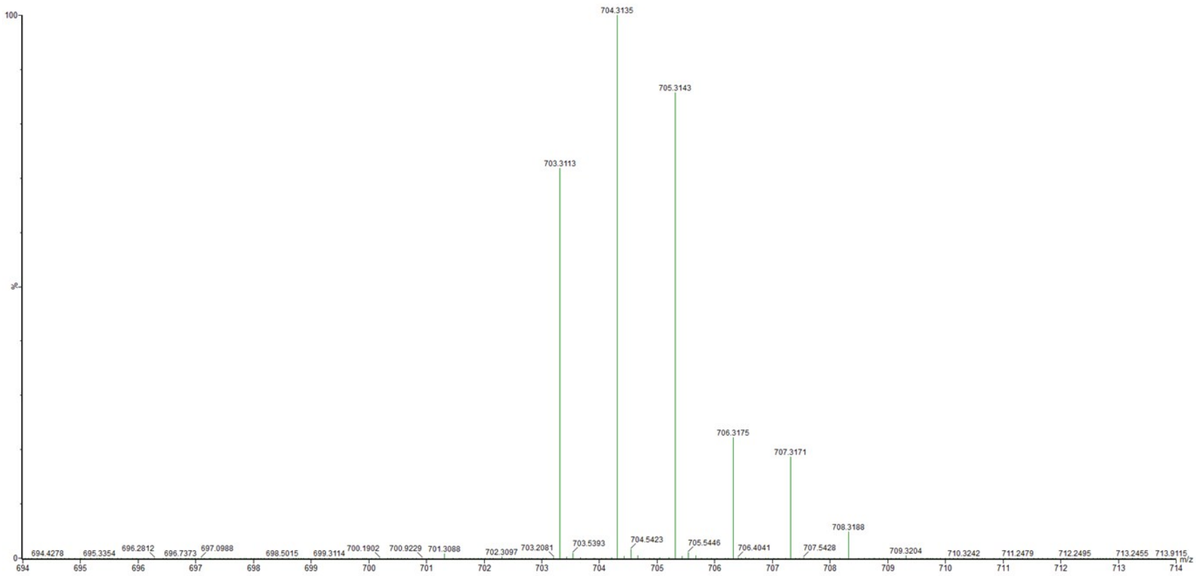

Figure D.3 ESI-MS spectrum of **[Pt(PHEN)(SSDACH)(OH)(Dodecanoate)](NO_3)$_2$** (**3**).

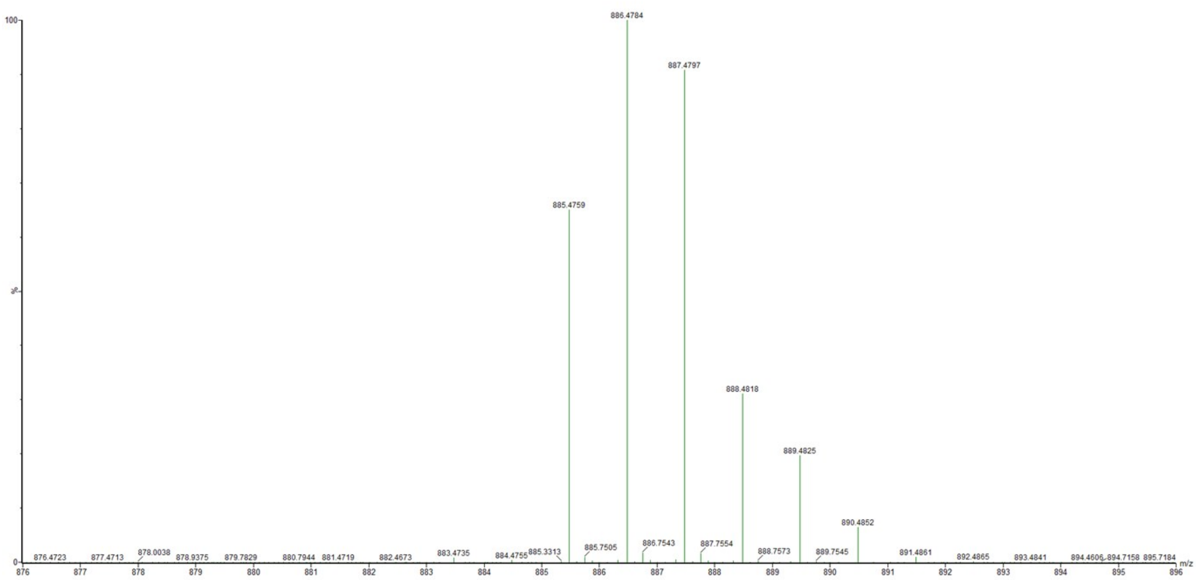

Figure D.4 ESI-MS spectrum of **[Pt(PHEN)(SSDACH)(Dodecanoate)$_2$](NO_3)$_2$** (**4**).

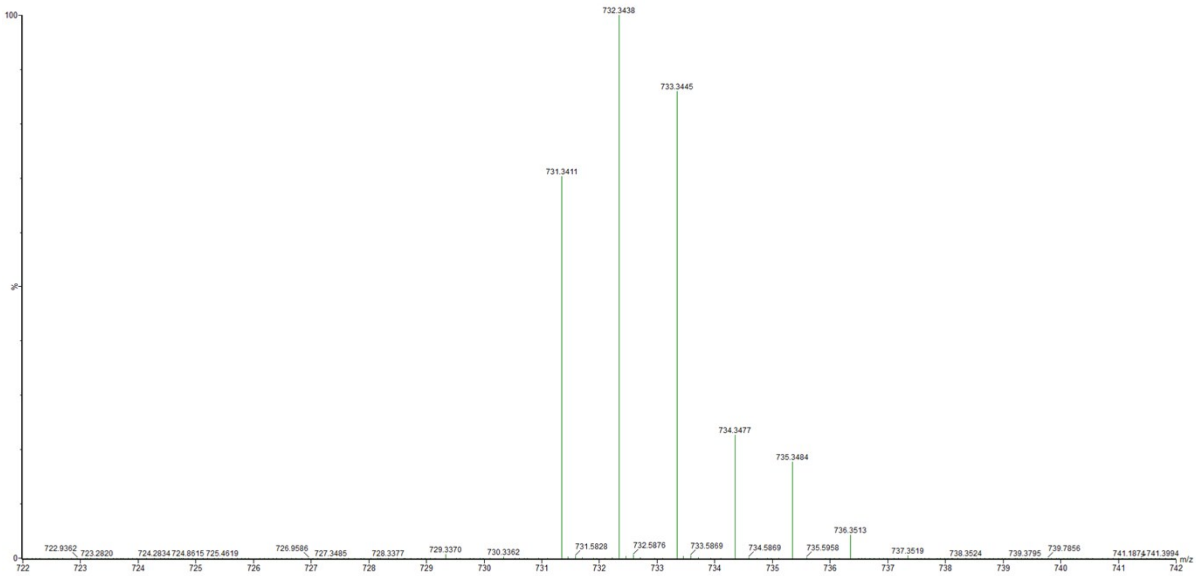

Figure D.5 ESI-MS spectrum of **[Pt(PHEN)(SSDACH)(OH)(Tetradecanoate)]$(NO_3)_2$ (5)**.

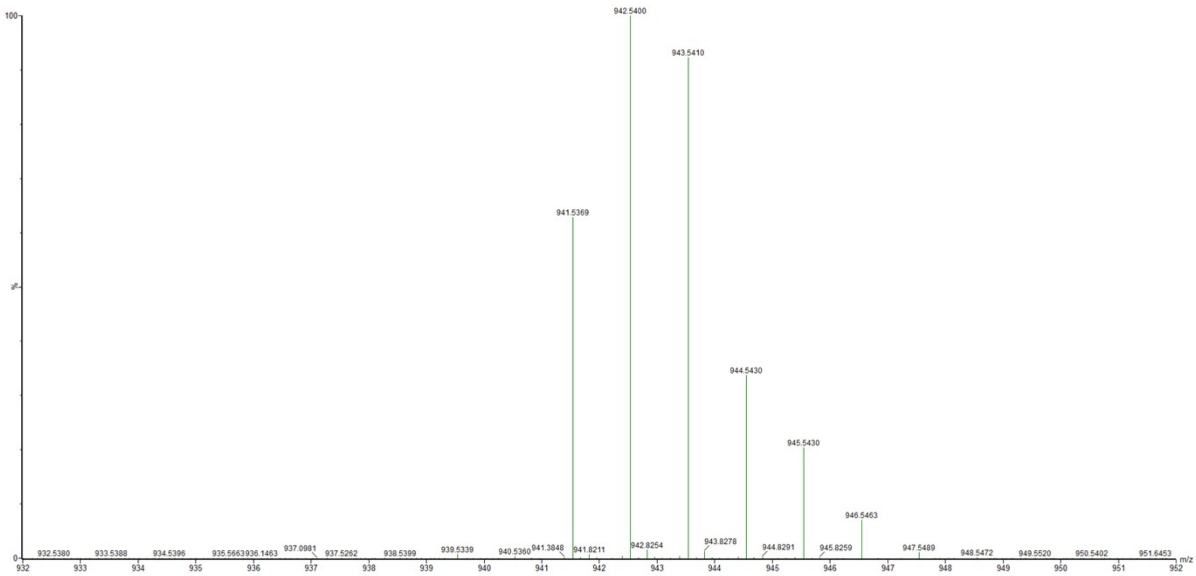

Figure D.6 ESI-MS spectrum of **[Pt(PHEN)(SSDACH)$(Tetradecanoate)_2$]$(NO_3)_2$ (6)**.

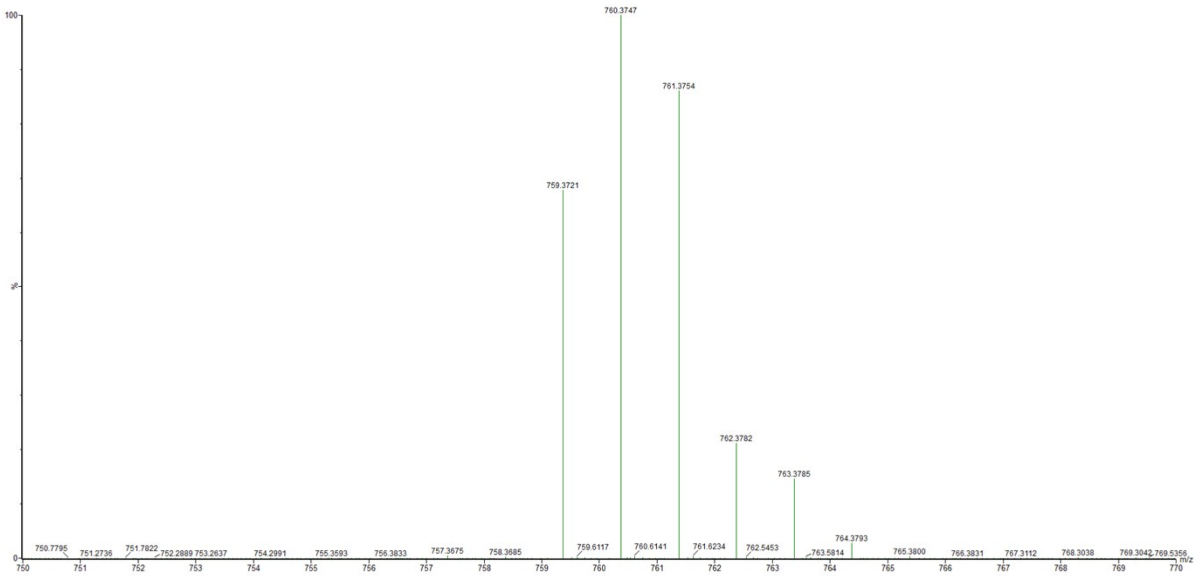

Figure D.7 ESI-MS spectrum of **[Pt(PHEN)(SSDACH)(OH)(Hexadecanoate)](NO_3)$_2$** (**7**).

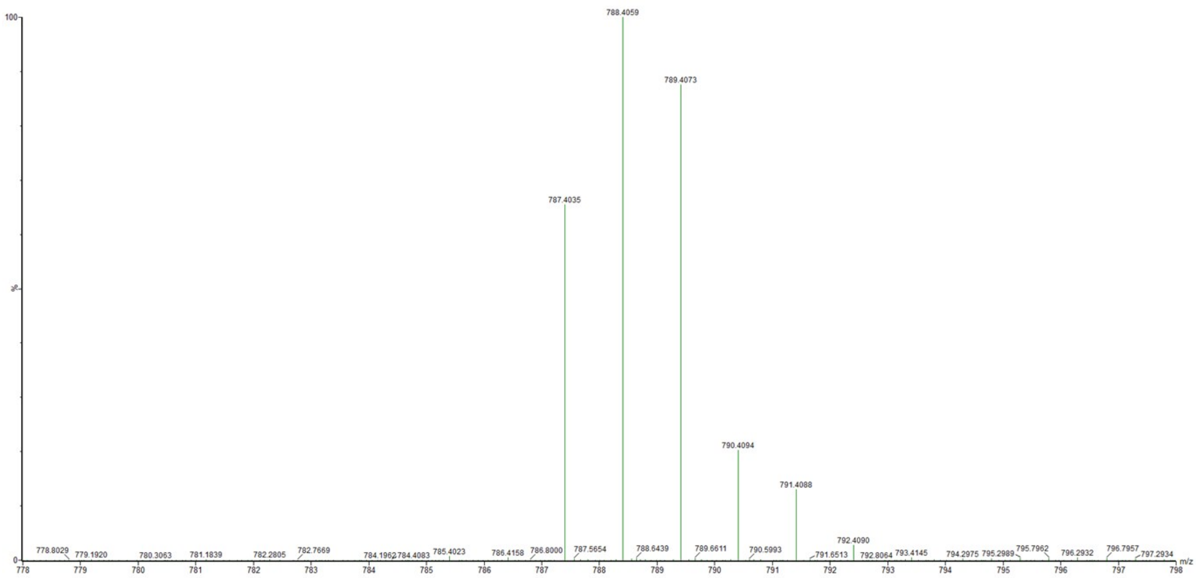

Figure D.8 ESI-MS spectrum of **[Pt(PHEN)(SSDACH)(OH)(Octadecanoate)](NO_3)$_2$** (**8**).

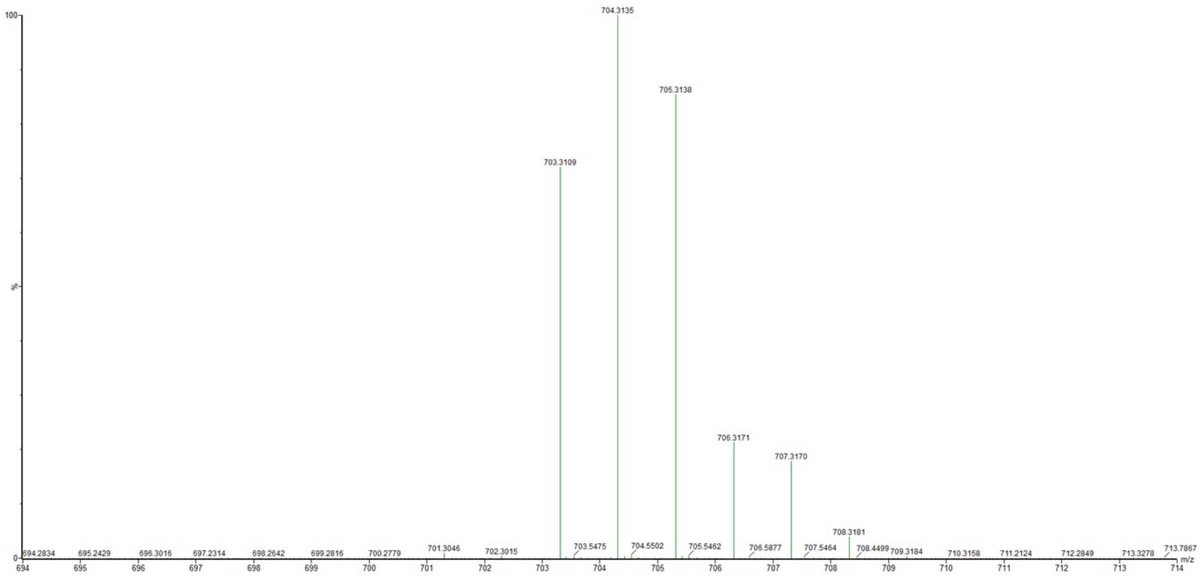

Figure D.9 ESI-MS spectrum of **[Pt(56Me$_2$PHEN)(SSDACH)(OH)(Decanoate)](NO$_3$)$_2$** (**9**).

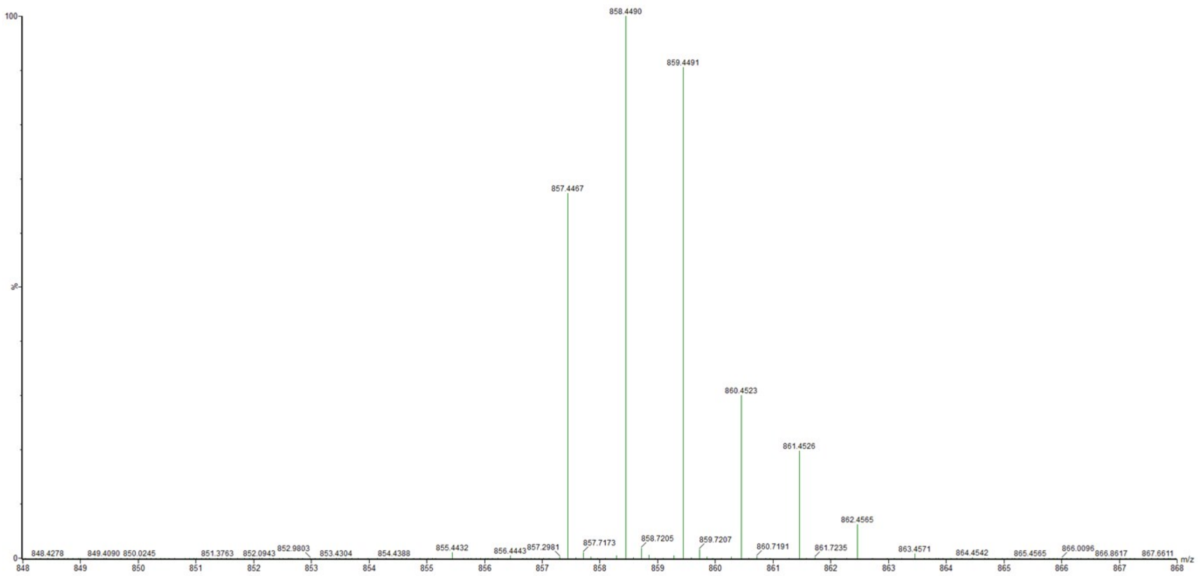

Figure D.10 ESI-MS spectrum of **[Pt(56Me$_2$PHEN)(SSDACH)(Decanoate)$_2$](NO$_3$)$_2$** (**10**).

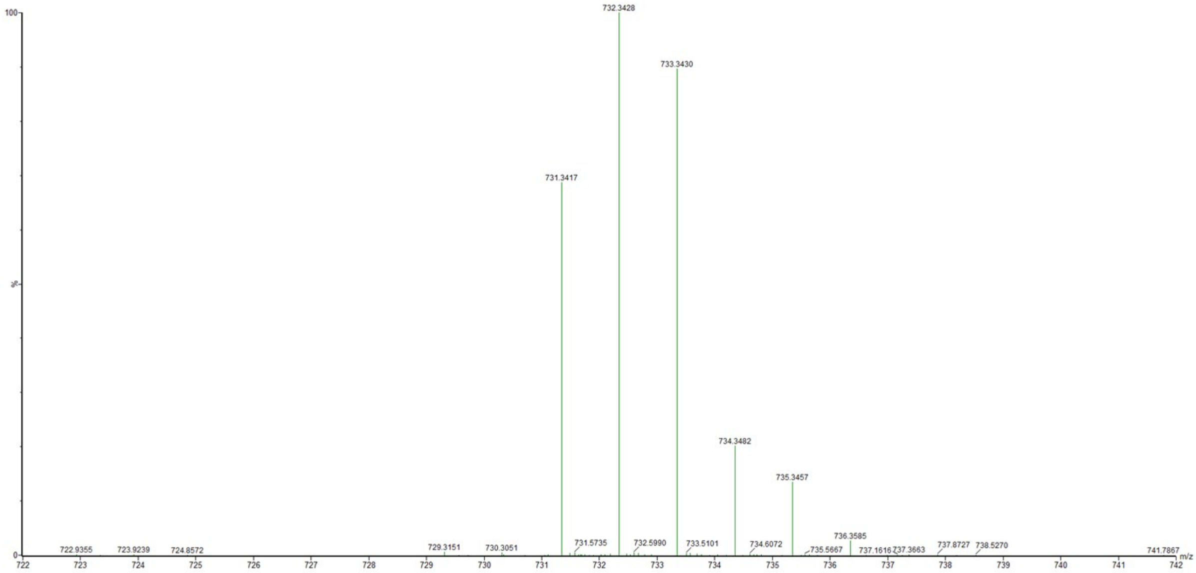

Figure D.11 ESI-MS spectrum of **[Pt(56Me$_2$PHEN)(SSDACH)(OH)(Dodecanoate)](NO$_3$)$_2$** (**11**).

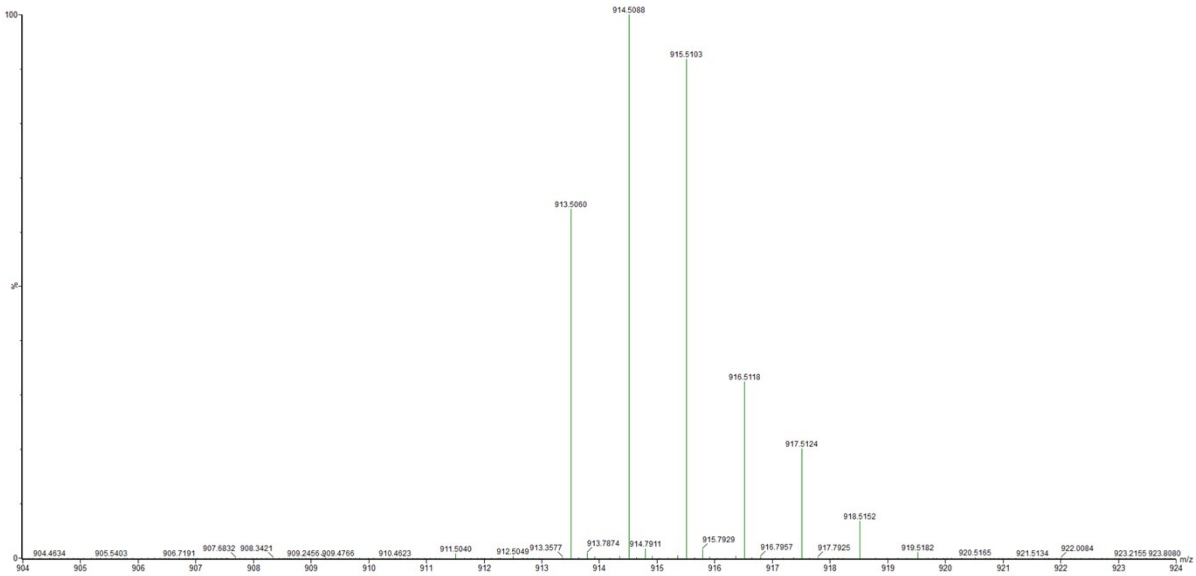

Figure D.12 ESI-MS spectrum of **[Pt(56Me$_2$PHEN)(SSDACH)(Dodecanoate)$_2$](NO$_3$)$_2$** (**12**).

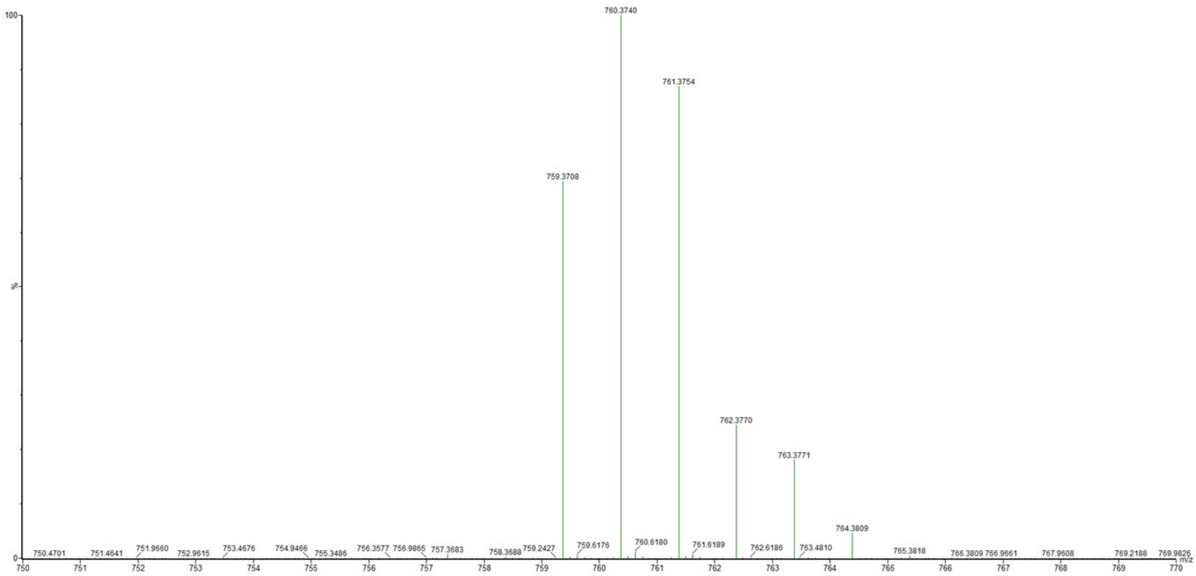

Figure D.13 ESI-MS spectrum of
[Pt(56Me$_2$PHEN)(SSDACH)(OH)(Tetradecanoate)](NO$_3$)$_2$ (**13**).

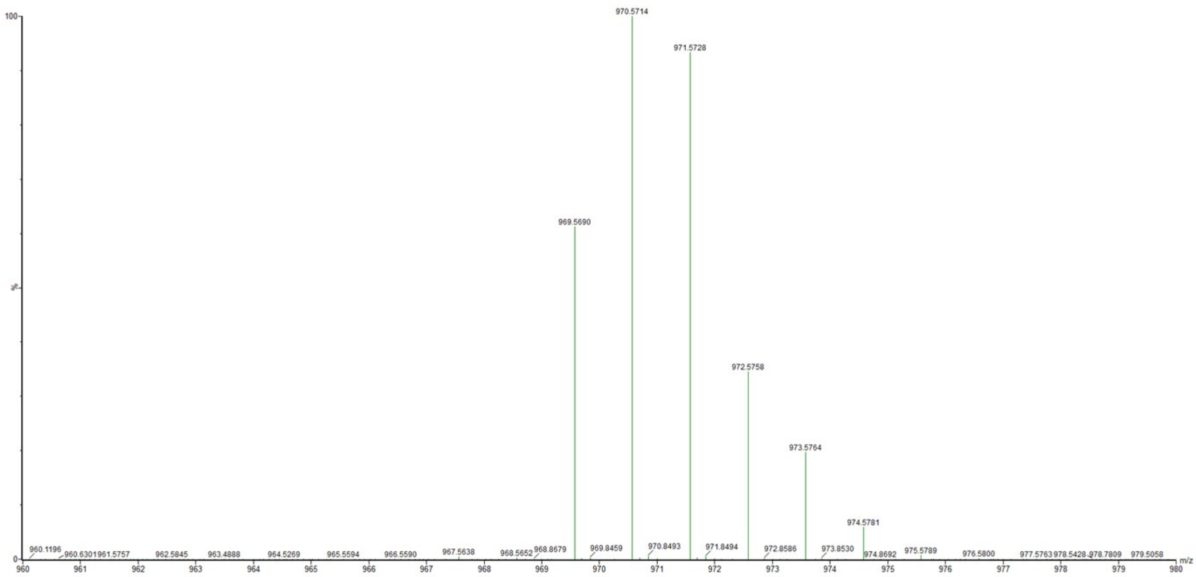

Figure D.14 ESI-MS spectrum of **[Pt(56Me$_2$PHEN)(SSDACH)(Tetradecanoate)$_2$](NO$_3$)$_2$** (**14**).

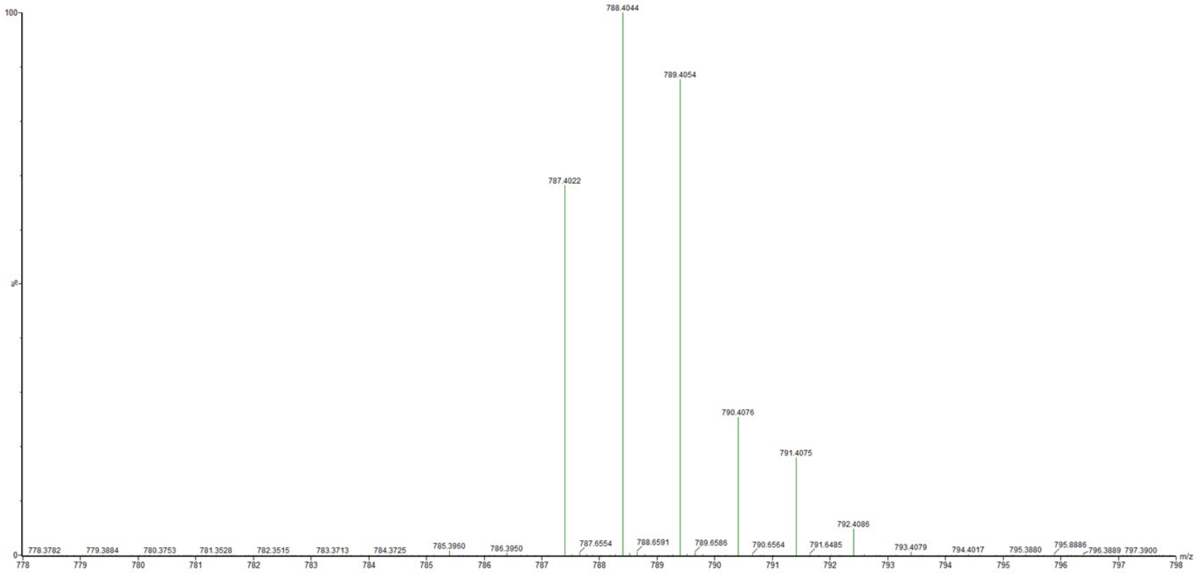

Figure D.15 ESI-MS spectrum of
[Pt(56Me$_2$PHEN)(SSDACH)(OH)(Hexadecanoate)](NO$_3$)$_2$ (**15**).

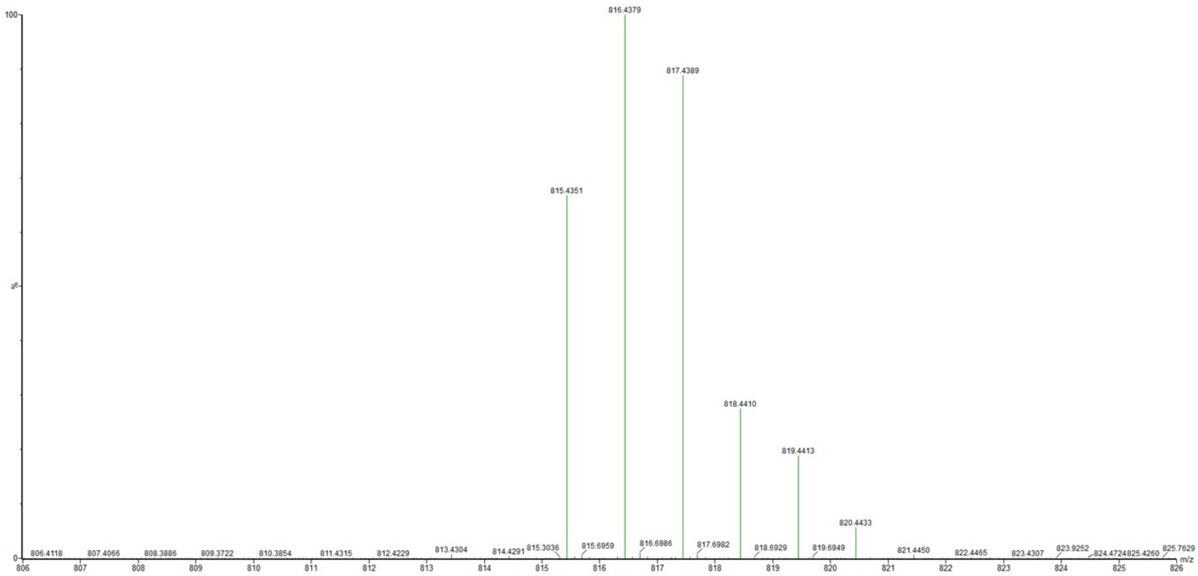

Figure D.16 ESI-MS spectrum of
[Pt(56Me$_2$PHEN)(SSDACH)(OH)(OctaDecanoate)](NO$_3$)$_2$ (**16**).

E. UV-Vis Spectra

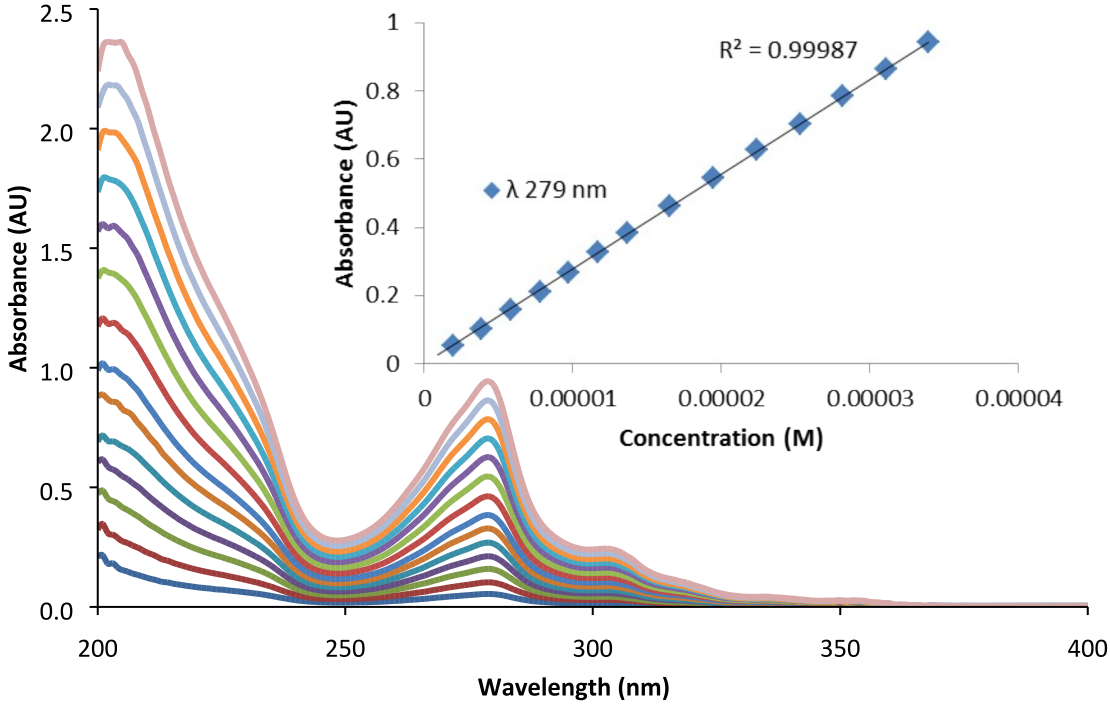

Figure E.1 Exemplar UV spectrum of **[Pt(PHEN)(SSDACH)(OH)(Decanoate)](NO_3)$_2$** (**1**) in MeOH.

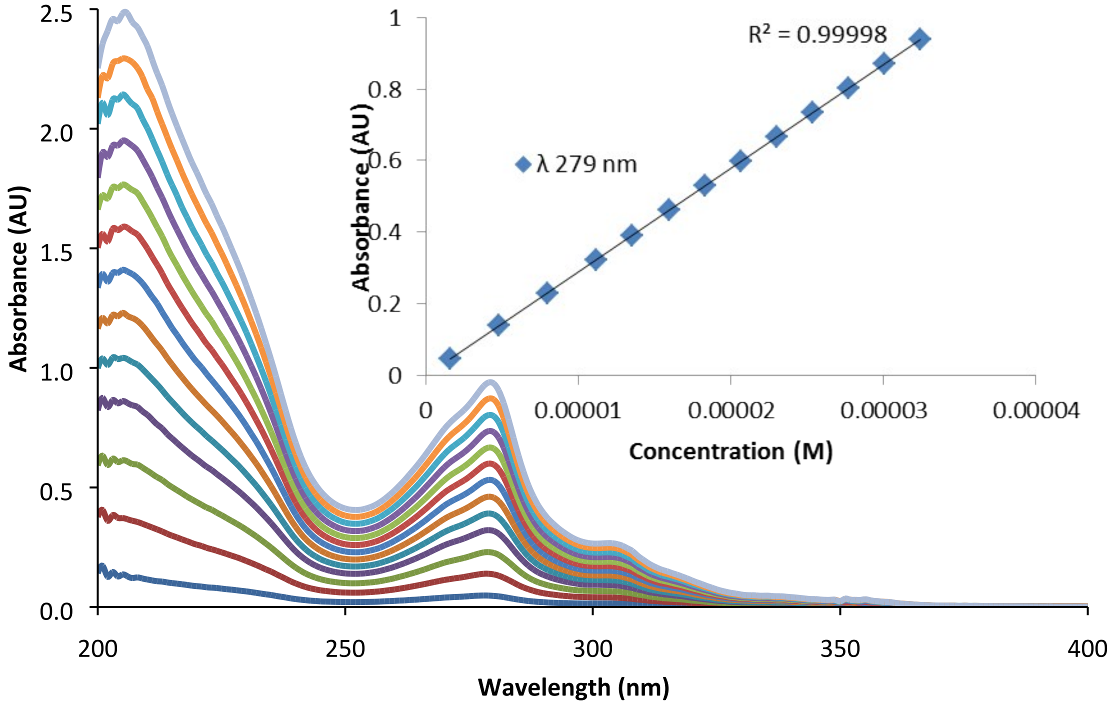

Figure E.2 Exemplar UV spectrum of **[Pt(PHEN)(SSDACH)(Decanoate)$_2$](NO_3)$_2$** (**2**) in MeOH.

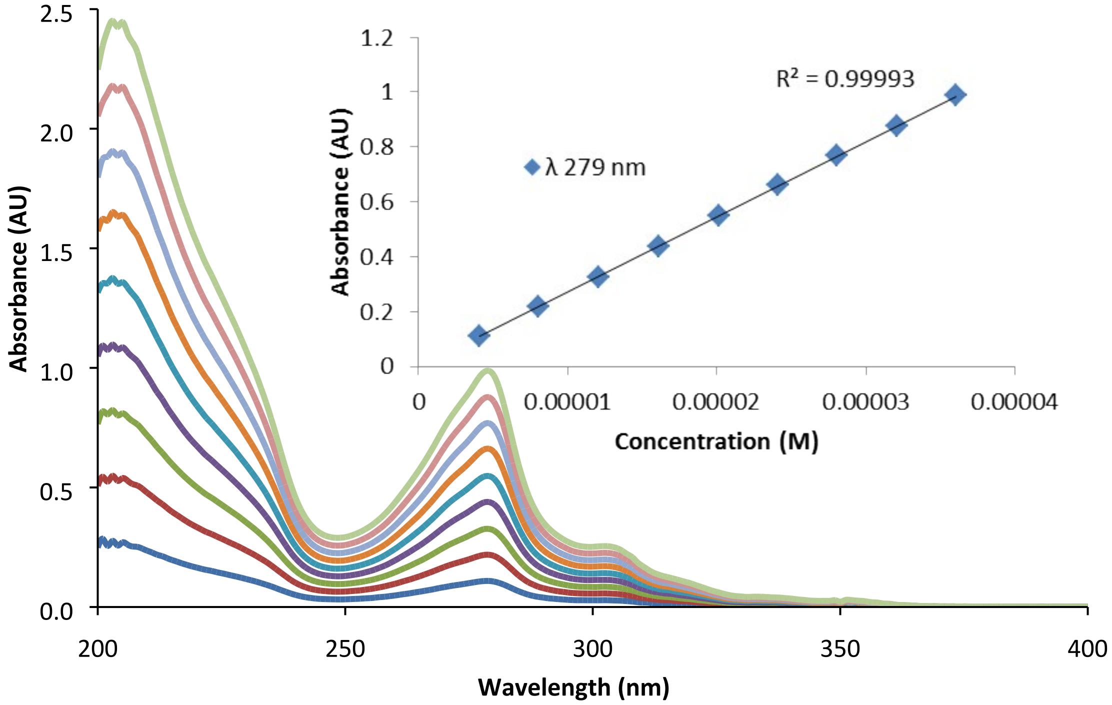

Figure E.3 Exemplar UV spectrum of **[Pt(PHEN)(SSDACH)(OH)(Dodecanoate)]$(NO_3)_2$** (**3**) in MeOH.

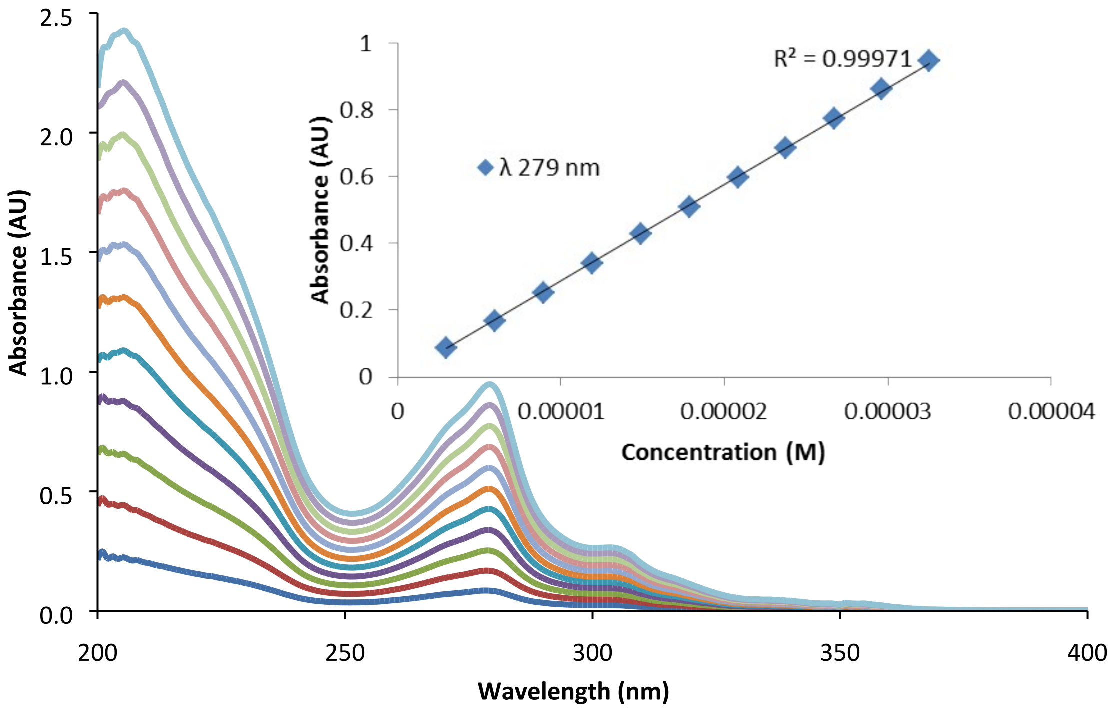

Figure E.4 Exemplar UV spectrum of **[Pt(PHEN)(SSDACH)$(Dodecanoate)_2$]$(NO_3)_2$** (**4**) in MeOH.

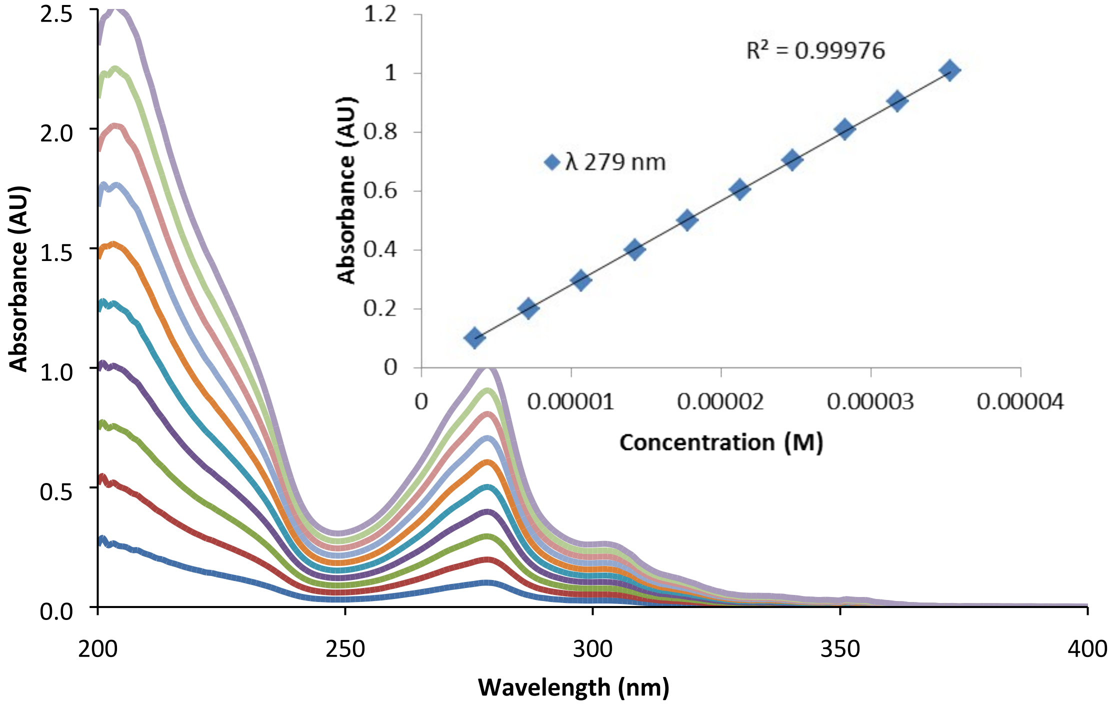

Figure E.5 Exemplar UV spectrum of **[Pt(PHEN)(SSDACH)(OH)(Tetradecanoate)]$(NO_3)_2$** (**5**) in MeOH.

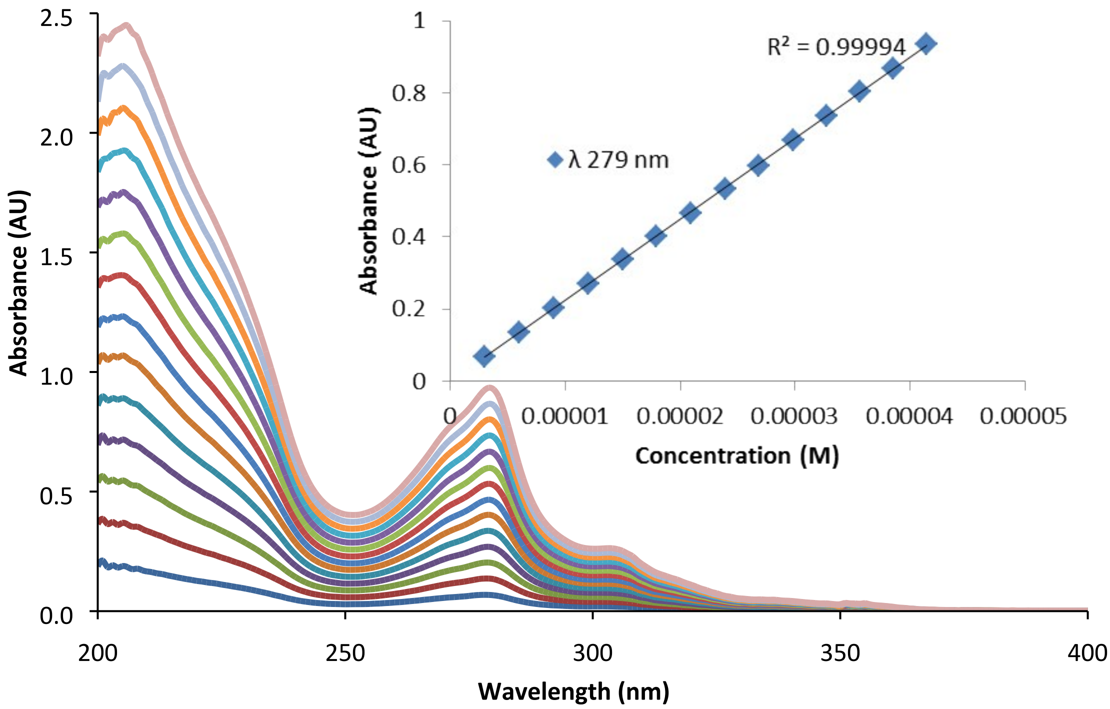

Figure E.6 Exemplar UV spectrum of **[Pt(PHEN)(SSDACH)$(Tetradecanoate)_2$]$(NO_3)_2$** (**6**) in MeOH.

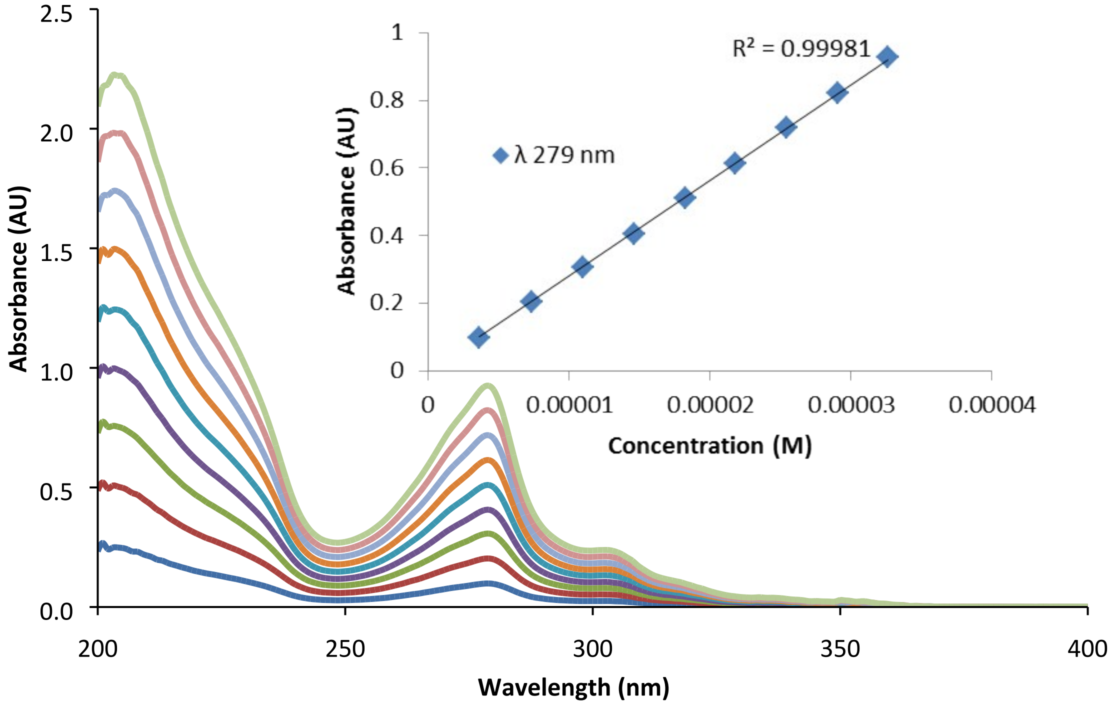

Figure E.7 Exemplar UV spectrum of **[Pt(PHEN)(SSDACH)(OH)(Hexadecanoate)]$(NO_3)_2$** (**7**) in MeOH.

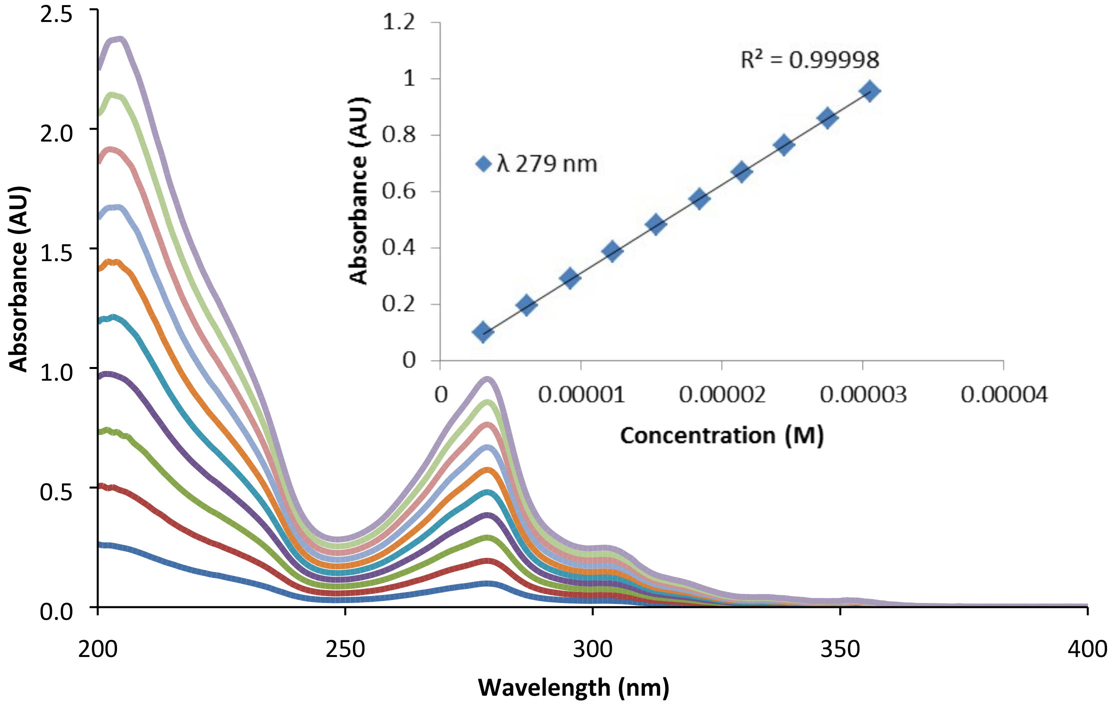

Figure E.8 Exemplar UV spectrum of **[Pt(PHEN)(SSDACH)(OH)(Octadecanoate)]$(NO_3)_2$** (**8**) in MeOH.

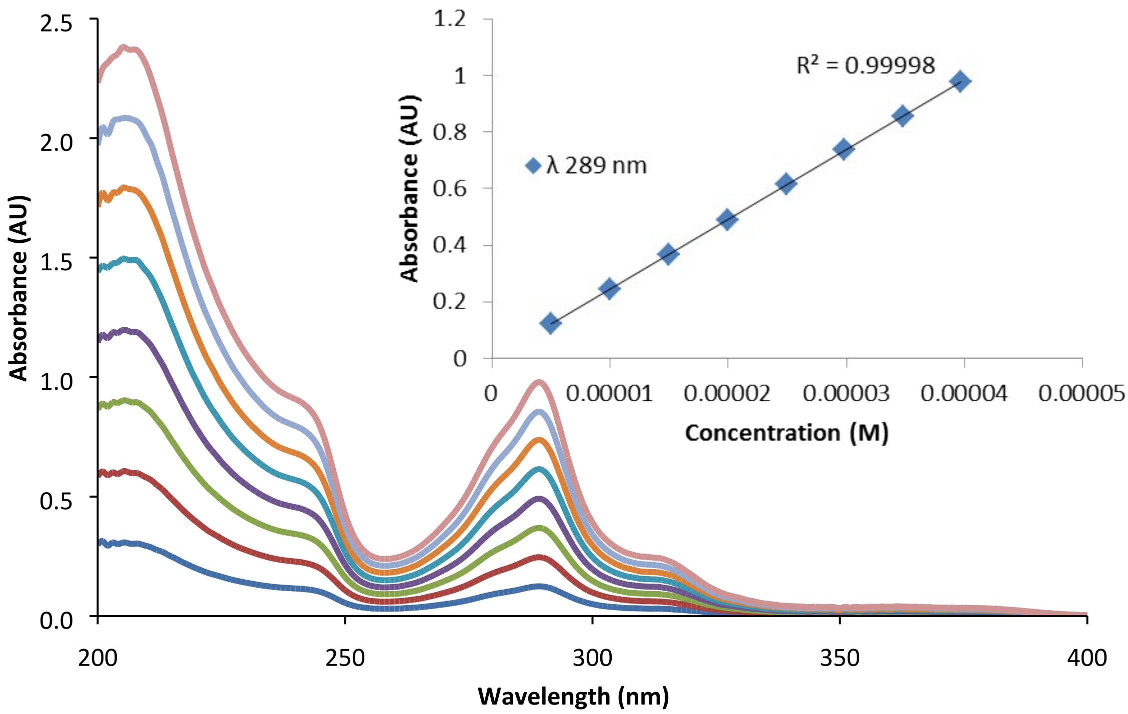

Figure E.9 Exemplar UV spectrum of **[Pt(56Me$_2$PHEN)(SSDACH)(OH)(Decanoate)](NO$_3$)$_2$** (**9**) in MeOH.

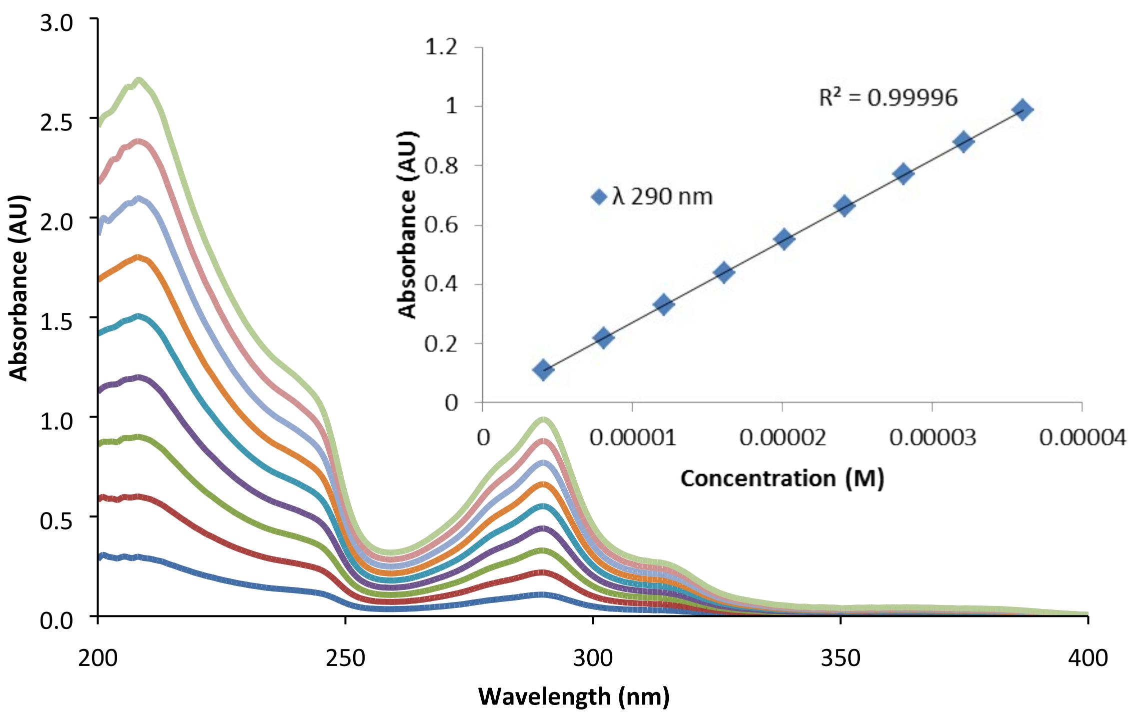

Figure E.10 Exemplar UV spectrum of **[Pt(56Me$_2$PHEN)(SSDACH)(Decanoate)$_2$](NO$_3$)$_2$** (**10**) in MeOH.

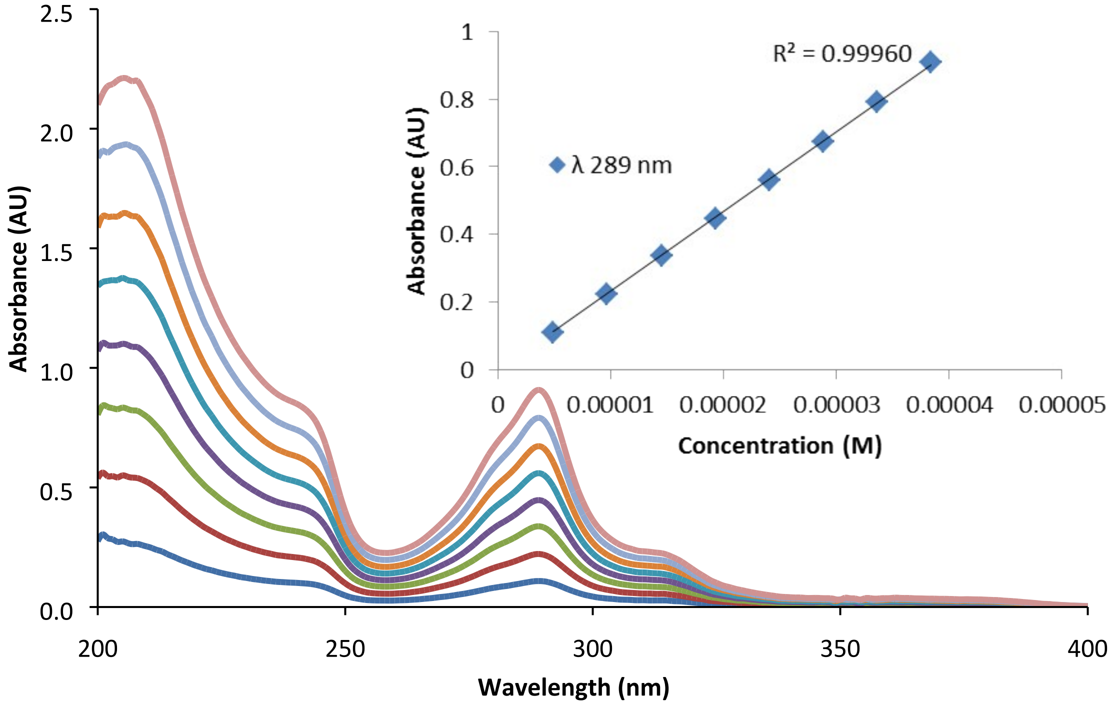

Figure E.11 Exemplar UV spectrum of
[Pt(56Me$_2$PHEN)(SSDACH)(OH)(Dodecanoate)](NO$_3$)$_2$ (**11**) in MeOH.

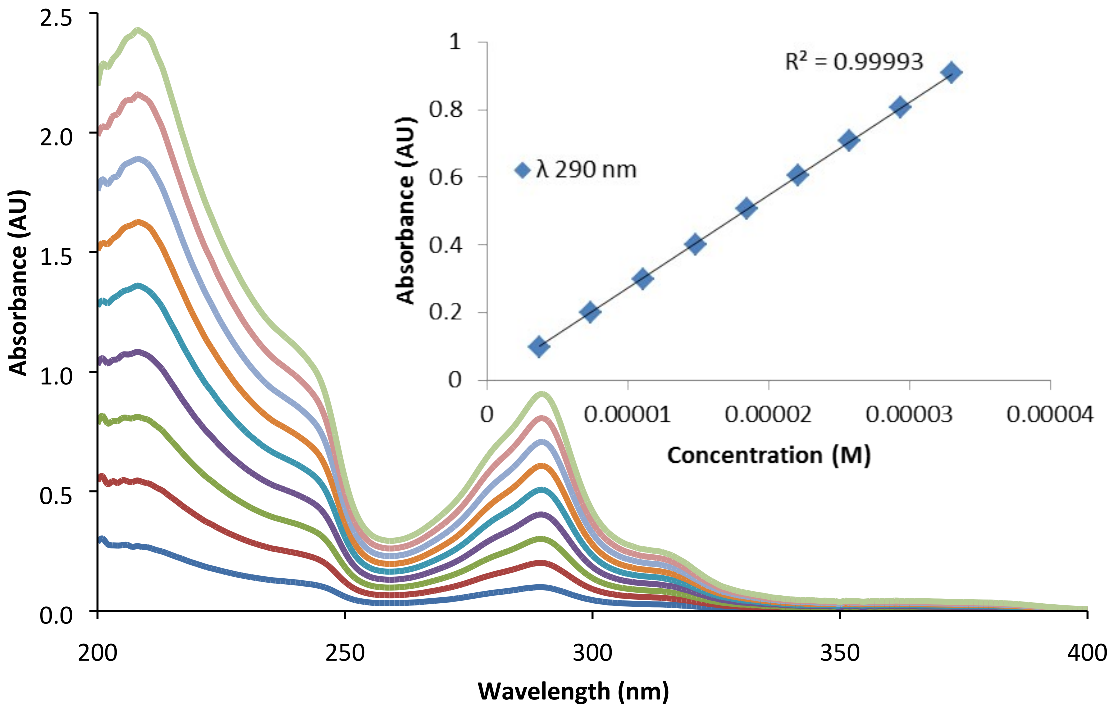

Figure E.12 Exemplar UV spectrum of
[Pt(56Me$_2$PHEN)(SSDACH)(Dodecanoate)$_2$](NO$_3$)$_2$ (**12**) in MeOH.

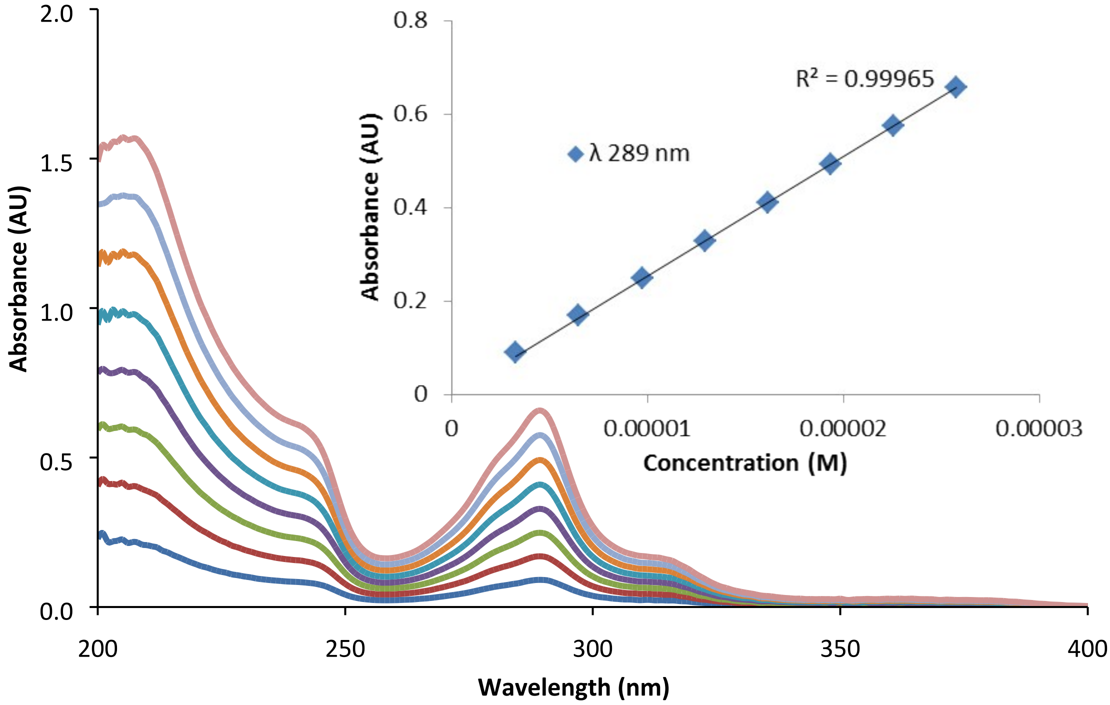

Figure E.13 Exemplar UV spectrum of
[Pt(56Me$_2$PHEN)(SSDACH)(OH)(Tetradecanoate)](NO$_3$)$_2$ (**13**) in MeOH.

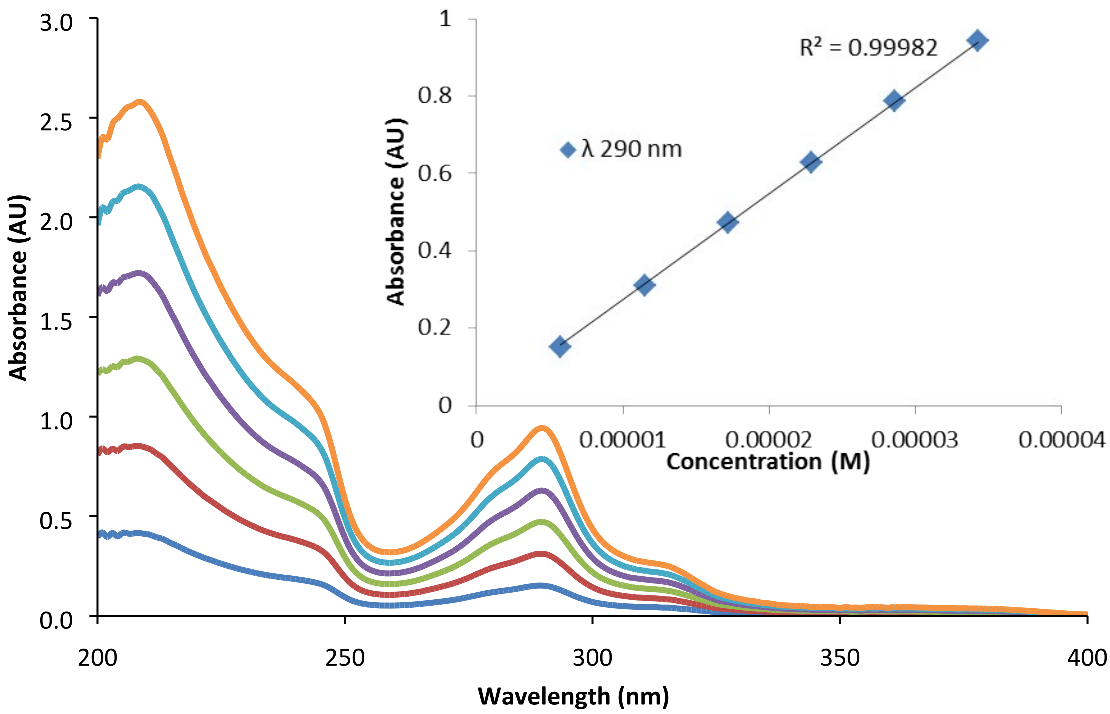

Figure E.14 Exemplar UV spectrum of
[Pt(56Me$_2$PHEN)(SSDACH)(Tetradecanoate)$_2$](NO$_3$)$_2$ (**14**) in MeOH.

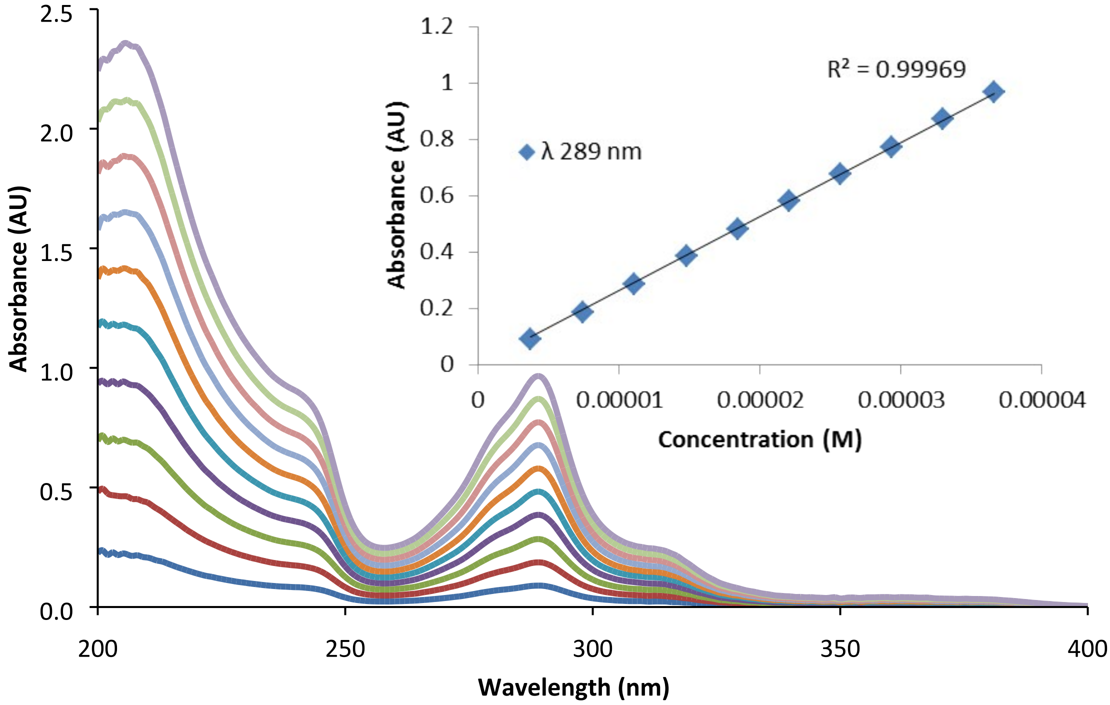

Figure E.15 Exemplar UV spectrum of **[Pt(56Me$_2$PHEN)(SSDACH)(OH)(Hexadecanoate)](NO$_3$)$_2$** (**15**) in MeOH.

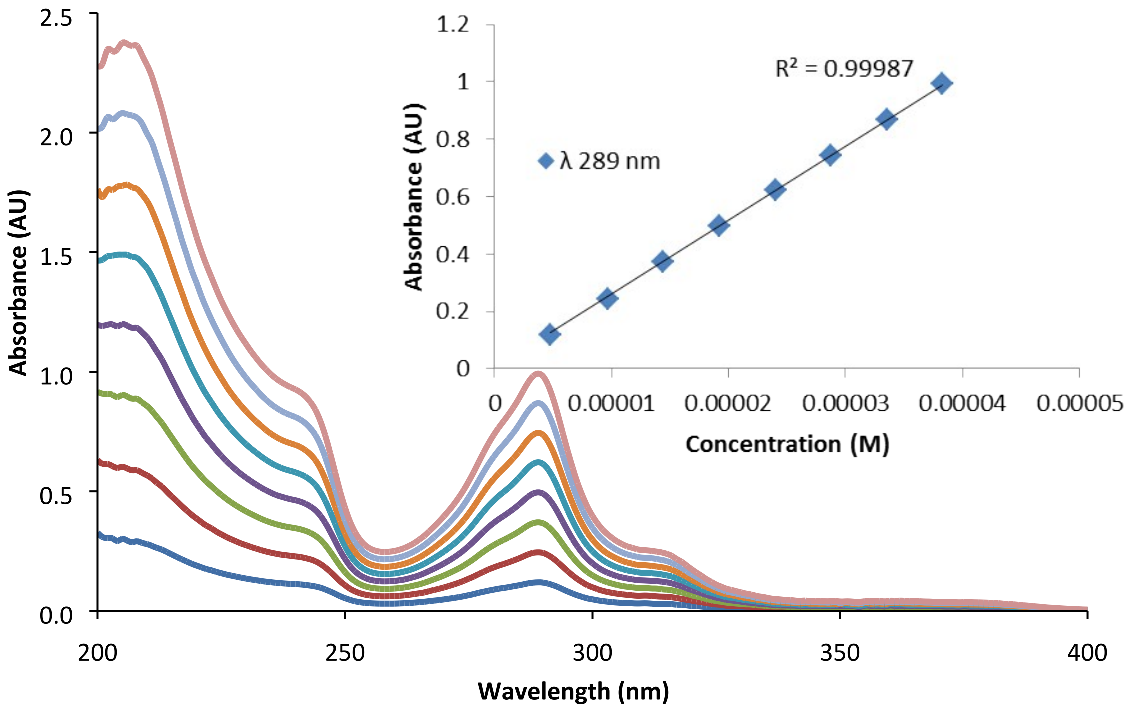

Figure E.16 Exemplar UV spectrum of **[Pt(56Me$_2$PHEN)(SSDACH)(OH)(Octadecanoate)](NO$_3$)$_2$** (**16**) in MeOH.

F. Circular Dichroism (CD) Spectra

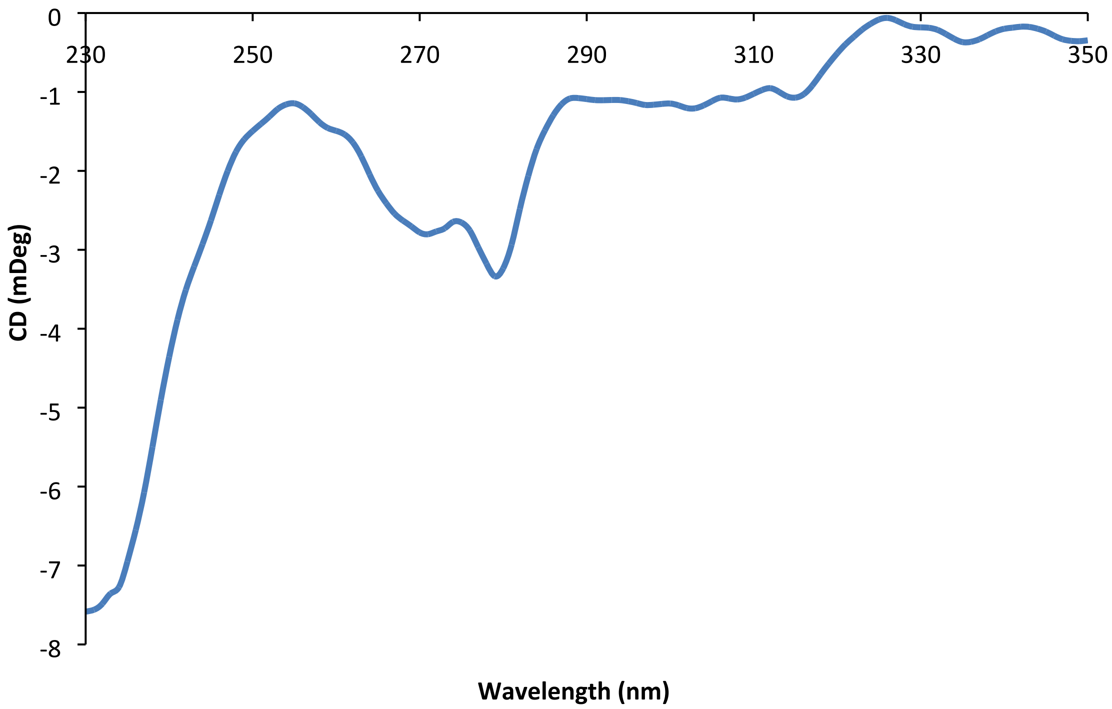

Figure F.1 CD spectrum of **[Pt(PHEN)(SSDACH)(OH)(Decanoate)]$(NO_3)_2$** (**1**) in MeOH:H_2O (1:4). 7pt smoothing applied.

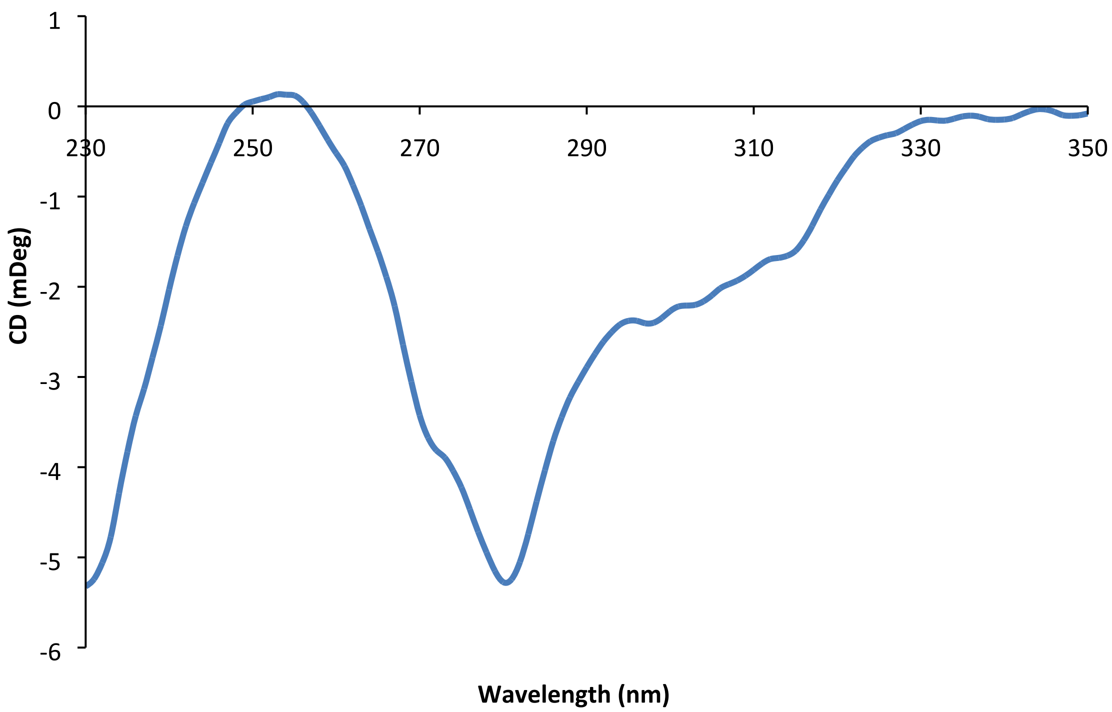

Figure F.2 CD spectrum of **[Pt(PHEN)(SSDACH)($(Decanoate)_2$]$(NO_3)_2$** (**2**) in MeOH:H_2O (1:4). 7pt smoothing applied.

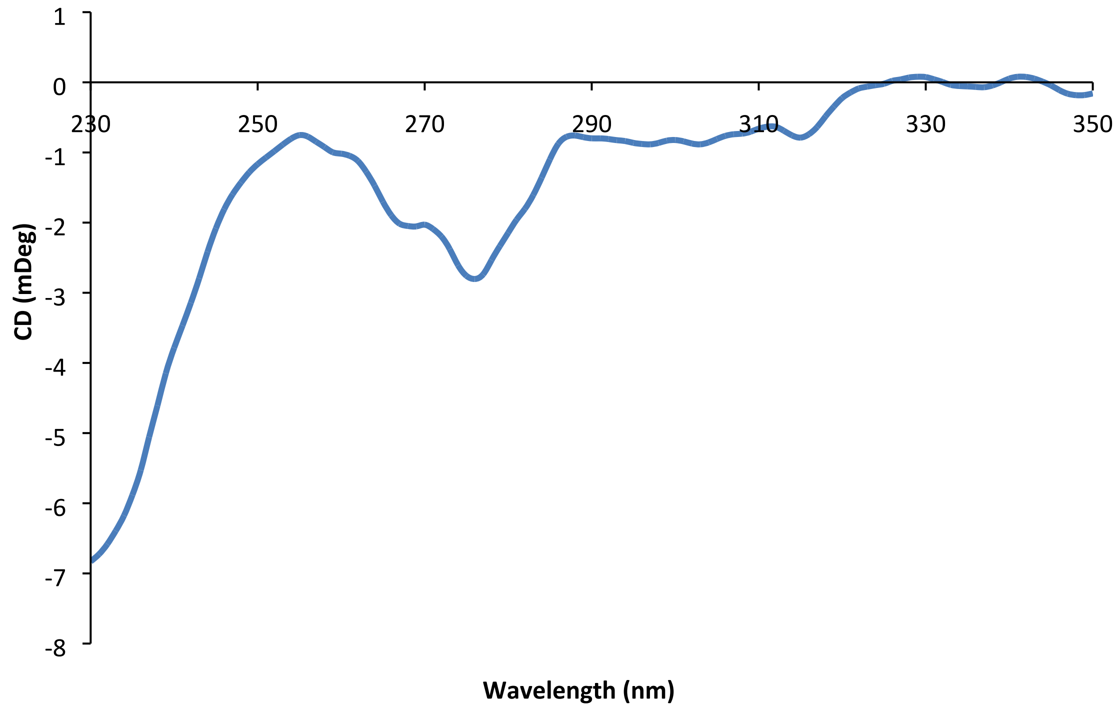

Figure F.3 CD spectrum of **[Pt(PHEN)(SSDACH)(OH)(Dodecanoate)](NO_3)$_2$** (**3**) in MeOH:H_2O (1:4). 7pt smoothing applied.

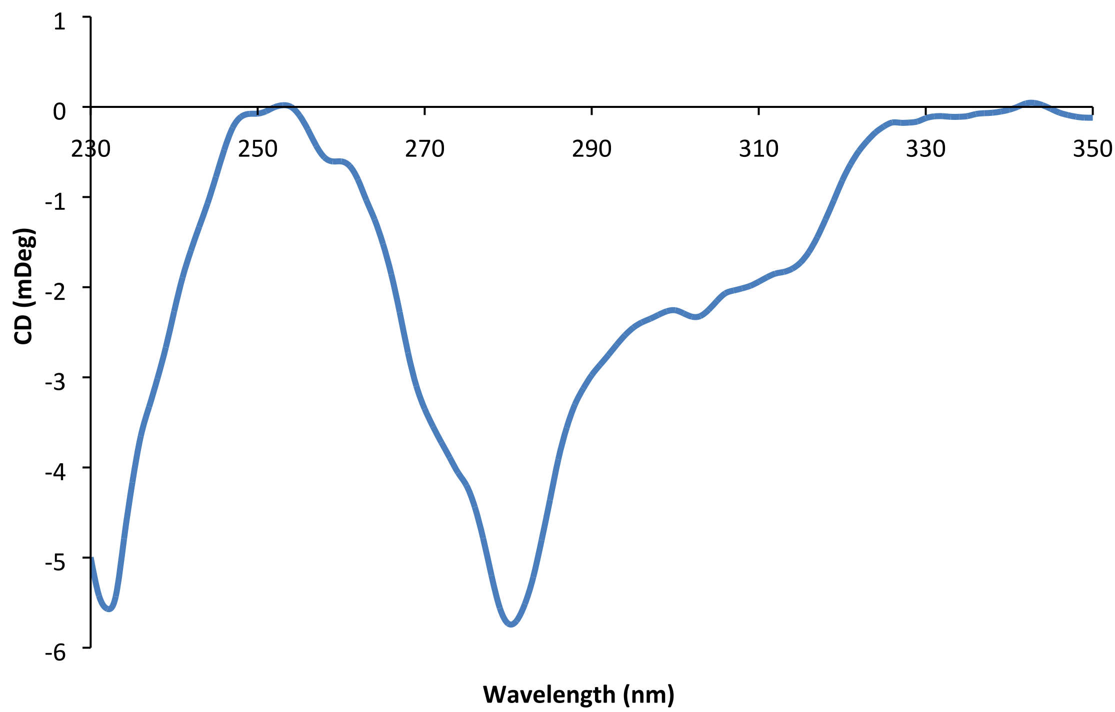

Figure F.4 CD spectrum of **[Pt(PHEN)(SSDACH)((Dodecanoate)$_2$](NO_3)$_2$** (**4**) in MeOH:H_2O (1:4). 7pt smoothing applied.

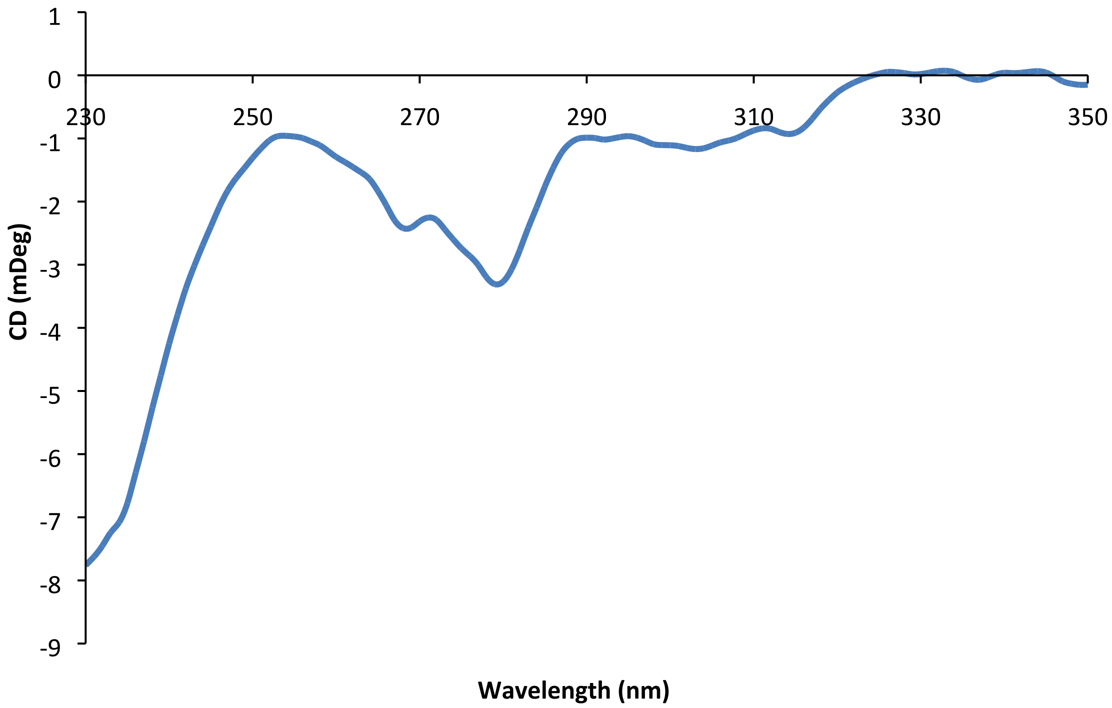

Figure F.5 CD spectrum of **[Pt(PHEN)(SSDACH)(OH)(Tetradecanoate)]$(NO_3)_2$ (5)** in MeOH:H_2O (1:4). 7pt smoothing applied.

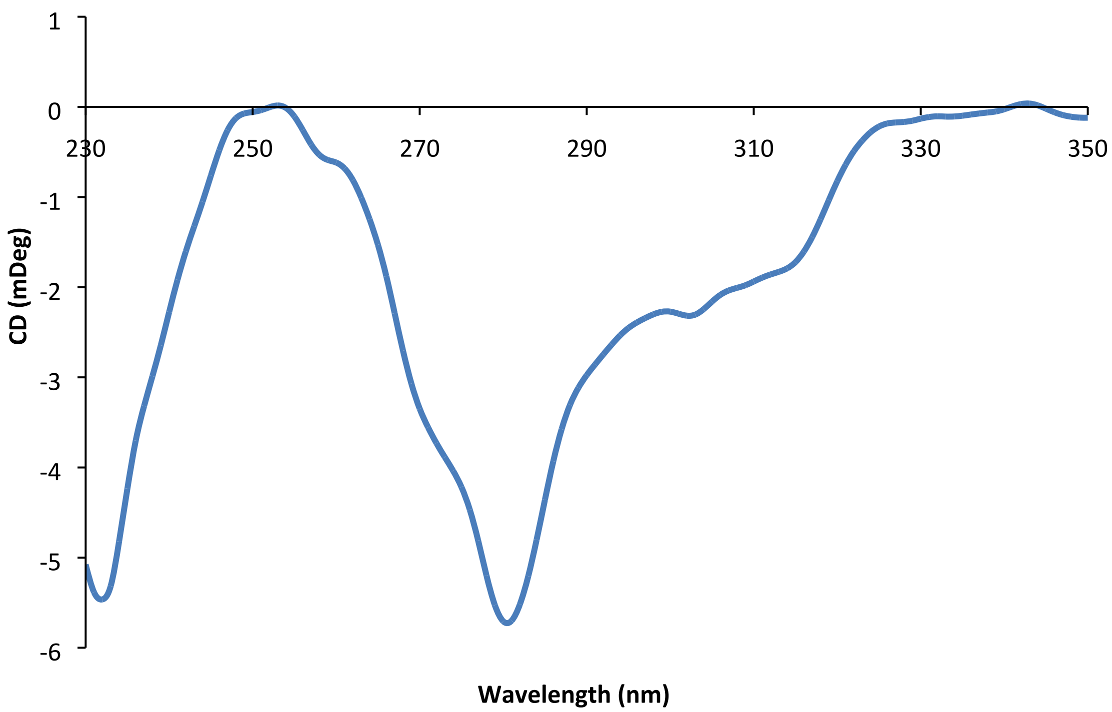

Figure F.6 CD spectrum of **[Pt(PHEN)(SSDACH)((Tetradecanoate)$_2$]$(NO_3)_2$ (6)** in MeOH:H_2O (1:4). 7pt smoothing applied.

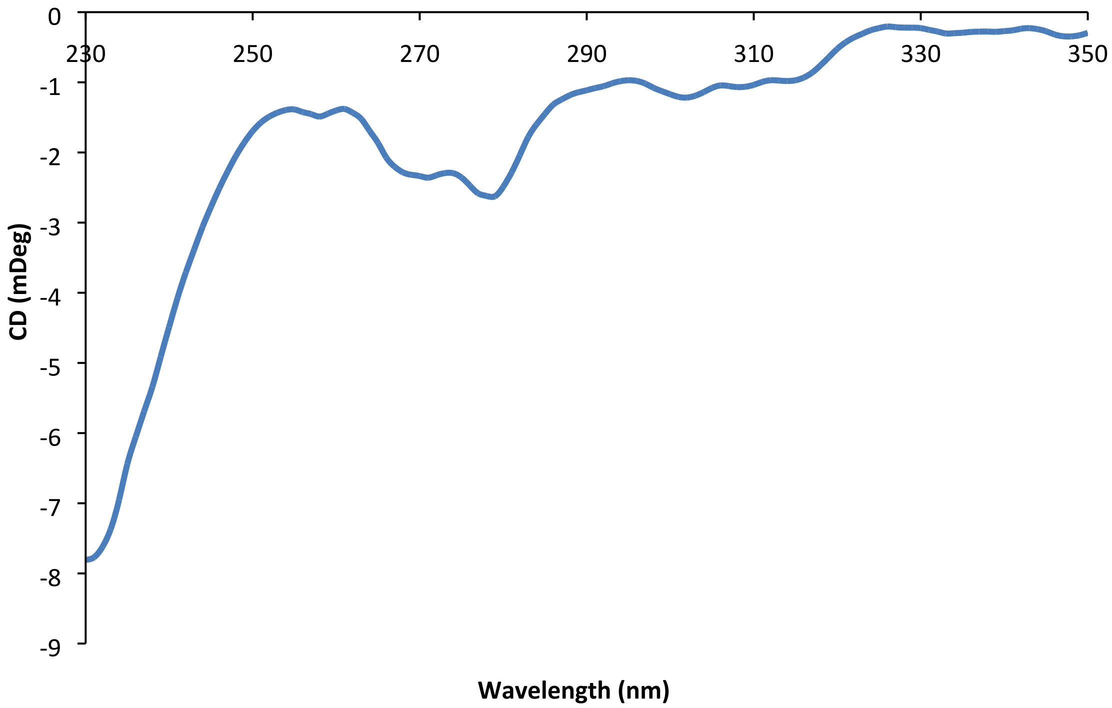

Figure F.7 CD spectrum of **[Pt(PHEN)(SSDACH)(OH)(Hexadecanoate)](NO_3)$_2$** (**7**) in MeOH:H_2O (1:4). 7pt smoothing applied.

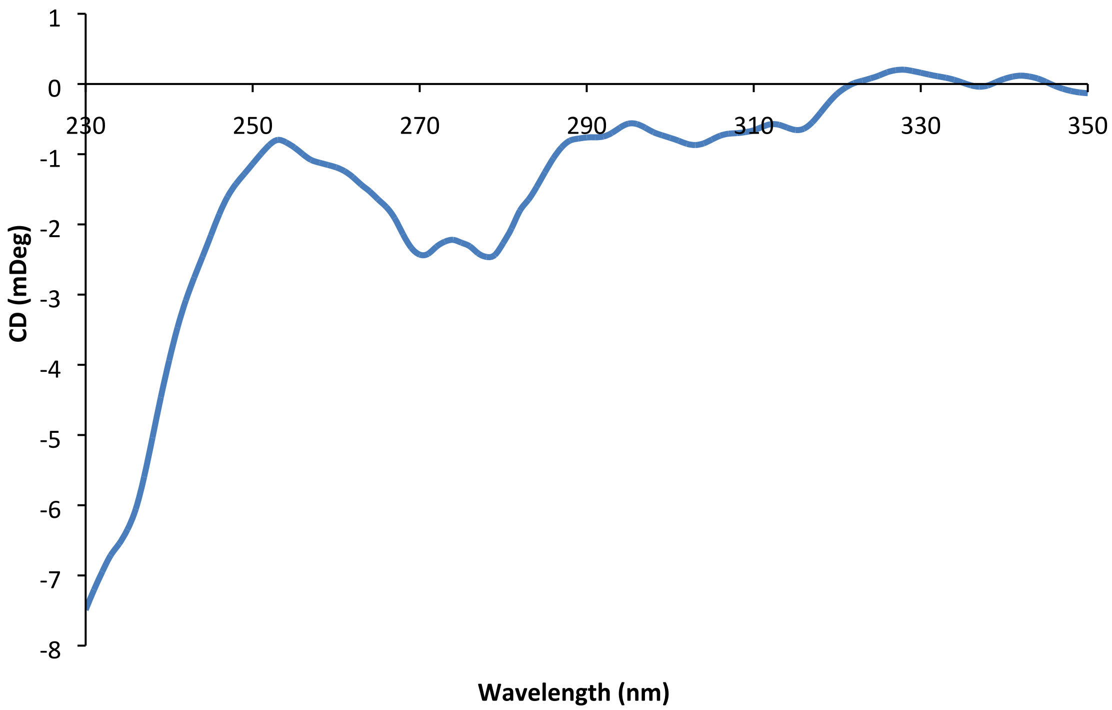

Figure F.8 CD spectrum of **[Pt(PHEN)(SSDACH)(OH)(Octadecanoate)](NO_3)$_2$** (**8**) in MeOH:H_2O (1:4). 7pt smoothing applied.

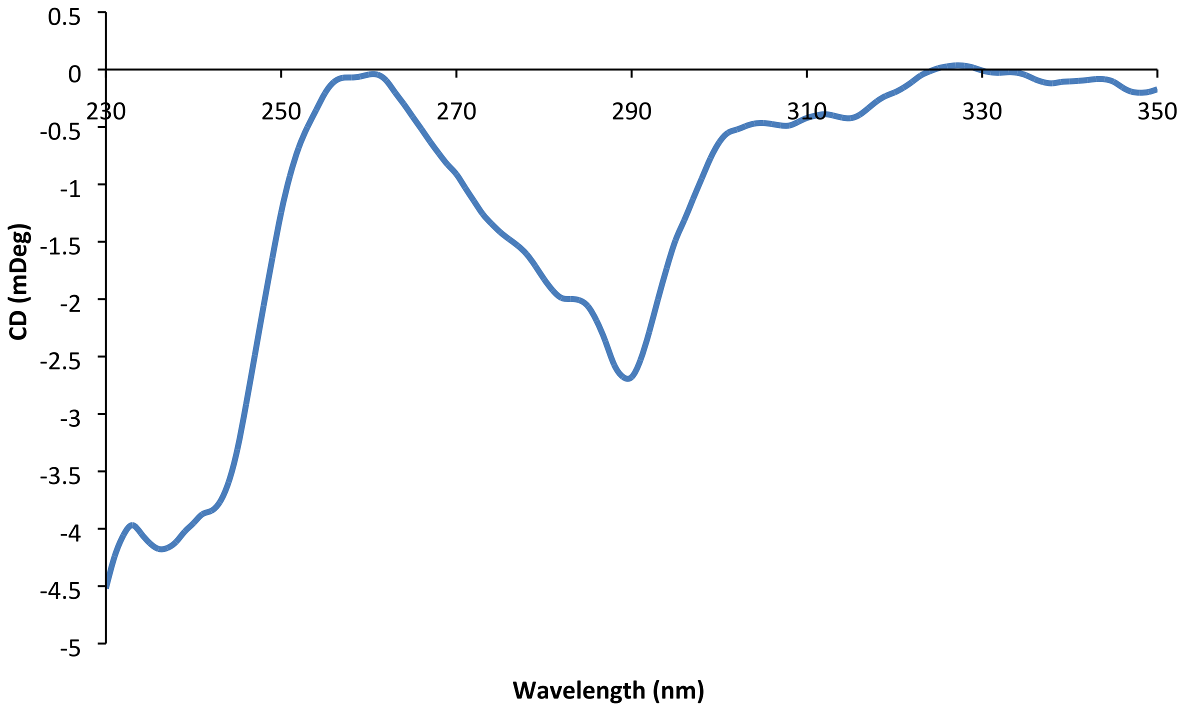

Figure F.9 CD spectrum of **[Pt(56Me$_2$PHEN)(SSDACH)(OH)(Decanoate)](NO$_3$)$_2$** (**9**) in MeOH:H2O (1:4). 7pt smoothing applied.

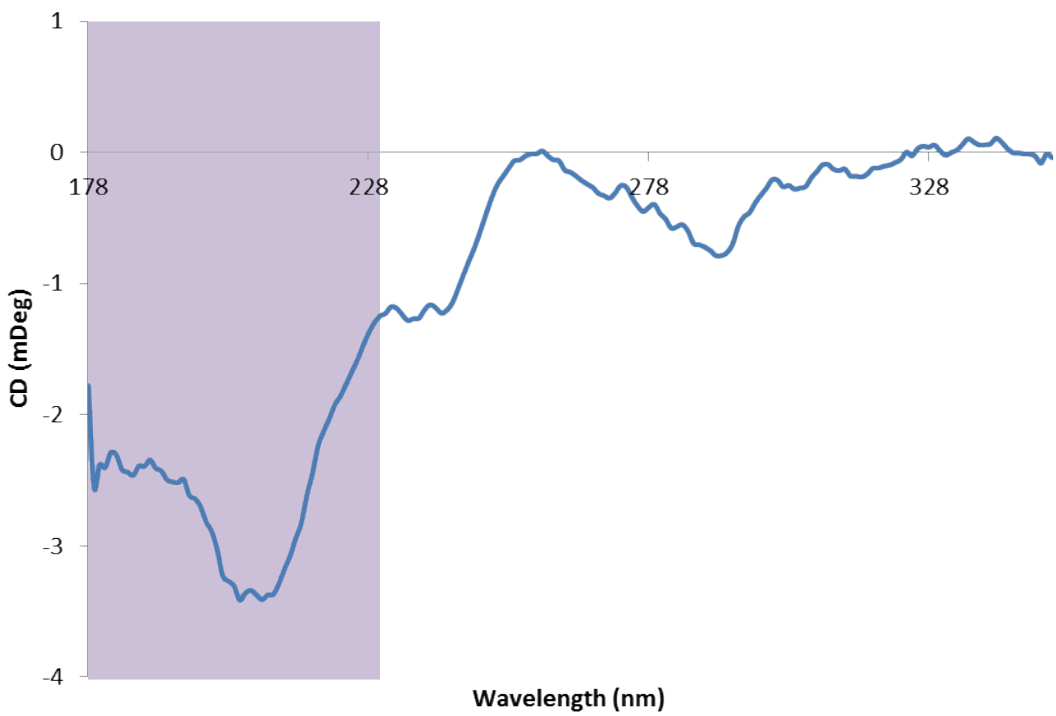

Figure F.10 SRCD spectrum of **[Pt(56Me$_2$PHEN)(SSDACH)(OH)(Decanoate)](NO$_3$)$_2$** (**9**) in MeOH:H_2O (1:4). 7pt smoothing applied. Additional spectral information has been highlighted in purple.

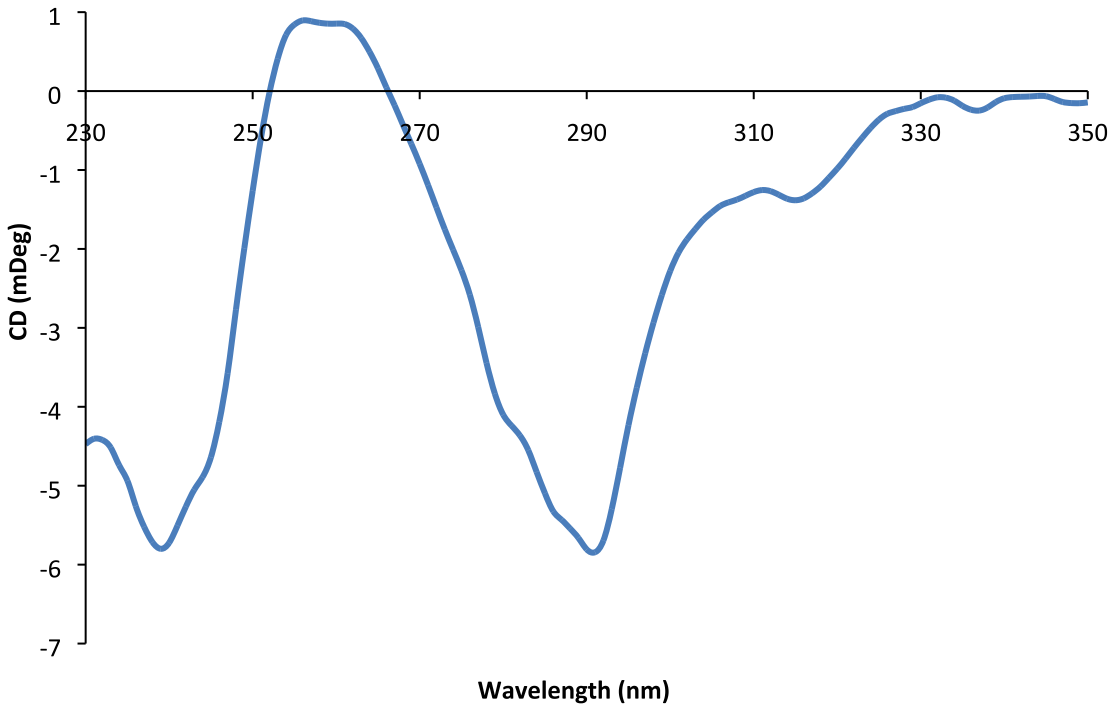

Figure F.11 CD spectrum of **[Pt(56Me$_2$PHEN)(SSDACH)(Decanoate)$_2$](NO$_3$)$_2$** (**10**) in MeOH:H2O (1:4). 7pt smoothing applied.

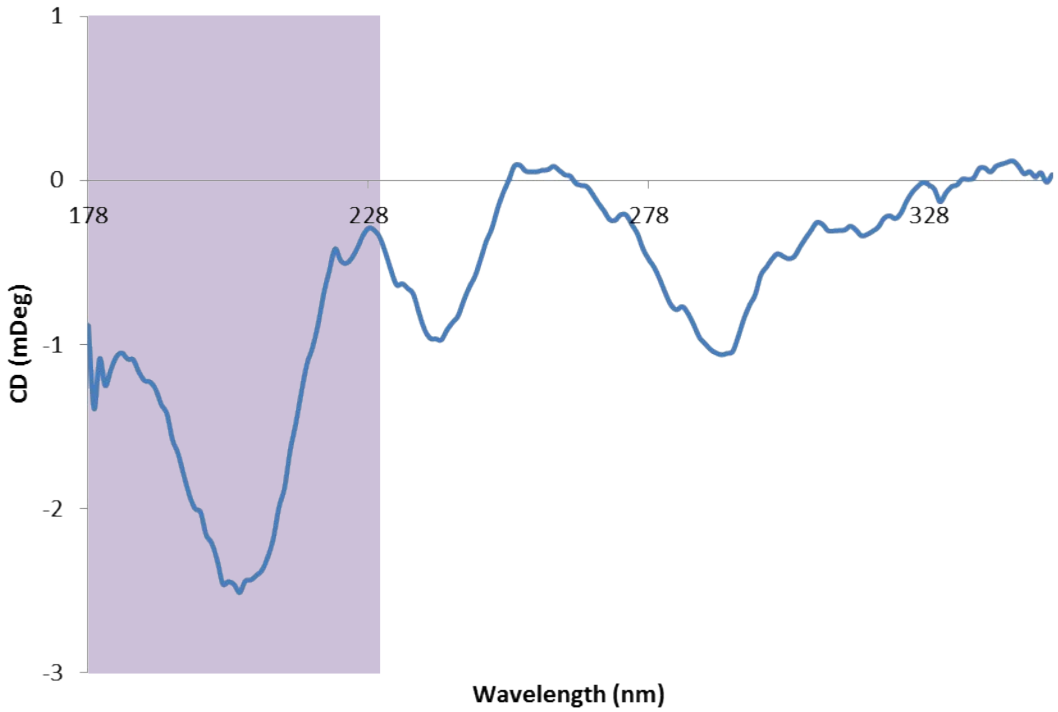

Figure F.12 SRCD spectrum of **[Pt(56Me$_2$PHEN)(SSDACH)(Decanoate)$_2$](NO$_3$)$_2$** (**10**) in MeOH:H_2O (1:4). 7pt smoothing applied. Additional spectral information has been highlighted in purple.

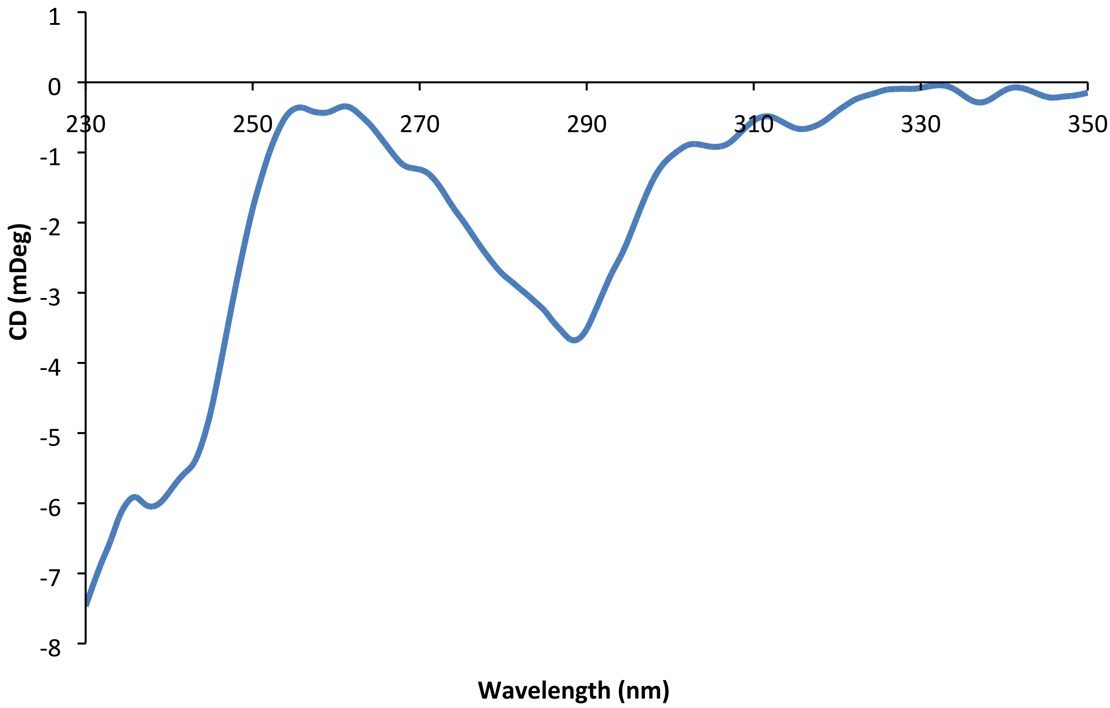

Figure F.13 CD spectrum of **[Pt(56Me$_2$PHEN)(SSDACH)(OH)(Dodecanoate)](NO$_3$)$_2$** (**11**) in MeOH:H2O (1:4). 7pt smoothing applied.

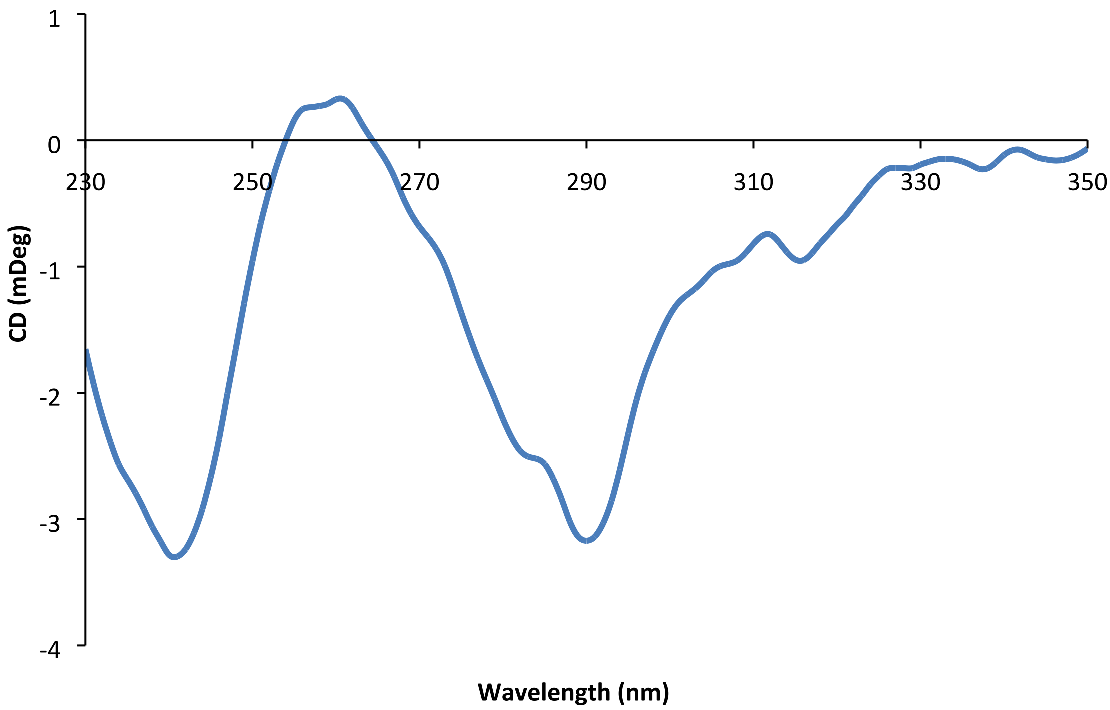

Figure F.14 CD spectrum of **[Pt(56Me$_2$PHEN)(SSDACH)(Dodecanoate)$_2$](NO$_3$)$_2$** (**12**) in MeOH:H2O (1:4). 7pt smoothing applied.

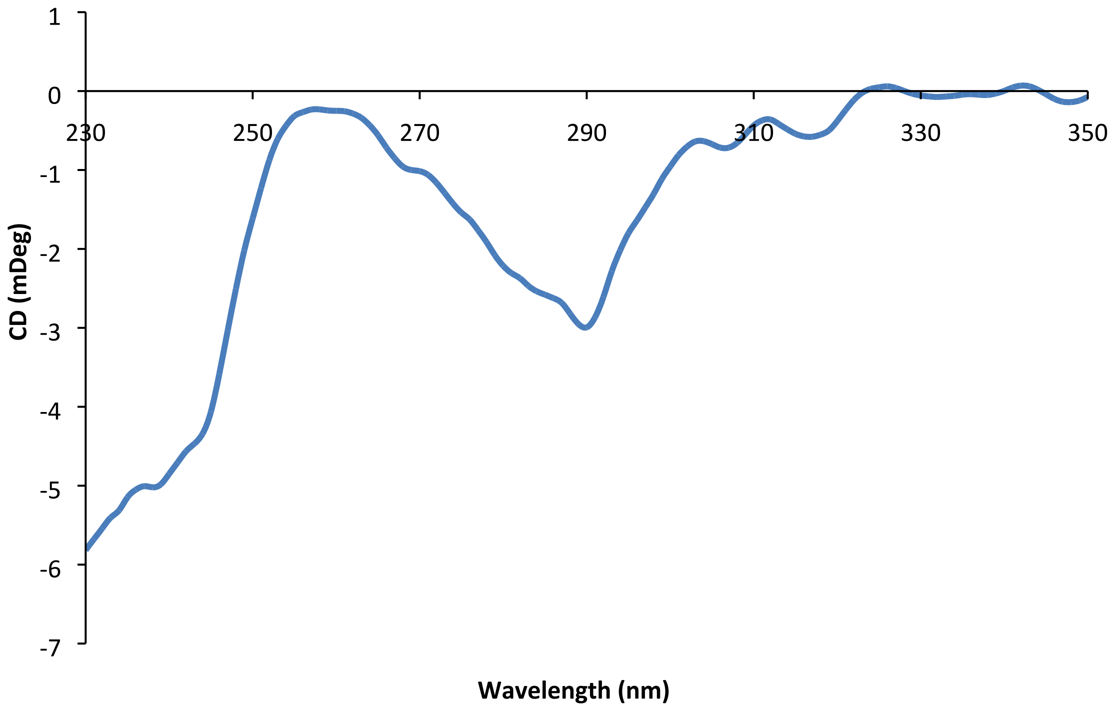

Figure F.15 CD spectrum of **[Pt(56Me$_2$PHEN)(SSDACH)(OH)(Tetradecanoate)](NO$_3$)$_2$** (**13**) in MeOH:H2O (1:4). 7pt smoothing applied.

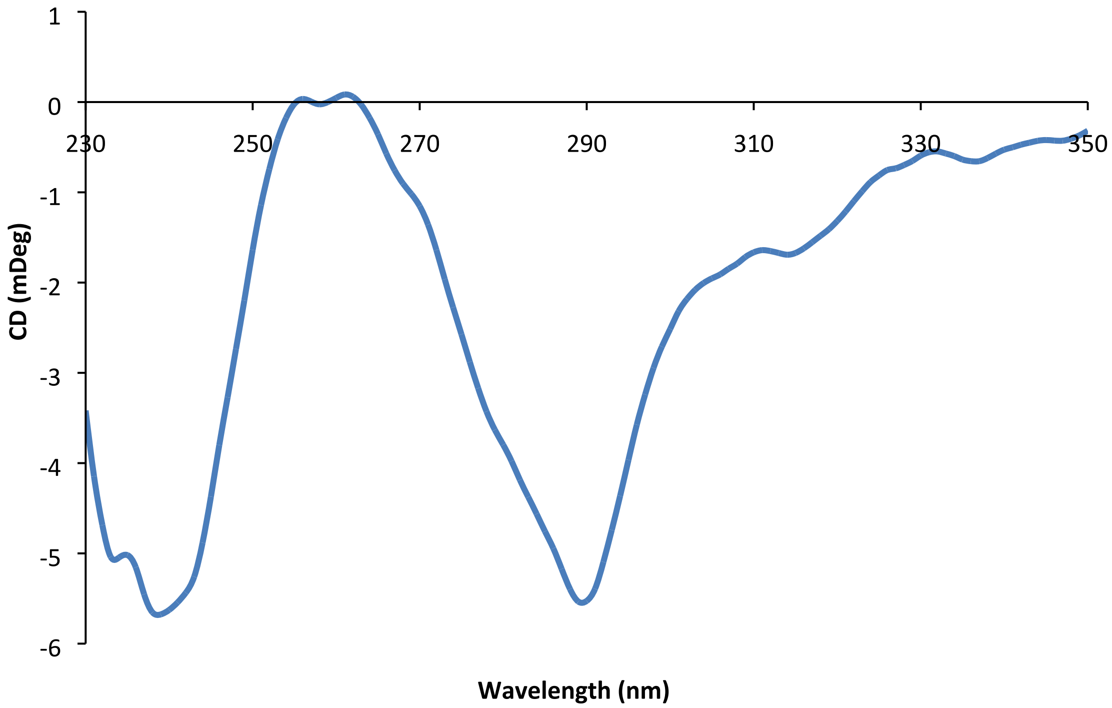

Figure F.16 CD spectrum of **[Pt(56Me$_2$PHEN)(SSDACH)(Tetradecanoate)$_2$](NO$_3$)$_2$** (**14**) in MeOH:H2O (1:4). 7pt smoothing applied.

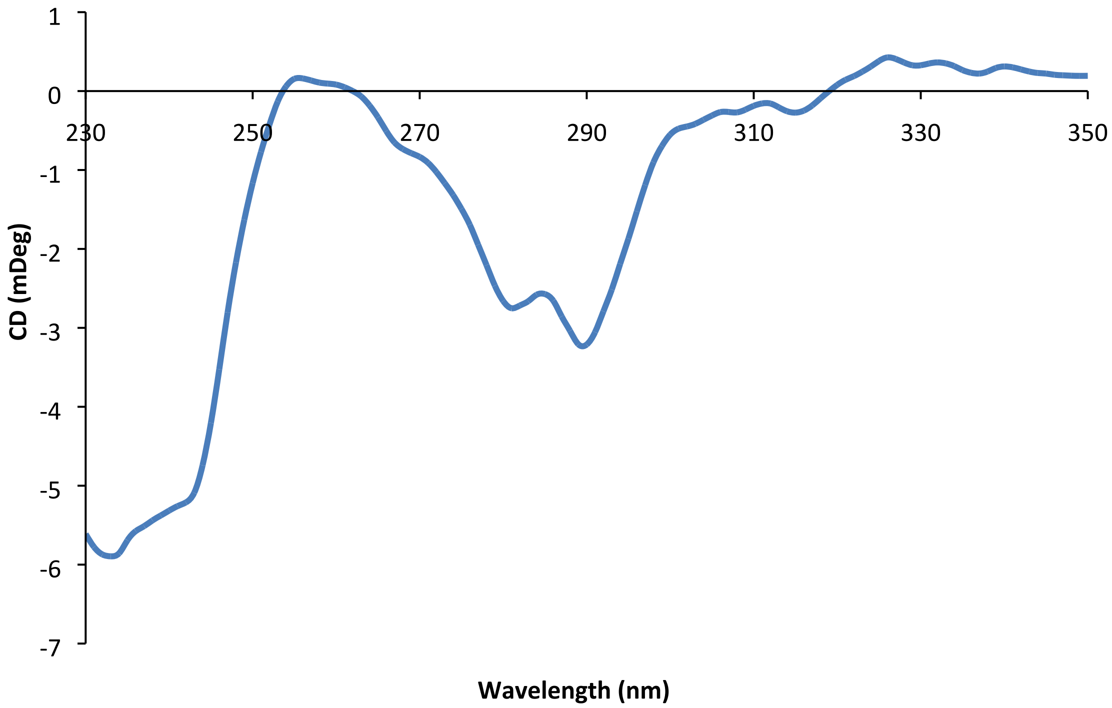

Figure F.17 CD spectrum of **[Pt(56Me$_2$PHEN)(SSDACH)(OH)(Hexadecanoate)](NO$_3$)$_2$** (**15**) in MeOH:H2O (1:4). 7pt smoothing applied.

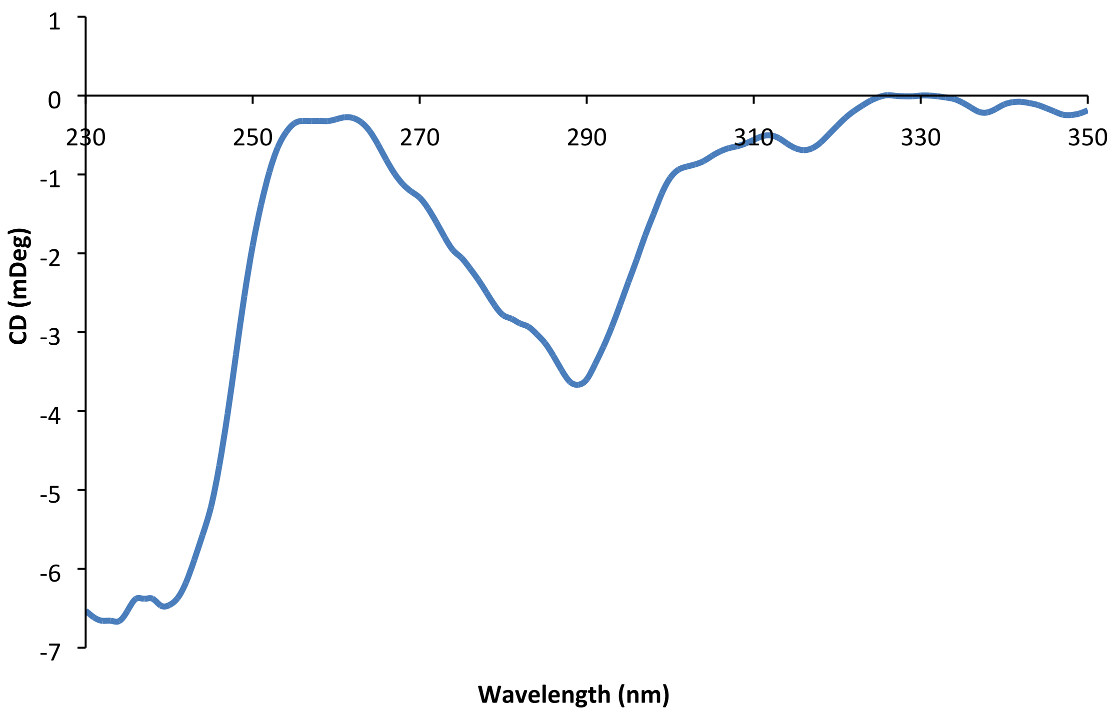

Figure F.18 CD spectrum of **[Pt(56Me$_2$PHEN)(SSDACH)(OH)(Hexadecanoate)](NO$_3$)$_2$** (**16**) in MeOH:H2O (1:4). 7pt smoothing applied.

G. Flash Chromatography Details

Table G.1 Flash chromatography gradients (H_2O:MeOH), flowrates and elution times of all mono- and di-substituted derivatives of **PHENSS(IV)** and **56MESS(IV)**.

<table>
<tr><th>Complex</th><th>Gradient (% MeOH)</th><th>Flowrate</th><th>Peak elution time (min)</th></tr>
<tr><td>1</td><td rowspan="2">3 % for 4 min
3–45 % over 6 min
45–55 % over 5 min
55–100 % over 2 min
100 % for 4 min</td><td rowspan="2">8 mL/min</td><td>9–12</td></tr>
<tr><td>2</td><td>13–16</td></tr>
<tr><td>3</td><td rowspan="2">3 % for 8 min
3–40 % over 12 min
40–55 % over 6 min
55–100 % over 9 min</td><td rowspan="2">8 mL/min</td><td>19–23</td></tr>
<tr><td>4</td><td>26–30</td></tr>
<tr><td>5</td><td rowspan="2">3 % for 9 min
3–40 % over 12 min
40–60 % over 10 min
60–90 % over 11 min
90–100 % over 3 min</td><td rowspan="2">8 mL/min</td><td>20–28</td></tr>
<tr><td>6</td><td>32–40</td></tr>
<tr><td>7</td><td>5 % for 5 min
5–50 % over 9 min
50–100 % over 5 min</td><td>12 mL/min</td><td>14–17</td></tr>
<tr><td>8</td><td>5 % for 4 min
5–50 % over 5 min
50–100 % over 3 min
100 % for 5 min</td><td>12 mL/min</td><td>9–12</td></tr>
<tr><td>9</td><td rowspan="2">3 % for 4 min
3–40 % over 8 min
40–76 % over 4 min
76–100 % over 2 min
100 % for 3 min</td><td rowspan="2">8 mL/min</td><td>12–14</td></tr>
<tr><td>10</td><td>15–17</td></tr>
<tr><td>11</td><td rowspan="2">3 % for 7 min
3–50 % over 7 min
50–100 % over 5 min
100 % for 5 min</td><td rowspan="2">8 mL/min</td><td>13–15</td></tr>
<tr><td>12</td><td>16-18</td></tr>
<tr><td>13</td><td rowspan="2">3 % for 7 min
3–40 % over 15 min
40–60 % over 12 min
60–100 % over 15 min</td><td rowspan="2">8 mL/min</td><td>22–31</td></tr>
<tr><td>14</td><td>34–46</td></tr>
<tr><td>15</td><td>5 % for 9 min
5–50 % over 12 min
50–100 % over 10 min</td><td>10 mL/min</td><td>19–24</td></tr>
<tr><td>16</td><td>5 % for 7 min
5–50 % over 15 min
50–100 % over 10 min</td><td>10 mL/min</td><td>24–28</td></tr>
</table>

H. Lipophilicity Studies

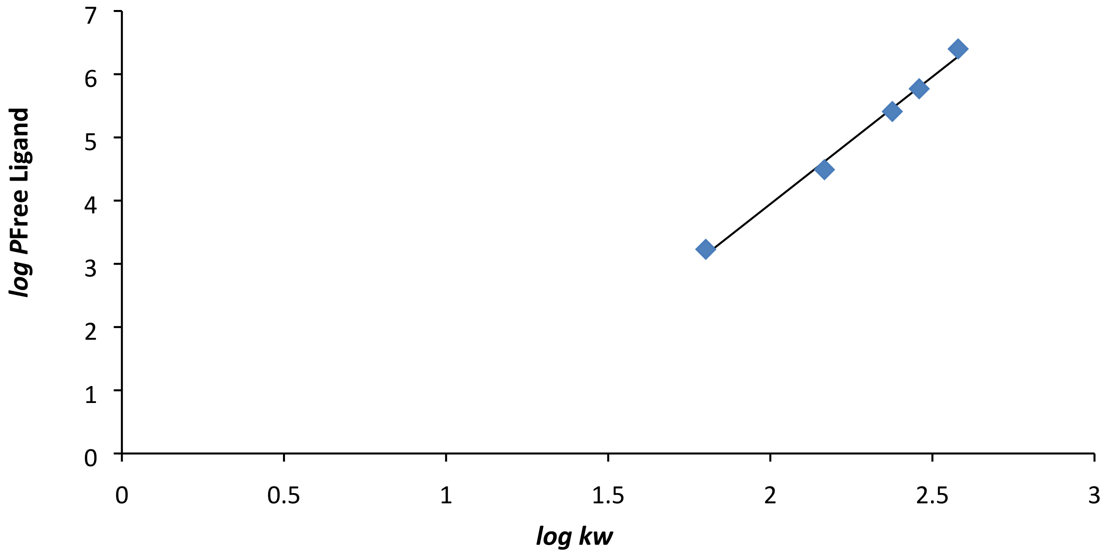

Figure H.1 Plot of *log P* values of carboxylic acid ligands vs. *log* k_w values of synthesised **PHENSS(IV)** derivatives.

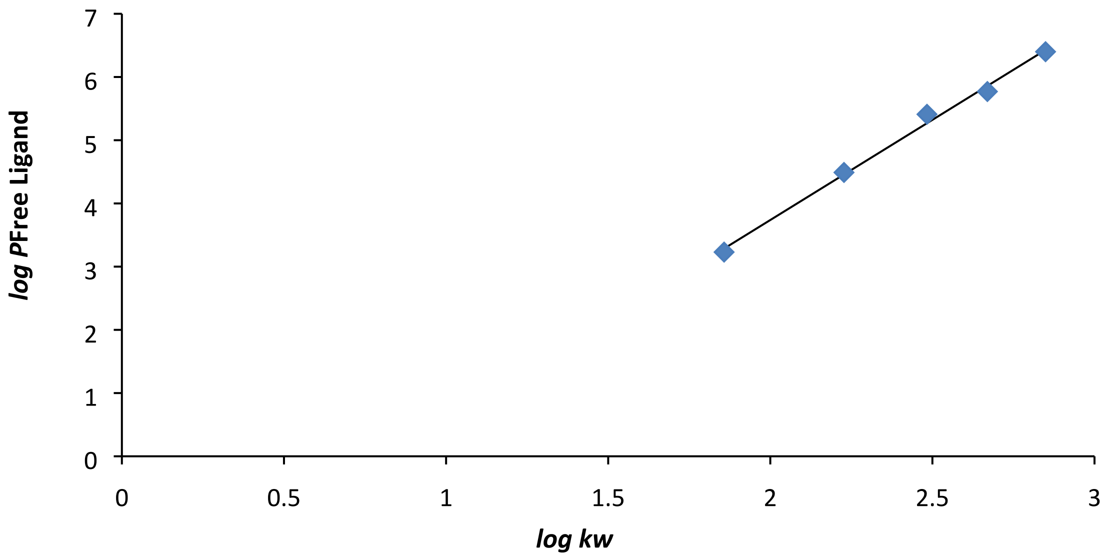

Figure H.2 Plot of *log P* values of carboxylic acid ligands vs. *log* k_w values of synthesised **56MESS(IV)** derivatives.

Log P values of carboxylic acids used to construct the plots against *log* k_w were obtained from literature.[1, 2]

I. *In vitro* cytotoxicity assay

All test agents were prepared as stock solutions (30 mM) in DMSO and stored at -20 °C. Cell lines used in the study included HT29 (colorectal carcinoma); U87 and SJ-G2 (glioblastoma); MCF-7 (breast carcinoma); A2780 (ovarian carcinoma); H460 (lung carcinoma); A431 (skin carcinoma); Du145 (prostate carcinoma); BE2-C (neuroblastoma); and MIA PaCa-2 (pancreatic carcinoma) together with one non-tumour derived normal breast cell line (MCF10A). All cell lines were incubated in a humidified atmosphere 5% CO_2 at 37 °C. The cancer cell lines were maintained in Dulbecco's modified Eagle's medium (DMEM; Trace Biosciences, Australia) supplemented with foetal bovine serum (10%), sodium bicarbonate (10 mM), penicillin (100 IU/mL), streptomycin (100 µg/mL), and glutamine (4 mM). The non-cancer MCF10A cell line was maintained in DMEM:F12 (1:1) cell culture media, 5% heat inactivated horse serum, supplemented with penicillin (50 IU/mL), streptomycin (50 µg/mL), HEPES (20 mM), L-glutamine (2 mM), epidermal growth factor (20 ng/mL), hydrocortisone (500 ng/mL), cholera toxin (100 ng/mL), and insulin (10 µg/mL). Cytotoxicity was determined by plating cells in duplicate in medium (100 µL) at a density of 2500–4000 cells per well in 96-well plates. On day 0 (24 h after plating) when the cells were in logarithmic growth, medium (100 µL) with or without the test agent was added to each well. After 72 h of drug exposure, growth inhibitory effects were evaluated using the MTT (3-[4,5-dimethylthiazol-2-yl]-2,5-diphenyl-tetrazolium bromide) assay and absorbance read at 540 nm. An eight-point dose-response curve was produced from which the IC_{50} value was calculated, representing the drug concentration at which cell growth was inhibited by 50% based on the difference between the optical density values on day 0 and those at the end of drug exposure.[3] Values presented for cisplatin, oxaliplatin and carboplatin were determined using this same method from a previous study.[4]

Table I.1 *In vitro* cytotoxicity of all synthesised complexes. IC_{50} values [nM] are reported with standard error; produced from 3-4 replicate experiments (n = 3-4); n.d. = not determined. [a]data taken from ref [5]. [b]data taken from ref [4].

	IC_{50} ± S.D. (nM)										
Complex	**HT29**	**U87**	**MCF-7**	**A2780**	**H460**	**A431**	**Du145**	**BE2-C**	**SJ-G2**	**MIA**	**MCF10A**
P-Dec (**1**)	130 ± 31	710 ± 170	1800 ± 120	270 ± 33	310 ± 13	430 ± 93	130 ± 24	490 ± 53	360 ± 110	280 ± 46	300 ± 40
$P(Dec)_2$ (**2**)	83 ± 12	210 ± 33	330 ± 70	160 ± 47	230 ± 60	220 ± 63	79 ± 21	350 ± 53	220 ± 49	160 ± 48	200 ± 64
P-DoDec (**3**)	90 ± 27	350 ± 63	1400 ± 230	280 ± 77	320 ± 70	340 ± 100	110 ± 35	440 ± 83	370 ± 80	270 ± 67	280 ± 49
$P(DoDec)_2$ (**4**)	67 ± 14	250 ± 15	500 ± 84	200 ± 6.7	240 ± 29	230 ± 29	290 ± 160	450 ± 41	260 ± 32	210 ± 17	140 ± 57
P-TetraDec (**5**)	150 ± 29	330 ± 27	1200 ± 150	270 ± 24	280 ± 24	210 ± 17	180 ± 19	450 ± 20	240 ± 37	260 ± 15	180 ± 89
$P(TetraDec)_2$ (**6**)	160 ± 13	420 ± 38	1200 ± 100	330 ± 23	310 ± 46	360 ± 67	160 ± 15	550 ± 30	390 ± 32	290 ± 42	210 ± 95
P-HexaDec (**7**)	170 ± 28	230 ± 33	1000 ± 200	310 ± 23	300 ± 3.3	190 ± 40	170 ± 65	350 ± 38	260 ± 28	210 ± 20	140 ± 46
P-OctaDec (**8**)	130 ± 28	210 ± 26	770 ± 180	260 ± 20	240 ± 6.7	150 ± 31	130 ± 34	340 ± 27	220 ± 45	170 ± 42	120 ± 25
56-Dec (**9**)	11 ± 4.6	47 ± 14	150 ± 30	27 ± 0	19 ± 3	24 ± 5.7	7.8 ± 4.1	390 ± 280	63 ± 9.4	17 ± 1.7	11 ± 0.79
$56(Dec)_2$ (**10**)	10 ± 2.8	22 ± 6	69 ± 8.3	23 ± 5	21 ± 3.3	29 ± 6.1	13 ± 7.1	92 ± 24	65 ± 7.4	16 ± 3.4	15 ± 2.7
56-DoDec (**11**)	19 ± 2.3	82 ± 14	180 ± 31	38 ± 4	35 ± 5	49 ± 0.3	15 ± 6.4	150 ± 41	110 ± 12	25 ± 2	28 ± 2
$56(DoDec)_2$ (**12**)	31 ± 24	24 ± 1	74 ± 8.2	23 ± 3	23 ± 2.7	20 ± 1.2	3.4 ± 0.6	140 ± 73	58 ± 16	28 ± 17	16 ± 4.4
56-TetraDec (**13**)	15 ± 4.6	44 ± 6	190 ± 44	37 ± 3.1	31 ± 5.8	35 ± 2.7	15 ± 2.6	100 ± 17	100 ± 33	92 ± 64	28 ± 8.7
$56(TetraDec)_2$ (**14**)	21 ± 5.7	62 ± 10	140 ± 33	39 ± 4.7	34 ± 7.8	56 ± 3.6	20 ± 2.1	150 ± 31	130 ± 34	31 ± 6.2	31 ± 2.1
56-HexaDec (**15**)	17 ± 8.4	24 ± 4	160 ± 60	34 ± 6	20 ± 1.7	24 ± 3.2	7.8 ± 2.2	54 ± 11	59 ± 26	21 ± 4.2	16 ± 5.9
56-OctaDec (**16**)	16 ± 0.9	23 ± 0	160 ± 19	29 ± 0.3	22 ± 1.7	20 ± 2.4	12 ± 2.3	88 ± 19	53 ± 12	15 ± 1.9	13 ± 3.4
PHENSS(II)[a]	130 ± 42	1500 ± 430	530 ± 150	270 ± 29	480 ± 150	870 ± 280	81 ± 50	400 ± 45	450 ± 60	800 ± 650	160 ± 74
PHENSS(IV)[a]	710 ± 300	4900 ± 610	16000 ± 4500	800 ± 84	1700 ± 200	4300 ± 530	310 ± 92	3000 ± 530	1700 ± 350	3400 ± 2200	1700 ± 200
56MESS(II)[b]	76 ± 61	76 ± 14	50 ± 4	30 ± 4	37 ± 9	51 ± 21	7 ± 2	100 ± 16	74 ± 18	15 ± 2	20 ± 5
56MESS(IV)[b]	22 ± 4	140 ± 23	140 ± 0	63 ± 16	53 ± 10	100 ± 15	9 ± 3	320 ± 61	110 ± 9	27 ± 2	30 ± 3
Cisplatin[b]	11300 ± 1900	3800 ± 1100	6500 ± 800	1000 ± 100	900 ± 200	2400 ± 300	1200 ± 100	1900 ± 200	400 ± 100	7500 ± 1300	n.d.
Oxaliplatin[b]	900 ± 200	1800 ± 200	500 ± 100	160 ± 0	1600 ± 100	4100 ± 500	2900 ± 400	900 ± 200	3000 ± 1200	900 ± 200	n.d.
Carboplatin[b]	>50000	>50000	>50000	9200 ± 2900	14000 ± 1000	24300 ± 2200	14700 ± 1200	18700 ± 1200	5700 ± 200	>50000	n.d.

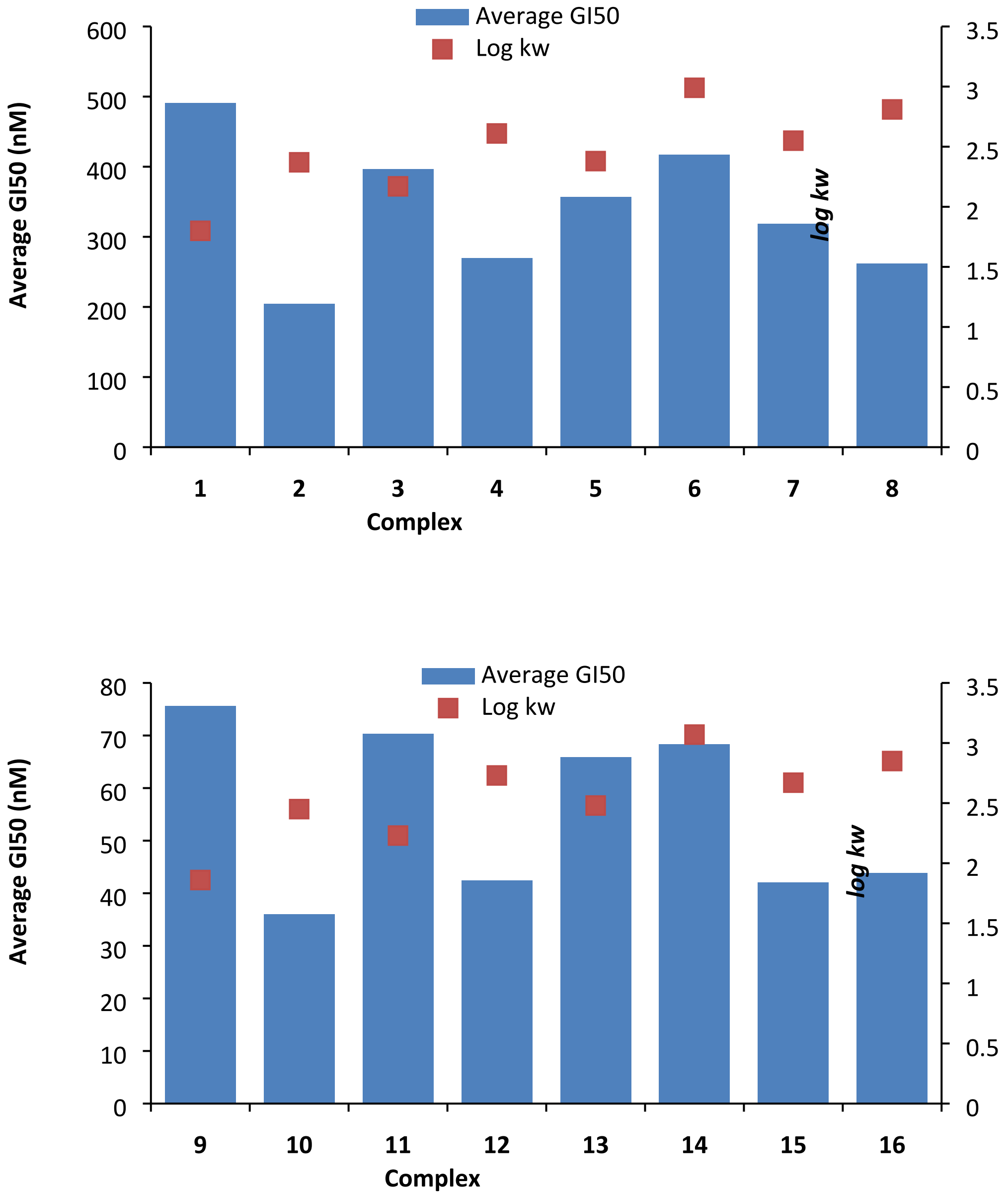

Figure I.1 Comparison of the average GI_{50} values across all cell lines for **PHENSS(IV)** derivatives (**1**–**8**, above) and **56MESS(IV)** (**9**–**16**, below), along with lipophilicity ($log\ k_w$) values.

REFERENCES

1. A. K. Ghose and G. M. Crippen, *J. Chem. Inf. Comput. Sci.*, 1987, **27**, 21-35.
2. V. N. Viswanadhan, A. K. Ghose, G. R. Revankar and R. K. Robins, *J. Chem. Inf. Comput. Sci.*, 1989, **29**, 163-172.
3. M. Tarleton, J. Gilbert, M. J. Robertson, A. McCluskey and J. A. Sakoff, *MedChemComm*, 2011, **2**, 31-37.
4. F. J. Macias, K. M. Deo, B. J. Pages, P. Wormell, J. K. Clegg, Y. Zhang, F. Li, G. Zheng, J. Sakoff, J. Gilbert and J. R. Aldrich-Wright, *Chem. Eur. J.*, 2015, **21**, 16990-17001.
5. K. M. Deo, J. Sakoff, J. Gilbert, Y. Zhang and J. R. Aldrich-Wright, *Dalton Trans.*, 2019, DOI: 10.1039/C9DT03339D.